UNIVERSITY OF THE WITWATERSRAND, JOHANNESBURG

FEASIBILITY OF INCINERATED SEWAGE SLUDGE ASH FOR PARTIAL REPLACEMENT OF PORTLAND CEMENT: PYRO-PROCESSING AND HYDRATION MECHANISMS ASSESSMENTS

Prepared by:

Ruth Katlego Juala (1367749)

School of Chemical and Metallurgical Engineering

A dissertation submitted to the Faculty of Engineering and the Built Environment, University of the Witwatersrand, Johannesburg, in fulfilment of the requirements for the degree of Master of Science in Engineering.

2021

DECLARATION

I declare that this thesis is my own unaided work. It is being submitted for the Degree of Master of Science to the University of the Witwatersrand, Johannesburg. It has not been submitted before for any degree or examination to any other University.

…………………………………………………………………………………

(Signature of Candidate)

…..06……. day of September……..in the year 2021……

(day) *(month)* *(year)*

ABSTRACT

Over 4 billion tons of cement is produced globally each year, resulting in approximately 0.95 tons of carbon dioxide (CO_2) per ton of cement produced. Over the years pozzolanic waste material has played a significant role in the construction industry as a partial replacement of Portland cement (PC) and other building materials. It seems likely that the greatest CO_2 reduction from the cement industry can be attained by the inclusion of these materials. This study considered the use of incinerated sewage sludge ash (ISSA) as a partial pozzolanic replacement of cement. The aim of this work was to evaluate the pozzolanicity of ISSA and its effect on the hydration and performance of Portland cement products. Dried sewage sludge (DSS) was incinerated at 700ºC, 800ºC and 900ºC to produce ISSA and cooled in the furnace (F_{ISSA}), air (A_{ISSA}) and in water (Q_{ISSA}) to study the effect of the incineration temperature and cooling rate on its performance.

Characterization of the ISSA was executed using scanning electron microscopy (SEM) equipped with energy dispersive spectroscopy (EDS), X-Ray Fluorescence (XRF), atomic absorption spectroscopy (AA) and a Malvern Mastersizer for particle size analysis to determine its feasibility as a partial replacement of Portland cement. Cement paste samples were prepared using 30% ISSA to replace PC and compared to a 100% PC mix as the primary reference sample and a mix of 30% coal fly ash and 70% PC as a secondary reference mix. All mixtures were prepared using a water/binder (w/b) ratio of 0.45 and used to study the pozzolanicity of ISSA after 6 hours, 7 days and 28 days of hydration. A SEM was used to study the hydration mechanism of ISSA and thermogravimetric analysis (TGA) to obtain the mass loss rate, calcium hydroxide ($Ca(OH)_2$) content and chemically combined water ($H_2O_{Q.comb}$). Mortar samples were also prepared at a PC replacement level of 30% and w/b ratio of 0.50 to study the effect of ISSA on the workability and compressive strength of PC mortar after 3, 7 and 28 days of hydration.

The chemical composition results of DSS/ISSA showed the presence of cementitious compounds and elements (Ca/CaO, Si/SiO_2, Fe/Fe_2O_3, Al/Al_2O_3, etc). These results suggested that ISSA could be used as a partial replacement of PC. The analysis showed that the concentrations of these elements/compounds were increased after incineration. In addition, a majority of the compounds showed an increase in concentration with an increase in incineration temperature, while the concentrations of elements of the ISSA varied with the different cooling methods.

Particle size analysis showed that ISSA particles were the largest in size compared to the particle sizes of PC and FA. These results were correlated with the SEM micrographs in which an irregular and amorphous morphology of ISSA was observed.

TGA results of cement pastes showed that cement pastes containing ISSA incinerated at 900ºC had a considerable reduction in $Ca(OH)_2$ after 28 days of hydration suggesting that effective pozzolanic reactions took place. The $H_2O_{Q.comb}$ content varied with each sample. Quenched ISSA incinerated at 900ºC showed better compatibility in the paste with the highest $Ca(OH)_2$ content and reduction of $Ca(OH)_2$ after 28 days of hydration. In general, an increase in the $Ca(OH)_2$ content was observed with an increase in the incineration temperature of ISSA. An increase of $Ca(OH)_2$ content in the order $F_{ISSA} < A_{ISSA} < Q_{ISSA}$ of the cooling rate of ISSA's was also observed. SEM analysis also showed that pastes containing ISSA had hydration products such as $Ca(OH)_2$, ettringite and calcium silicate hydrates (C-S-H), evidently developed after 6 hours and 7 days of hydration. However, due to the reduced amount of PC in the samples, the hydration was evidently slower compared to the reference sample, meaning that the ISSA pastes developed less heat during their hydration.

A reduction in mortar workability was obtained with the displacement of 30% PC by ISSA. This result was expected due to the irregular morphology of ISSA that reduced the flow of the mortar. A reduction in compressive strength was also obtained with the addition of 30% ISSA in PC mortar. These results were expected due to the reduced reactivity of ISSA compared to PC thus resulting in reduced compressive strength. The compressive strength results showed an increase with an increase in the incineration temperature of ISSA from 700ºC to 900ºC. The highest compressive strength on the ISSA blended mortars was that of sample MS9Q (70% PC and 30% quenched ISSA incinerated at 900ºC) with a compressive strength reduction percentage of 20.1%.

Although FA is generally considered to have higher pozzolanicity than ISSA, the compressive strengths obtained for ISSA blended mortars were comparable to that of MFA30 (FA blended mortar) and even slightly higher for sample MS9Q. The quenched ISSA generally showed better performance, establishing the lowest compressive strength reduction at all ages compared to furnace and air cooled ISSA's. To add to this, the rate of increase in compressive strength of MS9Q over time was higher than that of MFA30 and also higher than MC100 (reference sample). This result suggests that it is possible to achieve enhanced or even high compressive strength at later stages on mortar samples containing 30% ISSA with reduced PC content. In conclusion the highest cooling rate and the highest incineration temperature of 900ºC reduced the weakening effect of ISSA related to its low cementing properties compared to PC, and were regarded as the best methods to be considered when preparing ISSA for partial replacement in cement products.

DEDICATION

This work is dedicated to my mother, ***Merica Juala*** *the queen of my heart, my biggest cheerleader and best friend. Thank you for being my greatest inspiration, supporter and for walking with me throughout this journey. Your strength never ceases to amaze me. I would also like to extend my gratitude to my* ***siblings*** *for their endless support and encouragement throughout this journey. And to* ***God,*** *who made this possible.*

ACKNOWLEDGEMENTS

I would like to first thank my supervisor **Prof. Yunus Ballim** for taking up my project and seeing it through to completion, and for his guidance and tireless support throughout the course of the project. I would also like to thank my co-supervisor **Prof. Jean Mulopo** for his supervision. I would also like to thank **SASOL** for the financial, academic and emotional support. I have to mention **Dr Pheladi Mohlala, Vimal Bhimsan, Steyn Kobus,** and the entire **SASOL Bursary Team** for going out of their way to offer the support that was needed to complete this project. I would also like to thank the **technical staff** of the School of Chemical and Metallurgy and Materials Engineering. I have to mention, **Bruce Mothibedi** and **Motlatsi Phali**. Thank you to **Sonia Mavhungu** for her assistance, friendship and efforts in seeing my work proceed. Thank you to **Dr Diakanua Nkazi** for always checking the progress of my work and encouraging me to work hard. **Petra Dinham** for going out of her way to fit the analysis of my samples in her busy schedule. **Prof. Michael Daramola** for his contribution to my office equipment. **Dr David Whitefield** for his Malvern Mastersizer and **Francois Marais** for his assistance. I would also like to thank the **technical staff** of the School of Civil and Environmental Engineering for helping me with the initial set up of my experiments. Thank you to **Dr Mike Otieno** for giving me access to the compressive strength test machine and **Ms Janina Kanjee** for answering any questions I had about my experiment design. Thank you to **Mr Jacques Gerber** from MMU for helping me get my fragile samples coated immediately before microscopic analysis. Thank you to the East Rand Water plant **(ERWAT)** in Norkem Park for granting me permission to visit the plant and **Livhuwani** for talking me through their operation procedures. I would also like to thank **Afrisam** (Roodepoort Plant) for their assistance in running my XRF tests. And not to forget all the **postgraduate students** who always answered my never-ending admin questions.

CONTENTS

LIST OF FIGURES

LIST OF TABLES

ACRONYMS AND NOMENCLATURE

WWTP = wastewater treatment plant

SCM = supplementary cementitious material

DWA = Department of Water Affairs

ERWAT = East Rand Water

SCWO = supercritical water oxidation

w/c = water / cement ratio

w/b = water / binder ratio

CH = calcium hydroxide/$Ca(OH)_2$

CSH = calcium silicate hydrate

CS = calcium silicate

C_3S = tri-calcium silicate or Alite / $(CaO)_3.(SiO_2)$

C_2S = di-calcium silicate or Belite / $(CaO)_2.(SiO_2)$

C_3A = tri-calcium aluminate / $(CaO)_3.(Al_2O_3)$

Ettringite = $(CaO)_3.(Al_2O_3).(CaSO_4)_3.32H_2O$

Monosulphate = $(CaO)_3.(Al_2O_3).(CaSO_4).12H_2O$

PC = Portland cement

CEM I = Portland cement containing 95% (minimum) clinker

52.5N = cement strength class ($\geq$ 52.5 MPa at 28days, tested in accordance with SANS 50196-1)

CEM II = a composite cement containing a specified proportion of pozzolan or limestone

H_2O_{Qcomb} = chemically combined water

LOI = Loss on ignition (determined during chemical analysis)

FA = fly ash

SS = sewage sludge

DSS = Dry sewage sludge

ISSA = incinerated sewage sludge ash

A_{ISSA} = air cooled ISSA

F_{ISSA} = furnace cooled ISSA

Q_{ISSA} = quenched ISSA

7A = ISSA incinerated at 700ºC and air cooled

7F = ISSA incinerated at 700ºC and furnace cooled

7Q = ISSA incinerated at 700ºC and quenched

8A = ISSA incinerated at 800ºC and air cooled

8F = ISSA incinerated at 800ºC and furnace cooled

8Q = ISSA incinerated at 800ºC and quenched

9A = ISSA incinerated at 900ºC and air cooled

9F = ISSA incinerated at 900ºC and furnace cooled

9Q = ISSA incinerated at 900ºC and quenched

C100 = 100% PC (cement paste)

FA30 = 70% PC and 30% FA (cement paste)

S7A = 70% PC and 30% 7A (cement paste)

S7F = 70% PC and 30% 7F (cement paste)

S7Q = 70% PC and 30% 7Q (cement paste)

S8A = 70% PC and 30% 8A (cement paste)

S8F = 70% PC and 30% 8F (cement paste)

S8Q = 70% PC and 30% 8Q (cement paste)

S9A = 70% PC and 30% 9A (cement paste)

S9F = 70% PC and 30% 9F (cement paste)

S9Q = 70% PC and 30% 9Q (cement paste)

MC100 = 100% PC (mortar)

MFA30 = 70% PC and 30% FA (mortar)

MS7A = 70% PC and 30% 7A (mortar)

MS7F = 70% PC and 30% 7F (mortar)

MS7Q = 70% PC and 30% 7Q (mortar)

MS8A = 70% PC and 30% 8A (mortar)

MS8F = 70% PC and 30% 8F (mortar)

MS8Q = 70% PC and 30% 8Q (mortar)

MS9A = 70% PC and 30% 9A (mortar)

MS9F = 70% PC and 30% 9F (mortar)

MS9Q = 70% PC and 30% 9Q (mortar)

CHAPTER 1

INTRODUCTION

This chapter outlines the background of the study, problem statement, project aims, objectives, research questions and the overall dissertation layout.

1.1. Background

Waste recycling is one of the best ways to provide new, safe and renewable resources that contribute to the construction industry and thus protect the environment. Sewage sludge waste (residue from wastewater treatment plants), is one of the largest contributors to waste material worldwide. According to a research conducted by Fleishman *et al.* (2014), South Africa is one of the countries facing difficulties in the disposal of wastewater sludge. Environmental and public health concerns of sewage sludge disposal have historically been centered around the presence of harmful pollutants such as pathogens (e.g., viruses, parasites and bacteria); organic contaminants (e.g., dioxins; surfactants and pharmaceuticals) and inorganic contaminants (e.g., metals and trace elements) (National Research Council, 2002). These pollutants can cause intestinal, lung and viral infections (e.g., gastroenteritis) to those exposed to them (Lewis *et al.*, 2002). Hence, there is currently a need for much further analysis of sewage sludge disposal practices that includes the significance of economic criteria and environmental issues associated with sludge treatment.

Increased urbanization has brought about an escalation in the demand for cement in the construction industry. This increase has led to high emissions of carbon dioxide (Ing *et al.*, 2016). Various studies have shown that incinerated sewage sludge ash (ISSA) produced from raw sewage sludge can be used as supplementary cementitious material (SCM) in concrete production (Scrivener *et al.*, 2018). Incinerated sewage sludge ash contains components such as Al_2O_3, CaO and SiO_2 which are the primary compounds found in Portland cement (PC) (Tenza-abril *et al.*, 2011).

The most commonly used SCM's are ground granulated blast furnace slag and fly ash. Sewage sludge ash is another interesting alternative in this case. Sewage sludge is abundantly available and stockpiled in municipal wastewater treatment plants across South Africa. According to previous studies (Monzo *et al.*, 1997; Tantawy *et al.*, 2012; Dyer *et al.*, 2011; Pavlik *et al.*, 2016), ISSA has shown evidence of a certain level of pozzolanic activity. Pozzolans are siliceous or alumino-siliceous materials, which when finely divided, and in the presence of moisture, react chemically with calcium hydroxide released by the hydration of PC to form compounds found in hardened PC (Kosmatka *et al.*, 2002). Using these materials as a partial replacement of PC can reduce carbon dioxide (CO_2) emission from the cement manufacturing industry (Siddique & Cachim, 2018), and simultaneously reduce the amounts of waste material sent to landfill.

This project was aimed at evaluating the feasibility of using ISSA, as a partial replacement of PC in mortar. An important objective of this study was to investigate the effect of the post-incineration cooling rate of ISSA on the hydration mechanics when combined with PC. In support of the decision and for comparative purposes coal fly ash (a commonly used pozzolanic supplementary cementitious material) was also used to partially replace PC to compare the overall performance of ISSA as a partial replacement for PC.

1.2. Problem Statement

In South Africa, the large volumes of solid waste generated immobilize ever larger storage areas, thus reducing land availability without counting the environmental pollution consequences. South African population has experienced a rapid growth in the last two decades i.e. 48.8 million in 2005, 51.58 million in 2010 to 57.7 million 2018 (Worldometer, 2018) of which more than half currently lives and works in densely populated urban areas (DWA, 2013). This rapid population growth along with rapid urbanization has put extra pressure on the current existing wastewater treatment plant (WWTP) facilities which has resulted in an increased generation of sewage sludge at these facilities (Libhaber & Jaramillo, 2012). Several lines of evidence have suggested that sewage sludge disposal in landfill is not a sustainable option for sewage sludge management (Kacprzak, *et al.*, 2017; Tesfamariam, 2010; Devi & Saroha, 2017; He, *et al.*, 2015). Yet approximately 80% of wastewater treatment facilities still dispose their sewage sludge on dedicated sites (Herselman & Snyman, 2006) despite the potential dangers of contamination of the soil and subsoil (Kacprzak, *et al.*, 2017).

The South African department of Water Affairs and Forestry has identified five areas of utilization of sewage sludge namely: i) agriculture use (fertilizer), ii) on-site land application (within boundaries of WWTP) and off-site land application (outside the boundaries of WWTP), iii) thermal management practices (e.g., total or partial combustion of organic solids through incineration), iv) Beneficial use of sludge at high loading rates in agricultural practices and v) commercial products (e.g., manufacturing of pellet, bricks, paving and artificial rock) (Herselman & Snyman, 2009). However, the utilization of fertilizers produced from sewage sludge is still relatively limited because of the difficulty of satisfying the quality limitations (Faecal coliform maximum < 10000 CFU/g dry, Helminth Ova < 1 viable ova/g dry, pollution: As < 40 ppm, Cd< 40 ppm, Cr <1200 ppm, Cu < 1500 ppm, Pb < 300 ppm, Hg < 15 ppm, Ni < 420 ppm, Zinc < 2500 ppm) (Herselman & Snyman, 2009). These limitations result in large volumes of sewage sludge being disposed on open land. The need for creative methods that reduce the volumes of sewage sludge waste has become an environmental and social imperative. To reduce the above-mentioned environmental problems, sewage sludge ash produced from dried sewage could be used as a partial replacement of cement. Ultimately the goal of this project was to show that ISSA can be synergistically used as eco-materials in the local construction industry, in line with the global trend for the development of environmentally sustainable materials.

1.3. Research Questions

- Is ISSA a pozzolanic waste material?
- What incineration temperature enhances the pozzolanicity of ISSA?
- What effect do different cooling rates have on the feasibility of ISSA as a partial replacement of Portland cement?
- What effect does ISSA have on the hydration of cement paste?
- What is the influence of ISSA on the workability and compressive strength of PC mortar?

1.4. Aim

Increased urbanization has led to a high demand for Portland cement in the construction industry coupled with increased CO_2 emissions. The goal of this project was to study the possibility of using ISSA as a partial replacement of PC and comparing it with the performance of fly ash (a commonly used pozzolanic supplementary cementitious material) as reference. Effective utilization of ISSA can help reduce carbon dioxide emissions from the cement industry and reduce on-site/off-site disposal of sewage sludge.

1.5. Research objectives

Below are the summarized objectives of the study:

- To determine the effect of pyro-processing on the composition and morphology of sewage sludge through physical and chemical characterisation, i.e. silica content, pozzolanic activity and amorphous characteristics.
- To investigate the effect of the post-incineration cooling rates (furnace cooling, air cooling and quenching in water) of ISSA on the hydration mechanics when combined with PC.
- To determine the effect of ISSA on the hydration of PC paste by using TGA, SEM techniques at 6 hours, 7 days and 28 days of hydration.
- To test the performance of mortar produced with ISSA as part of the cementitious binder, at a PC replacement level of 30% by conducting workability and compressive strength tests at 3, 7 and 28 days of age.

1.4. Scope and limitations

The scope of this study is limited to the constraints mentioned below:

- Portland cement (52.5N), dried sewage sludge (ERWAT) and coal fly ash (Eskom)
- Water/binder ratio of 0.45 for cement pastes and 0.5 for PC mortar samples
- PC replacement percentage of 30%

1.5. Dissertation Layout

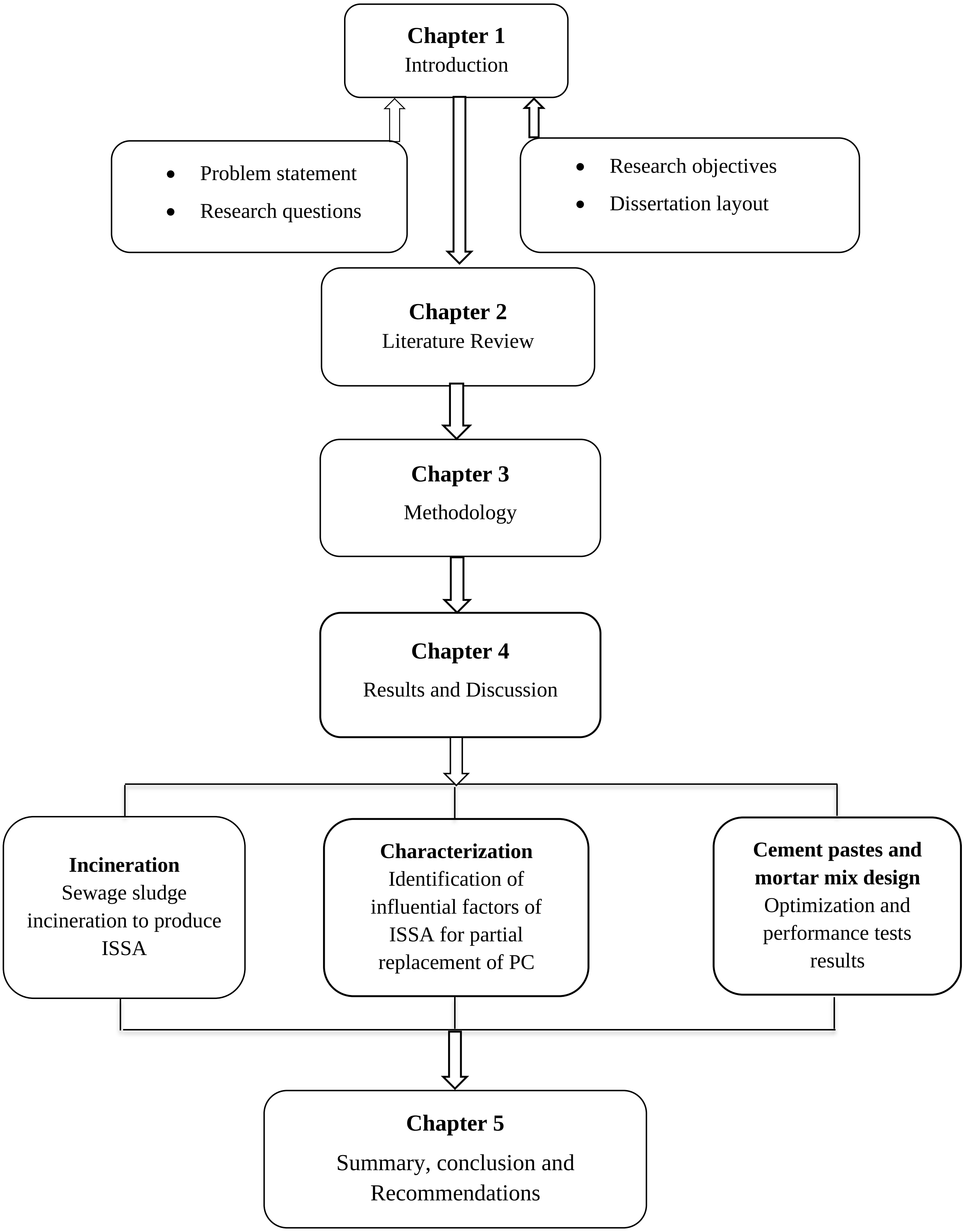

Figure 1.Dissertation layout

References

Devi, P. and Saroha, A.K., 2017. Utilization of sludge based adsorbents for the removal of various pollutants: a review. *Science of the Total Environment*, *578*, pp.16-33.

DWA. 2013. National Water Resource Strategy. Water for an equitable and sustainable future. 2nd Ed, *Department of Water Affairs.* Pretoria, South Africa.

Dyer, T.D., Halliday, J.E. and Dhir, R.K., 2011. Hydration chemistry of sewage sludge ash used as a cement component. *Journal of materials in civil engineering*, *23*(5), pp.648-655.

Scrivener, K.L., John, V.M. and Gartner, E.M., 2018. Eco-efficient cements: Potential economically viable solutions for a low-CO2 cement-based materials industry. *Cement and Concrete Research*, *114*, pp.2-26.

Fleischman, N.D., Botha, M.F. and Germanis, J.P., 2014. Sewage sludge and biomass incineration in South Africa using a fluidized-bed reactor. *South African Journal of Chemical Engineering*, *19*(3), pp.35-47.

He, Q., Xie, D., Xu, R., Wang, T. and Hu, B., 2015. The utilization of sewage sludge by blending with coal water slurry. *Fuel*, *159*, pp.40-44.

Herselman, J.E. and Snyman, H.G., 2009. *Guidelines for the utilisation and disposal of wastewater sludge*. Water Research Commission.

Ing, D.S., Chin, S.C., Guan, T.K. and Suil, A., 2016. The use of sewage sludge ash (SSA) as partial replacement of cement in concrete. *ARPN Journal of Engineering and Applied Sciences*, *11*(6), pp.3771-3775.

Kacprzak, M., Neczaj, E., Fijałkowski, K., Grobelak, A., Grosser, A., Worwag, M., Rorat, A., Brattebo, H., Almås, Å. and Singh, B.R., 2017. Sewage sludge disposal strategies for sustainable development. *Environmental research*, *156*, pp.39-46.

Kosmatka, S.H., Kerkhoff, B. and Panarese, W.C., 2002. Fly ash, slag, silica fume, and natural pozzolans. *Design and Control of Concrete Mixtures, EB001.* , 14th Ed, Portland Cement Association, Skokie, Illinois, USA, pp 57-72.

Lewis, D.L. and Gattie, D.K., 2002. Peer reviewed: Pathogen risks from applying sewage sludge to land. *Environmental Science & Technology*, *36*(13), pp.286A-293A.

Libhaber, M. and Orozco-Jaramillo, Á., 2012. *Sustainable Treatment and Reuse of Municipal Wastewater: For decision makers and practising engineers*. Iwa publishing, London, UK.

Monzo, J., Paya, J., Borrachero, M.V., Bellver, A. and Peris-Mora, E., 1997. Study of cement-based mortars containing spanish ground sewage sludge ash. In *Studies in environmental science* (Vol. 71, pp. 349-354). Elsevier.

National Research Council, 2002. *Biosolids Applied to Land: Advancing Standards and Practices*. National Academies Press, Washington DC, USA.

Pavlík, Z., Záleská, M. and Pavlikova M., 2016. Thermally treated sewage sludge as a potential pozzolanic additive in cement-based composites. *International Multidisciplinary Scientific GeoConference: SGEM*, *2*, pp.373-380.

Siddique, R. and Cachim, P., 2018. *Waste and Supplementary Cementitious Materials in Concrete: Characterisation, Properties and Applications*. Woodhead Publishing.

Tantawy, M.A., El-Roudi, A.M., Abdalla, E.M. and Abdelzaher, M.A., 2012. Evaluation of the pozzolanic activity of sewage sludge ash. *ISRN Chemical Engineering*, 2012.

Tenza-Abril, A.J., Saval, J.M. and Cuenca, A., 2015. Using sewage-sludge ash as filler in bituminous mixes. *Journal of Materials in Civil Engineering*, *27*(4), p.04014141.

Tesfamariam, E.H., 2010. *Sustainable use of sewage sludge as a source of nitrogen and phosphorus in cropping systems* (Doctoral dissertation, University of Pretoria).

Worldometer., 2018. *South Africa Population*. Accessed: 12 February 2020. Available at: <https://www.worldometers.info/world-population/south-africa-population/>

CHAPTER 2

LITERATURE REVIEW

This chapter focuses on the state of knowledge and research of Portland cement, sewage sludge, incinerated sewage sludge ash and the use of pozzolanic waste material, particularly ISSA. The chapter begins by outlining the history of PC, its production and the use of pozzolanic waste material as a partial replacement of PC. The various types of pozzolanic waste material are introduced and furthermore, the current state of knowledge on sewage sludge and ISSA as the material of interest is outlined.

2.1. Portland cement

Portland cement (PC) is an adhesive and cohesive material used to bind fragments of solid matter (Blezard, 1998). PC is one of the most important manufactured materials in the construction industry. When mixed with water PC forms a paste that hardens as a result of the hydration process (Jackson, 1998). When used in the production of mortar and concrete, cement produces a strong and rigid composite by binding aggregate material together (Grieve, 2009).

2.1.1. A brief history of Portland cement

As one of the most indispensable materials in the construction industry today, Portland cement was invented in 1824 by Joseph Aspdin (Screed Scientist, 2014). This was done through the thermal treatment of limestone and clay followed by crushing of the product to a powder which was then called "Portland cement". The name was inspired by the popularity and high quality of Portland stone at the time (Halstead, 1961). In an effort to upgrade and refine the invention, Portland cement was improved by William Aspdin (1843) through the use of enhanced grinding and heating equipment.

In South Africa, the first cement plant began operation in Pretoria in 1892, established as *"De Eerste cement Fabrieken Beperkt"* and was later re-established as "*Pretoria Portland Cement Company Limited" (PPC)* in the year 1908 (PPC, 2018). The company has grown over the years and engages in both the production and selling of cement through engagements with subsidiaries (PPC, 2018). The cement industry has shown tremendous growth over the years with other company developments such as "*Afrisam"*. The first cement plant under the company was built in Roodepoort in the year 1934, along with a limestone factory (the primary ingredient used in the production of cement) (Afrisam, 2020). Over the years the cement production industry expanded with the development of companies such as Lafarge, Natal Portland Cement (NPC), Sephaku Cement and Kwikbuild Cement.

2.1.2. The production of Portland cement

Portland cement is characterized by its principal raw material, oxides of silica, aluminium, lime and iron. (Grieve 2009). It can be produced through a dry or wet method. The major difference in these methods is the blending of raw material as a slurry in the wet process before thermal treatment is conducted (Screed Scientist, 2014). The dry method is commonly used due to its higher efficiency compared to the wet process (PCA, 2014; Screed Scientist, 2014). According to previous experiments, the wet method uses more fuel for evaporating water in the slurry and results in high CO_2 emission during heating (PCA, 2014). Portland cement is manufactured in five steps (see Figure 2).

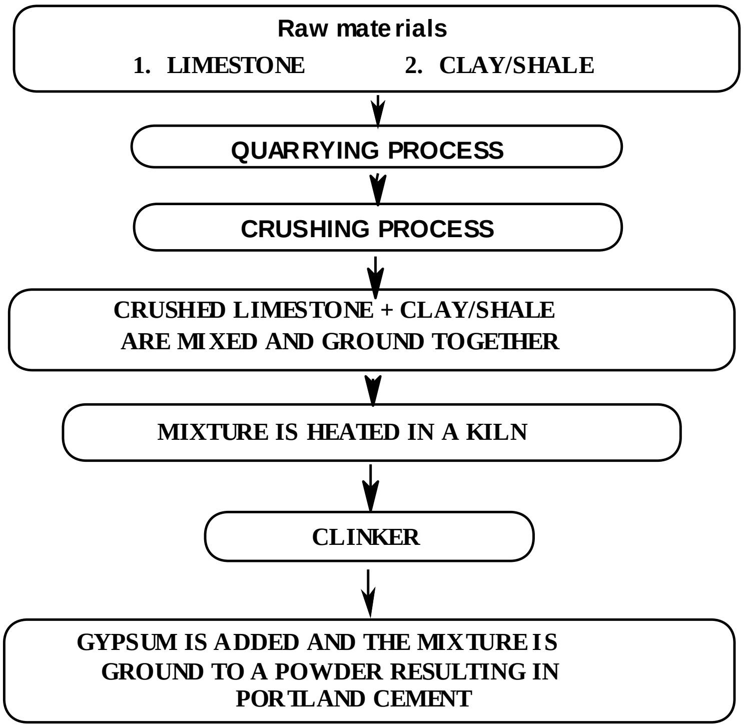

Figure 2: Schematic diagram of the production of Portland cement (Chamberlain et al., 1995)

The initial step is size reduction of raw materials (clay and limestone). The fine powder material is then proportioned and mixed together in preparation for heat treatment to melting point at 1400°C to 1500°C using a rotary kiln. In the kiln the decarbonation process to occurs according to the following PC chemistry.

$$CaCO_3 = CaO + CO_2 \qquad (1)$$

This is followed by further heating to form tri- and di-calcium silicates which are the major constituents of the clinker formed in the hottest part of the kiln. The product from the rotary kiln (red-hot in appearance) is rapidly cooled in preparation for milling. The final step (milling) is usually conducted using a ball mill to produce fine particles (≤ 0.075 mm). To help manage the setting of the cement when mixed with water, gypsum is mixed with the clinker during the milling process. Gypsum is used to lower the rate of reaction of cement and water during the hydration process; this allows sufficient time to transport and cast cement before hardening takes place (Ylmén, 2013). The typical composition of South African PC is given in Table 1 below.

Table 1: Typical chemical composition of PC (Grieve, 2009)

Oxide	**% by mass**
CaO	63 - 69
SiO_2	19 - 24
Al_2O_3	4 - 7
Fe_2O_3	1 – 6
MgO	0.5 – 3.6
Na_2O + 0.658 K_2O	0.2 – 0.8

2.1.3. Hydration of Portland cement

The reaction between water and cement is known as the hydration process. During hydration, cement paste changes from a thixotropic fluid state to a clay form and finally hardens to a rigid state (Roussel *et al.*, 2012). The major compounds of cement form chemical bonds with water molecules to produce hydration products (Chamberlain *et al.*, 1995). Tri- and di-calcium silicates are the main crystal components of PC that react with water to produce calcium silicate hydrates (Equation 2 and 3 respectively). The calcium silicates form over 80% of the total mass of most cement (Barron, 2014). Alite (C_3S) is known to contribute to the hydration and strength development of cement at the early stage of hydration (about 28 days of age), while belite (C_2S) tends to be responsible for the strength and hydration of cement at a later stage of the hydration process (Barron, 2014).

$$2(CaO)_3\,(SiO_2) + 7H_2O = (CaO)_3\,(SiO_2)_2 \bullet 4(H_2O) + 3Ca(OH)_2 \qquad (2)$$

$$2(CaO)_2\,(SiO_2) + 5H_2O = (CaO)_3\,(SiO_2)_2 \bullet 4(H_2O) + Ca(OH)_2 \qquad (3)$$

The produced calcium silicate hydrates (C-S-H) are the main components that bind PC paste and contributes to the early development of compressive strength at up to 7 days of age (Bensted, 1983). The C-S-H produced are also responsible for the main heat of reaction and grow rapidly, leaving a limited amount of space for water molecules to react with unhydrated C_3S (Scrivener *et al.,* 2015). At this stage the rate at which the reaction proceeds is led by the diffusion of water molecules through C-S-H coating, which thickens over time causing the production of C-S-H to decrease (Chamberlain *et al.,* 1995).

2.1.4. Evolution of heat during cement hydration

Heat flow is an important aspect when analysing the nature of cement (Ylmén, 2013). Most reactions that occur during the hydration of cement are exothermic (release heat). The heat of the reaction is usually measured using a calorimetric device. Figure 3 shows a typical isothermal calorimetry curve of the hydration stages of cement. The hydration process stages are described by Ballim and Graham, (2009).

Initial heat liberation starts immediately after cement comes in contact with water. This occurs due to the hydration of tricalcium aluminate (C_3A) and some of the C_3S (Odler, 1998). Thereafter, ettringite is produced by the reaction of calcium sulphate resulting in a reduction in the heat rate. The ettringite produced slows down the hydration of C_3A by forming a protective coating (Odler, 1998). Stage 2 entails a high rate of heat evolution and thereafter a decrease in the rate of heat evolution. At this point a second hydration peak is produced by hydrates C-S-H and $Ca(OH)_2$ (Odler, 1998). The C-S-H is produced as a result of the setting that occurs close to the inflection point that comes after the second peak in stage 2. Setting is the stiffening of the mixture that occurs due to the formation of ettringite and early-stage calcium silicate hydrates. The third and last stage results from the reaction of ettringite, which produces monosulphate hydrate (Odler, 1998). The ferrite phase also contributes to the formation of ettringite and C_2S to produce C-S-H (Ballim and Graham, 2009).

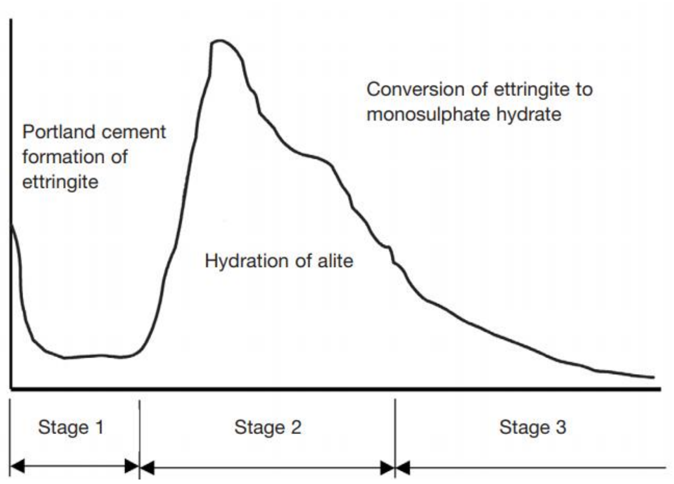

Figure 3: Isothermal calorimetry curve of the hydration stages of cement (Roy, 1989)

2.1.5. Strength development in concrete/mortar/cement paste

The strength of concrete/mortar/cement paste mixtures stems from the hardening process that takes places after the mixture has been poured and installed. When the cement begins to hydrate, calcium silicate hydrates form and induce the hardening process (Barron, 2014). The rate at which the mixture hardens is independent of the rate at which it sets (Anon, 2005). The strength of concrete, particularly the compressive strength, is often measured by preparing cubes or prisms and curing them for measurement at specific times. The most common curing times are 2, 7, 28 and 90 days at a typical curing temperature of 20ºC (Anon, 2005). Factors that affect concrete strength include but are not limited to:

- Porosity – the more porous the concrete is, the weaker it will be. The concrete voids may be filled with either air or water. The most significant cause of porosity in concrete is the ratio of water to cement in the mix (see below).
- Water/cement ratio – this ratio is calculated by dividing the mass of water in the mixture by the mass of cement in the mixture. An increase in the water cement ratio (w/c ratio) results in the increase in the porosity of the cement paste in the concrete. Consequently, as the porosity increases, the compressive strength of concrete decreases.
- Particle size – the fineness of cement affects the rate at which the cement hydrates and consequently the rate of strength growth. Coarser cement particles tend to lower the rate of the hydration reaction.
- Cement composition – the proportion of individual cement minerals can affect the rate of growth of strength and the final strength obtained. These include the alite content,

alite and belite reactivity and the cement sulphate content (Aligizaki, 2005; Anon, 2005; Bullard *et al.,* 2011).

2.1.6. Blended Portland cement

Supplementary cementitious materials (SCM's) are broadly used to replace a part of clinker during the production of cement (Berodier, 2015). Examples of SCM's include, ground granulated blast furnace slag, fly ash and silica fume (see Section 2.2). Studies have reported that the utilization of these materials has provided a way of improving and stabilizing the cementitious matrix while also reducing the amount of CO_2 emissions in the production of cement (Lothenbach *et al.,* 2011; Silva *et al.,* 2014). Concretes made with blended cements have also been reported to have higher durability than those made with pure Portland cement. This effect is predominantly attributed to the reduced permeability and ion transportation determined by the microstructure (Berodier, 2015), and the availability of new calcium silicate hydrates and calcium aluminate hydrates from additional pozzolanic reactions (Mendoza *et al.,* 2013; Silva *et al.,* 2014).

2.1.7. Hydration of blended Portland cement

It is important to understand the effect of SCM's on the performance of cement products. The use of SCM's in cement paste mixtures has been found to influence the nature and amount of hydrates formed during the hydration process, thus changing the volume, durability and porosity of the material (Lothenbach *et al.,* 2011). The hydrates (C-S-H) produced in blended cements are similar to the ones produced in PC, but have a changed chemical composition (Berodier, 2015). The hydration reaction of supplementary cementitious material only starts reacting after the first two days of the hydration process when the clinker phases react. Berodier, (2015) also showed that the reaction of SCM's in blended cements only starts during the second dissolution of calcium silicate hydrates. This, however, is predominantly affected by the level of substitution and type of the SCM's which is attributed to the early depletion of sulphate ions and formation of C-S-H (Berodier, 2015).

2.2. Pozzolanic supplementary materials used in cement

Pozzolanic materials are a type of SCM. Pozzolans play a vital role in the cement and concrete industry. These materials contain aluminous and siliceous material, which when finely divided react with $Ca(OH)_2$ to produce compounds found in hardened PC (Kosmatka *et al.,* 2002; Grieve, 2009). The name "pozzolana" was derived from the "*Roman source of zeolitic tuff at Pozzuoli in the foothills of Mount Vesuvius"* (Sims & Brown, 1998). In the past centuries, the use of pozzolans which had originated from Italy and Greece was restricted to countries where the substantial reserves of pozzolans were found (Massazza, 1998). Years later, other countries began to adapt to the use of pozzolans due to the rise in the need to reduce waste material such as silica fume and fly ash (artificial or man-made pozzolans).

Pozzolans react with $Ca(OH)_2$ in water and do not hydrate (i.e. react with water as PC) to form cementing compounds on their own (Grieve, 2009). The cementing compounds produced by pozzolans are similar to those produced by the hydration of PC (Grieve, 2009). Pozzolans are generally referred to as SCM's or mineral admixtures and may be used in addition to or as a partial replacement of cement (Kosmatka *et al.,* 2002). The use of pozzolans has been found to reduce CO_2 emissions from the production of cement due to their additional cementing compounds that contribute to the cement matrix structure and pozzolanic reactivity effect (Escalante-Garcia *et al.,* 2003). According to Boualleg *et al.* (2017), the reduction of $Ca(OH)_2$ caused by pozzolanic material is also associated with an increase in the durability of cement products due to the vulnerability of $Ca(OH)_2$ to chemical attack.

2.2.1. Measuring pozzolanicity

Pozzolanicity is a measure of the reactivity of cementitious material. Calcium hydroxide consumption is often used as means of determining the pozzolanicity of cementitious material. Traditionally, thermal procedures are used to identify and quantify hydration products in cement together with the loss of chemically combined water in the cement matrix (Silva *et al.,* 2014). Thermogravimetric analysis (TGA) is a broadly used technique in this aspect. TGA measures volatile components and the thermal stability of material by determining the fraction of weight loss that occurs when the material is heated at a constant rate (Groenewoud, 2001). For cementitious material, the analysis is used to identify the calcium hydroxide fixation percentage as a measure of mass loss due to the calcium hydroxide dehydroxylation process that occurs at a temperature range of 425ºC to 550ºC (Mendoza *et al.,* 2013). This is calculated with the addition of the calcium hydroxide that converts to calcium carbonate during sample preparation. The decomposition of $CaCO_3$ occurs at a temperature range of 600ºC to 800ºC (Lothenbach *et al.,* 2016).

An alternative method to determine the pozzolanicity of material was also introduced by Mendoza *et al.* 2013. In this method a moisture analyser (MA) measures the mass loss as a result of the dehydration of pozzolans in the reaction of cementitious material. Although the method was found to be less expensive and timesaving, most researchers on the topic consider the TGA technique as the most fitting technique to determine the consumption of $Ca(OH)_2$ of cement paste. This is due to the ease with which the decomposition of $Ca(OH)_2$ to $CaO + H_2O$ in the temperature range of 425ºC and 550ºC can be determined thus determining the level of pozzolanicity of the material (Menendez *et al.,* 2012; Galan *et al.,* 2012; Silva *et al.,* 2014; Anjos *et al.,* 2019).

2.2.2. Coal fly ash

Coal fly ash (FA) is a pozzolanic material commonly used as a partial replacement of cement in the construction industry (Bendapudi & Saha, 2011; Harison *et al.,* 2013; Patil, 2017). The use of fly ash in Portland cement has an effect on the kinetics of hydration (Berodier, 2015). FA is produced by the mechanical or electrostatic precipitation of dust particles from furnace flue gases during the combustion of coal in power plants (Jackson, 1998; Grieve, 2009). South Africa is abundant in FA produced from coal-fired power station in the country. Table 2 shows the typical chemical composition of South African FA.

Table 2: Typical chemical composition of South African coal fly ash (Grieve, 2009)

Oxide	**% by mass**
SiO_2	48 - 55
Al_2O_3	28 - 34
CaO	4 – 7
Fe_2O_3	2 – 4
MgO	1 – 2
$Na_2O + 0.658\ K_2O$	1 – 2

The market for FA in South Africa is shown in Figure 4. The chart shows that South Africa has adapted to the use of FA in cement making, with over 72% of FA used in the industry. The vast use of FA in cement and concrete stems from the effectiveness of FA in increasing the strength of the product over time. According to various studies, concrete containing FA has a lower strength than pure cement concrete for a period of 30 days. However, this concrete starts to show an increase in strength equal to that of the pure cement concrete in 30 – 40 days, and may measure higher strength in a year’s time (Kruger, 2015; Ayub *et al.,* 2014).

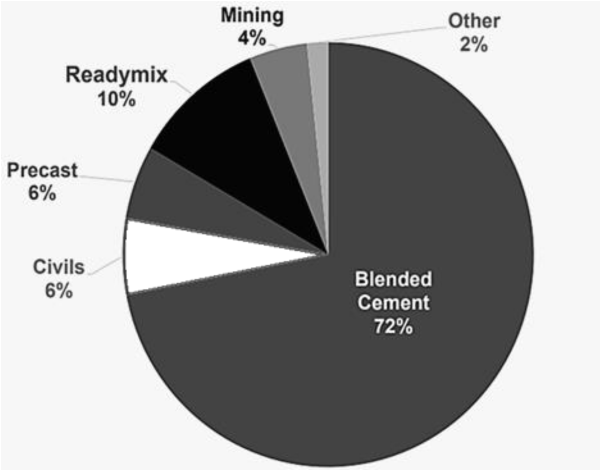

Figure 4: South Africa's Market Breakdown for coal fly ash with a total volume of 2.5 million tons (Kruger, 2015)

FA is a pozzolanic material that reacts with the $Ca(OH)_2$ in cement to produce cementitious compounds (Paya *et al.,* 2001; Goni *et al.,* 2003). During the reaction with water acts as a binding agent, calcium hydroxide merges with the FA to produce supplementary hydrate compounds (Paya et al., 2001), enabling it to partially replace cement.

2.2.3. Effect of pozzolanic materials in the construction industry

Over the years pozzolanic material has been found to improve the mechanical properties of concrete structures. These include modification of the thermal stability of cementitious matrix and the reduction of post-cooling cracking through the use of pozzolanic material (Fu *et al*., 2004; Wang, 2008). This behaviour is attributed to the availability of new calcium aluminosilicate hydrates from the pozzolanic reactions that take place between $Ca(OH)_2$ and silica-alumino rich minerals in the pozzolanic material (Silva *et al.,* 2014). According to previous studies the use of fly ash (Xu, 2003; El-Didamony *et al.,* 2012), silica fume (Morsy *et al.,* 2008) and metakaolin (Morsy *et al.,* 2008; Vu *et al.,* 2001) as a partial replacement of cement was found to enhance the physicochemical properties, microstructure and thermal stability of cement products. In another study, it was found that the use of these materials also reduced cracking that tends to occur during the post-cooling period as a result of the rehydration of dissociated calcium oxide (Petzold & Roehrs, 1970).

2.3. Sewage sludge waste

Waste disposal is a recognized global health problem and, with the human population growing, the demands for safe waste disposal are increased. Amongst these wastes is sewage sludge waste from WWTP's. The sludge is of a semi-solid nature produced as a by-product from treatment of municipal sewage and industrial wastewater (Dermibas *et al.,* 2017). On average it is estimated that one person can produce up to 10 – 15 kg sewage sludge per year, resulting in approximately 70 – 105 million tons of sewage sludge waste produced annually worldwide (Grobelak *et al.*, 2019). With the rapid increase in population, this number is certainly going to increase in the future. In studying the environmental impacts of sewage sludge, the chemical properties of the sludge are of great interest. Sewage sludge is made up of a complex matrix of both organic and inorganic material (Van Berg, 1993), and also contains heavy metals such as Cr, Pb, Ni, Zn, Cd and Cu, as well as pathogens and nutrients (refer to Section 4.2) (Ing *et al.*, 2016).

2.3.1. Sewage sludge disposal practices in South Africa

South Africa is home to over 824 wastewater treatment plants (Kings, 2017). The rapid increase in population in South Africa has led to overcrowded urban areas and townships across provinces in the country. Municipalities across the country are experiencing difficulties in solid waste disposal mainly due to a lack of landfill capacity (Rasmeni & Madyira, 2019). The two major disposal techniques employed for sewage sludge waste management in South Africa includes, stockpiling and land application (Grobelak *et al.*, 2019; Snyman, 2007). Figure 5 shows an example of land application of sewage sludge. According to Herselman *et al.* (2005), sewage sludge waste treatment processes applied in South Africa only account for 0.06% of the total waste produced in the country. Amongst these, poorly treated sludge applied to land may also contribute to the emission of greenhouse gases as a result of the organic degradation of the sewage sludge over time (Chen & Kuo, 2016). Due to the increase in urbanisation and industrialisation, sludge production has increased. From an environmental standpoint, ploughing and stockpiling in paddies have become unsustainable sewage sludge treatment methods.

Figure 5: Sludge disposal in landfill at ERWAT plant after treatment (Thusi, 2016)

2.3.2. Wastewater treatment plant processes

Primary treatment of the sewage sludge is conducted by screening to remove large objects that do not form part of the sludge (Anon, *n.d*). Secondary treatment takes place with the use of biological processes to break down suspended organic matter prior to disposal or possible incineration (Ambulkar, *n.d*; Simpkins, 2005). Incineration of sewage sludge is discussed further in Section 2.3.3. Figure 6 shows a typical wastewater treatment process. The material of interest is the dried/dewatered sludge from the WWTP which is disposed to landfill. Further studies on the use of this material can enable sustainable utilization and reduce the negative environmental impacts.

2.3.2.1. Wastewater treatment plant technologies

Wastewater treatment plants use various techniques to manage and reduce the overall volume of sewage sludge waste prior to disposal or usage; these techniques may include thickening, anaerobic/aerobic digestion, gasification and supercritical water oxidation (SCWO) and incineration. Figure 7 shows the different types of sewage sludge generated by South Africa's WWTP's, in terms of mass percentage (Snyman, 2007). A common method used to treat sludge containing about 1% of wastewater entering plants is anaerobic digestion and dehydration. Anaerobic digestion is a biological process that produces stable substances by decomposing organic solids (Mata-Alvarez, 2003). This process also obliterates pathogens and makes dewatering the sludge easier (Simpkins, 2005). Sewage sludge incineration (refer to Section 2.3.3) is seldom executed to reduce sewage sludge volume which would thus reduce the costs of storage and pumping (Ambulkar, *n.d*). Moreover, previous studies also reveal that incinerated sewage sludge has reduced odour, which makes it easier to handle without difficulty (DiStefano & Ambulkar, 2006).

Sewage sludge produced in WWTP's has over the years been found to contain nutrients that are vital for the growth of plantations (Dean & Suess, 1985). Although sewage sludge is of use in agriculture, only a certain regulated amount can be utilized. Excessive usage has been found to lead to infectious organisms that pose threat to the health of consumers (Dean & Suess, 1985). With an increase in sewage sludge production in the country, the current methods are unsustainable in managing sewage sludge waste.

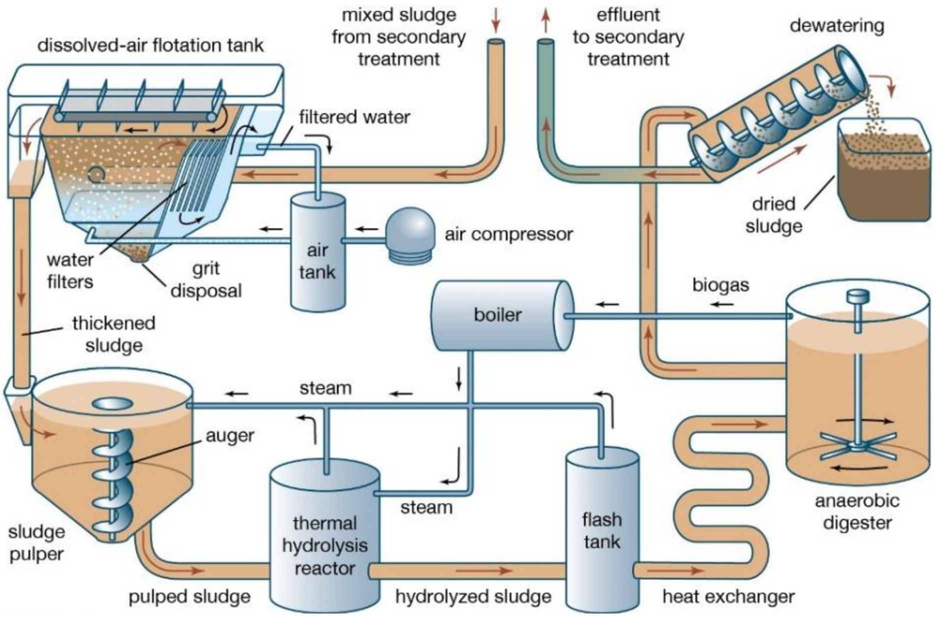

Figure 6: Wastewater treatment plant process (Ambulkar, n.d)

The dominant sludge treatment technique employed by South African WWTP's is anaerobic digestion and activated sludge (25%) as shown in Figure 7. Blended sludge accounts for both primary and activated sludge mixed before or after digestion, and only 1% of petro sludge is produced (mixture of waste oil, wastewater, sand and mineral matter (Islam, 2015; Snyman, 2007).

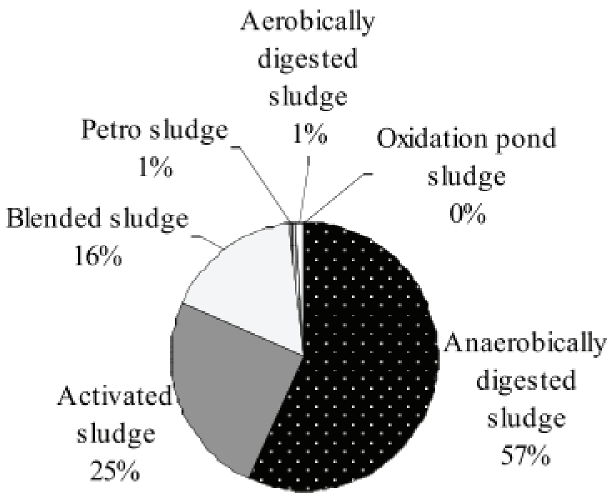

Figure 7: Sludge (dry mass wt% base) produced in SA's WWTP (Snyman, 2007)

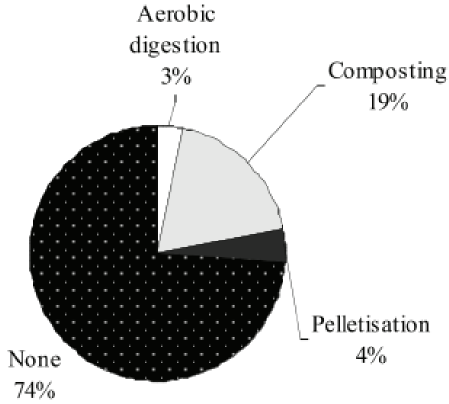

Figure 8: Tertiary treatment and additional stabilization technologies employed in SA (Snyman, 2007)

2.3.2.2. Additional stabilization technologies

Figure 8 shows the additional stabilization technologies for sewage sludge waste. Over 74% of the sludge generated by the WWTP's does not proceed to tertiary treatment or additional stabilization. Aerobic digestion (3%) is used as a secondary digestion method. Sewage sludge composting is relatively high (19%) because it is employed by treatment plants in small towns and metropolitan councils compared to pelletization, which is only employed in metropolitan councils (Snyman, 2007). The majority of the sewage sludge ends up disposed on-site and off-site in WWTP's and takes up valuable land space. For this reason, it is vital to conduct further research that supports the potential of using disposed sewage sludge.

2.3.3. Incineration of sewage sludge

Sewage sludge from WWTP's is characterised by an easy flow and poor engineering strength due to the high amount of organic matter and water content, in addition to the hazardous pollutants found in the sludge (Diliunas *et al.*, 2010; Yang *et al.,* 2017; Tan *et al.,* 2020; Chen *et al.*, 2020). Incineration is a thermal technique carried out to reduce the overall volume of sewage sludge. Incineration also reduces toxic organic compounds found in the raw sewage sludge (Khiari *et al.,* 2004). During incineration the mineralogy and microstructure of sewage sludge changes. The process is usually conducted at high temperatures ranging from 450ºC to 1300ºC (Vouk *et al.,* 2017). During the process, a change in chemical composition of the sludge occurs. A portion of the toxic substances in the sludge is removed, and some of the substances remain immobilized in the sludge (Lin & Chang, 2006), producing a considerable amount of ISSA primarily consisting of bottom ash (90%) and fly ash (10%) (Vouk *et al.,* 2017). Although sewage sludge is often converted into organic fertilizers, some researchers in Canada maintain that incineration is the best solution of sewage sludge disposal (Thomas Nutrient Solutions, 2014).

2.3.3.1. Sewage sludge incineration methods

Sewage sludge incineration has been gaining popularity in many countries such as the United States of America, which runs over 170 sewage sludge incineration plants (Federal Highway Administration, 2020). Some of the incineration equipment used includes, fluidized bed, multiple hearth and electric infrared incinerators, rotary kiln, single hearth cyclone and wet air oxidation, smelting furnaces (Werther & Ogada, 1999). Overall, incineration has been gaining popularity in many countries due to a decline of usage in agriculture, landfilling and environmental industries (Tammemagi, 1999). The fluidized bed furnace has become the most favoured method of incineration due to ease of operation, intermittent method of operation available and fewer moving mechanical parts (Dhir *et al.*, 2017). During the process dried or wet sewage sludge waste is heated in a fluidized bed reactor. Fuel is often used when heating wet sewage sludge due to its high-water content. The ash is produced as powdered solid material, inert dust and in some cases solid residue (Payá *et al.*, 2019).

2.3.3.2. Incinerated sewage sludge ash properties

Sewage sludge incineration facilitates the reduction in mass as shown in Figure 9 extracted from a study by David and Nair, (2018). It was noted that after grinding the sewage sludge ash was labelled as "SSA as cement", but it can be more correctly referred to as sewage sludge ash for partial replacement of cement. Treatment of the sewage sludge changes its composition and reduces its volume. According to Halliday *et al.* (2012), incineration reduces the mass of sewage sludge by approximately 65%. After incineration, sewage sludge ash is found to have an increased concentration of compounds commonly found in PC, such as SiO_2, Al_2O_3, Fe_2O_3, CaO and MgO as its main components (Tenza-abril *et al.*, 2011; Ing *et al.*, 2016; Kosior-Kazberuk, 2011; Yusuf *et al.*, 2012). These compounds make ISSA a potential SCM/pozzolanic material that can be used in the manufacturing of bricks, concrete, cement, lightweight aggregate, geopolymers and tiles (Tay, 1987; Gomes *et al.*, 2019; Payá *et al.*, 2019).

Figure 9: Forms of sewage sludge in relation to processing degree (David & Nair, 2018)

Table 3 shows the typical comprehensive chemical compositions of ISSA according to previous studies (Park *et al.*, 2003; Wang *et al.*, 2005; Merino *et al.*, 2007). These results were compared with the chemical composition of the ISSA used in this study.

Table 3: Typical chemical composition of ISSA (Park et al., 2003 (a); Wang et al., 2005 (b); Merino et al., 2007 (c)

Component	**wt% (a)**	**wt% (b)**	**wt% (c)**
SiO_2	39.52	43.6	25.40
Al_2O_3	17.17	16.6	7.64
Fe_2O_3	11.91	10.4	20.00
P_2O_5	7.55	12.1	14.20
CaO	7.16	5.61	21.05
K_2O	2.72	2.34	0.78
MgO	2.13	1.40	1.63
Na_2O	1.23	0.82	0.48
TiO_2	0.81	-	0.29
ZnO	0.52	-	-
MnO	-	-	0.03
LOI	7.31	-	8.36
Total	98.03	92.87	99.86

Figure 10 shows a comparison of calcium, silicon and aluminium oxide contents of various SCM’s compared to PC in a ternary diagram. The ISSA used in this study was added to the diagram. The differences observed contribute to the behaviour of the materials when used as a partial replacement of PC.

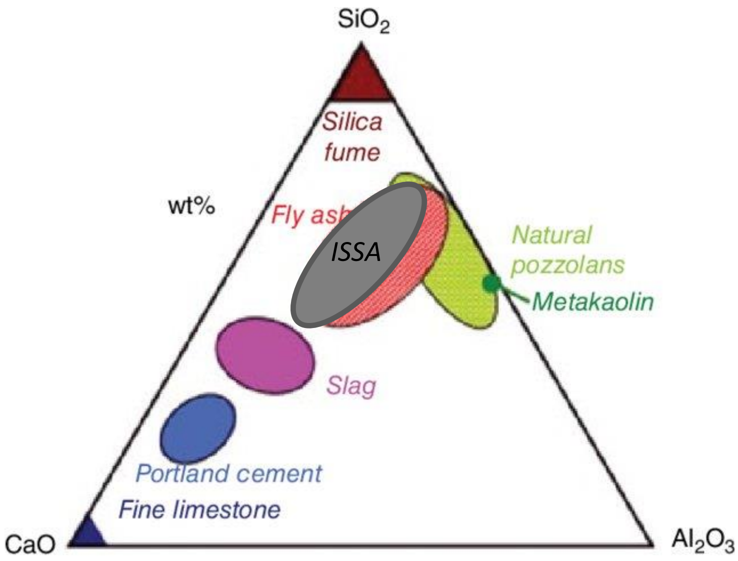

Figure 10: The ternary diagram of silica, alumina and calcium oxide content in cementitious material (Rakhimov et al., 2015) reproduced with an indication of ISSA

According to various studies, heat treatment of sewage sludge produces an irregular morphology and uneven texture of sewage sludge, changes the porosity (Johnson, 2014) and the pozzolanic activity of the sewage sludge (Tantawy *et al.*, 2012) while also removing organic materials in the sludge (Choo, 2016). According to Naamane *et al.* (2016), the aforementioned compounds increase with an increase in incineration temperature, due to the reaction with oxygen to form oxides during the incineration process. Figure 11 shows the SEM analysis from the study conducted by Naamane *et al.*, (2016).

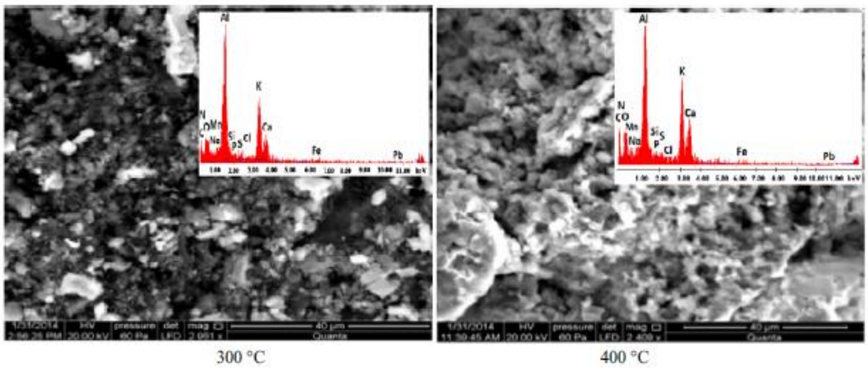

Figure 11: SEM micrographs of ISSA incinerated at 300°C - left and 400°C – right (Naamane et al., 2016)

The analysis showed a decrease in organic content (appears black) with an increase in the incineration temperature from 300ºC to 400ºC leaving behind inorganic matter which appears whitish in colour. The same trend was observed in a study conducted by Tantawy *et al.* (2012) as shown in Figure 12. However, according to Tantawy *et al.* (2012), amorphous silica captures fixed carbon at incineration temperatures below 800°C due to incomplete combustion. This leads to a reduction in pozzolanic activity of ISSA. In this study it was concluded that an incineration temperature of 800°C better preserves the amorphous nature of ISSA by removing fixed carbon captured by silica of ISSA.

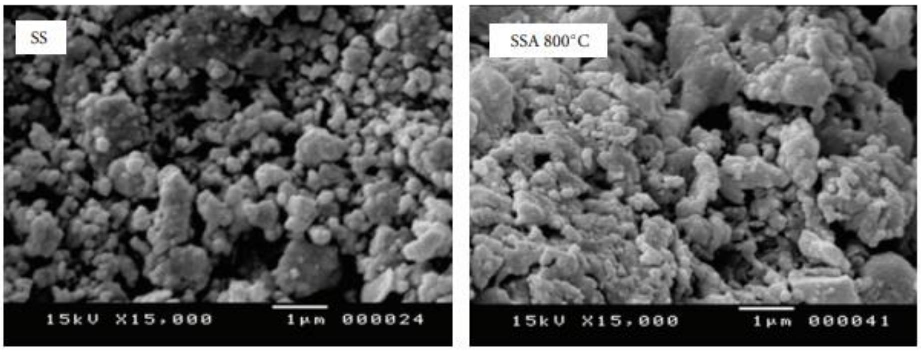

Figure 12: SEM of raw sewage sludge - left and ISSA incinerated at 800°C – right (Tantawy et al., 2012)

The micrographs of ISSA show an amorphous and irregular morphology with rare traces of rectangular or spherical grains (Kosior-Kazberuk, 2011; Horiguchi *et al.*, 2011; Naamane *et al.*, 2016; Zabielska-Adamska, 2020). However, according to Tantawy *et al.* (2012), incinerating sewage sludge at temperatures above 800°C is not recommended as it leads to the crystallization of amorphous silica (Figure 13) and reduces the adsorption capacity of the produced ISSA. To add to this, different cooling rates of ISSA were considered in this study in an attempt to suppress the possible crystallization of amorphous silica.

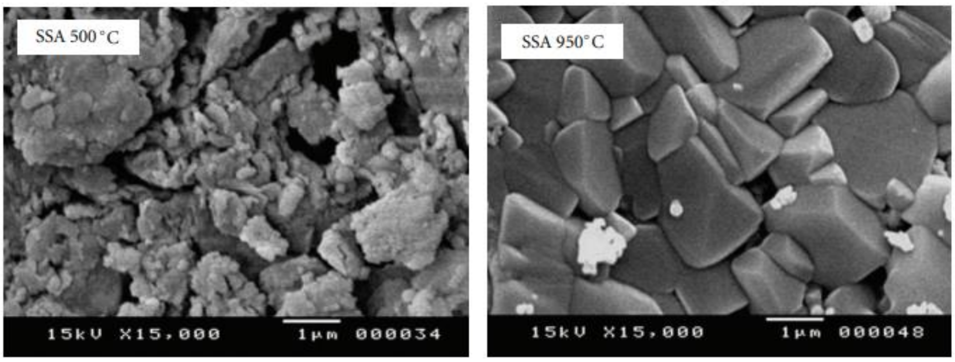

Figure 13: SEM micrographs of ISSA incinerated at 500°C - left and 950°C – right (Tantawy et al., 2012)

Figure 14 shows SEM and EDS analysis of sewage sludge ash incinerated at 850ºC. The ISSA had various compositions and was made up of irregular grains. The identified compositions are whitlockite and silico-alumina phase (A and C), calcium sulphate/gypsum (B) and Quartz (D) (Lin *et al.*, 2008).

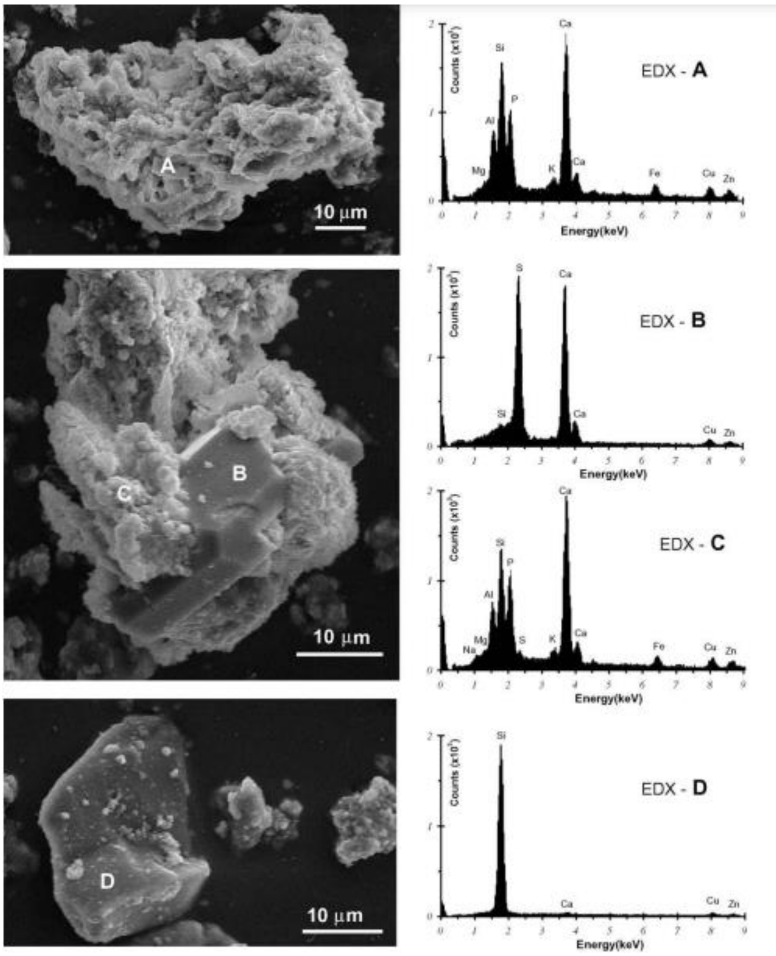

Figure 14: Sewage sludge incinerated at 850ºC (Lin et al., 2008)

2.3.4. The use of ISSA as a partial replacement of cement

The use of ISSA as an alternative pozzolanic material in the construction industry has been introduced and studied by several researchers (Chen *et al.*, 2013; Jonson *et al.,* 2014; Gomes *et al.,* 2019; Tantawy *et al.,* 2012). ISSA is characterized by a relatively high phosphate content ranging from 13.7% to 25.7% (Xu *et al.,* 2012). For this reason, it has mostly been used as an essential phosphate resource in the production of phosphoric acid and fertilizers (Xu *et al.,* 2012). However, the emerging use of ISSA as a partial replacement of cement in the manufacturing of commercial products such as concrete or bricks has been identified (Herselman *et al.,* 2009; Smol *et al.,* 2015). In this study the utilization of the ISSA as a partial replacement of cement in cement paste and mortar was investigated.

The potential utilization of ISSA as a SCM depends on its physical and chemical properties. According to Feenstra *et al.* (2003) and Tantawy *et al.* (2012), the organic material in sewage sludge tends to retard the setting of concrete mixtures whilst the toxic metals found in the sludge may disrupt hardening reactions that occur over time. Incineration of the sewage sludge to produce ISSA is often conducted to reduce the amount of organic material and toxic metals in the sewage sludge.

2.4. Effects of ISSA on the properties of cement/mortar

2.4.1. Effect of ISSA on the reactivity of Portland cement (TGA)

In a study conducted by Piasta *et al.* (2016), the reactivity of ISSA in cement mortar was investigated and compared to that of FA in terms of pozzolanic activity. The results showed that FA was more reactive than ISSA. Similar results were obtained by Pavlik *et al.* (2016) who found moderate reactivity of ISSA. Contrary to their results, Chen & Poon (2017) obtained a high reactivity of ISSA mortar compared to FA blended mortar in the early stages. From this study it was concluded that these results were attributed to the irregular shape of ISSA particles that gave rise to an interlocked structure on the unreacted particles and the slow water removal of ISSA which enabled further cement hydration (Chen & Poon, 2017).

The reactivity of ISSA was investigated using thermogravimetric analysis (TGA) and physicochemical evaluation by Dyer *et al.* (2001) and Monzo *et al.* (1997). Results from the study conducted by Monzo *et al.* (1997) showed that the calcium hydroxide consumption of ISSA blended cement paste was reduced from 29% to 16% after three days of curing. To study the hydration of ISSA blended cement paste, Dyer *et al.* (2001) used XRD and isothermal conduction calorimetry. Through these analyses, aluminates and aluminosilicates were detected along with monosulphate and other minerals. These findings implied that ISSA is a good pozzolanic material for partial use in cement. Moreover, hydration reactions studies conducted by Dyer *et al.* (2011) indicated that the amorphous phases in ISSA exhibit pozzolanic activity when used as a partial replacement of cement (CEM 1).

2.4.2. Effect of ISSA on the hydration of Portland cement

Several studies have been conducted to evaluate the effect of ISSA on the hydration of cement. According to Mejdi *et al.* (2020), mixing PC with ISSA influenced the kinetics of hydration and more notably the alite dissolution. This result was attributed to orthophosphate ions (PO_4^{3-}) released by ISSA. In a similar study conducted by Tantawy *et al.* (2013), the addition of ISSA in cement paste improved the hydration of cement due to its pozzolanic reaction with calcium hydroxide thus contributing to the formation of crosslinked fibrous calcium silicate with a low Ca/Si ratio.

Figure 15 shows less traces of well-formed crystals as a result of hydration. This was attributed to the age of the cement paste (Tantawy *et al.*, 2013). According to Stutzman, (2000), cement pastes generally tend to contain large void spaces where crystals can form at the early stages of hydration. Such crystals tend to form only in high porosity or in air voids at later stages (Stutzman, 2000). Furthermore, the use of ISSA was also found to reduce thermal damage to cement paste such as cracking and loss of mechanical strength after exposure to high temperatures by up to 20%. These results were attributed to the presence of crosslinked fibrous calcium silicate that reinforced the cement matrix (Tantawy *et al.,* 2013).

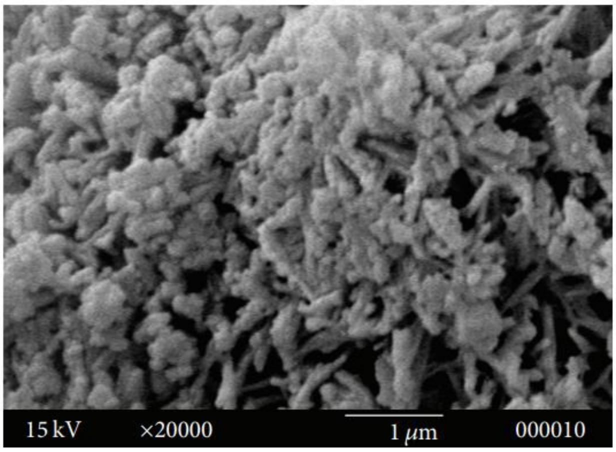

Figure 15: SEM micrographs of ISSA blended with cement and hydrated for 28 days (Tantawy et al., 2013).

Figure 16 shows the combined water contents of ISSA blended cement from the study conducted by Tantawy *et al.* (2013). The overall chemically combined water content showed reduction with the addition of sewage sludge ash in the cement paste. This result was attributed to the reduced cementitious properties in the sewage sludge. The overall results of studies on this topic show considerable differences in the effectiveness of ISSA as a SCM. The differences are largely attributed to the change in composition of ISSA which may sometimes be influenced by additives used for sludge conditioning in WWTP's (Yusuf *et al.,* 2012), different cement replacement ratios and sludge incineration temperature.

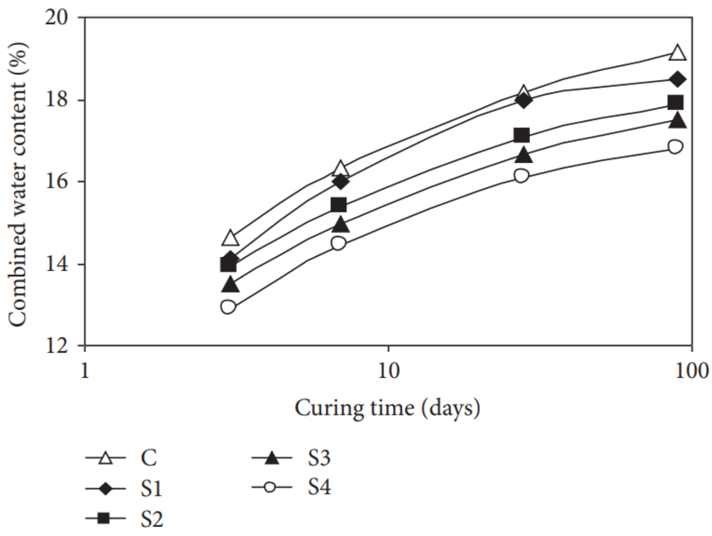

Figure 16: Combined water content of sewage sludge ash blended cement paste, C (100% OPC), S1 (5% ISSA, 95% OPC), S2 (10% ISSA, 90% OPC), S3 (15% ISSA, 85% OPC) and S4 (20% ISSA, 80% OPC) (Tantawy et al., 2013)

2.4.3. Effect of ISSA on the heat evolution of Portland cement

Cyr *et al.* (2007) conducted calorimetric studies on the heat evolution of mortars containing ISSA and found that the flow of heat commenced at 4.5 and 6.5 hours for mortar samples containing 25% and 50% ISSA respectively. Whereas the reference sample containing 0% ISSA took 3 hours. It was concluded that this result was due to the dilution effect and the presence of elements such as phosphorus and zinc in the ISSA.

2.4.4. Effect of ISSA on workability

Previous studies have shown that the partial replacement of PC by ISSA tends to influence both the strength and workability of cement (Donatello & Cheeseman, 2013; Pan *et al.*, 2003; Monzo *et al.*, 2003). The workability of cement mortar is highly dependent on the w/c ratio. According to various studies, using ISSA as a SCM in mortar was found to increase the water absorption and simultaneously resulted in longer setting time and a reduction of mortar workability (Vouk *et al.*, 2016; Naamane *et al.*, 2016). These results were attributed to the high amounts of P_2O_5 and SO_3 found in the ISSA (Vouk *et al.*, 2016; Naamane *et al.*, 2016). According to some authors, the significantly high need for water can be resolved by increasing the fineness of the ash or adding coal fly ash (Vimonsatit *et al.*, 2015).

Vouk *et al.* (2016) investigated the effect of ISSA on the workability of cement mortar. The results showed that 10% replacement of cement by ISSA caused a 19% reduction of the mortar workability giving a flow diameter of 140 mm compared to 172 mm that was obtained on the reference sample (0% ISSA). Similar results were obtained by Monzo *et al.* (1996), who used ashes of three different particle sizes (ash received from an incineration plant, ash that passed through a 40 µm sieve and 80 µm sieve) at replacement levels of 15%. The workability obtained from the use of these ashes in cement mortar samples was less than that of the reference sample especially for the ISSA with the largest particle sizes. In this study it was concluded that the reduction in workability of the cement mortar is attributed to irregular morphology and the increased water absorption of ISSA.

In another study conducted by Pan *et al.* (2003) it was concluded that the reduced workability of mortar produced from blending PC and ISSA can be improved by using finer ash particles which may in return also increase the pozzolanic activity, leading to an increased compressive strength of the mortar. Different results were obtained by Tay, (1987). The concrete samples containing ISSA (that passed through a 150 µm sieve) at replacement levels of 15% and 20% had similar workability to that of the reference sample containing 0% ISSA.

2.4.5. Effect of ISSA on the durability of Portland cement

According to various studies, the pozzolanic activity of ISSA is lower than the pozzolanic activity of most pozzolanic materials such as fly ash (Piasta *et al.*, 2016; Pavlik *et al.*, 2016; Chen & Poon, 2017). A lower pozzolanic activity is the source of strength reduction in cement mixtures containing ISSA (Manjunatha, 2017). Studies are presently underway to determine applications in which FA and ISSA can be blended for use in civil engineering applications without causing a reduction in compressive strength (Sahu & Gayathri, 2014). The use of ISSA in the presented study is mainly related to the application of mono-incinerators that allow processing of sewage sludge without adding lime or FA for improving combustion and fineness.

According to Vouk *et al.*, (2017), increasing the ISSA replacement ratio results in a reduced compressive strength of mortar, whilst increasing the fineness of ISSA particles can simultaneously increase the compressive strength. Adding ISSA within a 10% limit was found to have no effect on the mechanical characteristics of the mortar (Vouk *et al.*, 2017). In another study, an increase in the compressive strength of mortars containing ISSA was reported in comparison with reference samples (containing 0% ISSA) (Monzó *et al.*, 1997). However, Pan *et al.* (2003) found a 30% reduction in compressive strength when 10% PC was partially substituted by ISSA. The results from these studies show that the overall effect of ISSA as a replacement of cement is highly dependent on the amount of ISSA added to the mixture and its chemical composition (SiO_2, Fe_2O_3, Al_2O_3 and CaO).

Monzo *et al.* (1996) investigated the effect of ISSA on the compressive strength of cement mortar cured at 40°C, wherein 15% ISSA was used to replace PC using coarse (SSAC), medium (SSAM) and fine ISSA particles sizes. The results obtained showed an increase in compressive strength of mortars containing ISSA observed at ages of 3 - 28 days. Moreover, the compressive strength increased with the fineness of ISSA. An increase from 8.3% to 15.3% when 15% PC was replaced with ISSA was reported. A graphical representation of the results from the study is illustrated in Figure 17. In a separate study Monzo *et al.* (1997) concluded that a 15% to 30% partial substitution of PC by ISSA only led to a moderate reduction in compressive strength of mortar. This result was attributed to the curing of samples in water at 40ºC.

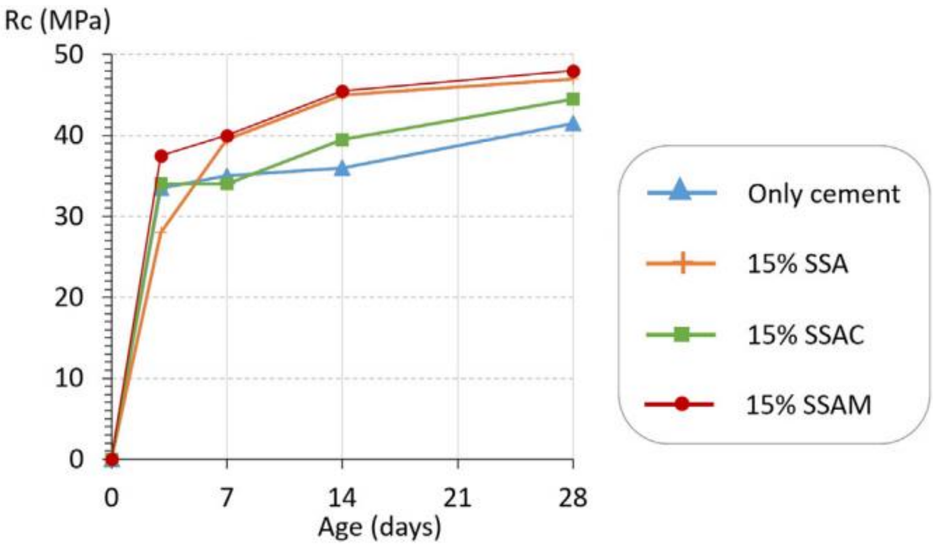

Figure 17: Compressive strength profiles of mortars at ages 3-28 days cured at 40°C (Monzo et al., 1996)

Naamane *et al.* 2016 investigated the effect of sewage sludge incineration temperatures (300°C - 800°C) on the compressive strength of mortar produced by partially replacing cement with ISSA (0 – 30% replacement levels). After 90 days of curing, incineration temperatures of 300°C – 500°C showed no improvement of the compressive strength of mortars compared to incineration temperatures of 700°C – 800°C which showed better results. From the study it was also discovered that an incineration temperature of 800°C for a period of 2.5 hours yielded the highest compressive strength of the mortar after 90 days.

Several compressive strength tests at the ages of 1, 3, 7, 14, 28 and 78 days on mortars containing 10% ISSA (M_2) compared to a controlled sample (M_1) containing cement (CEM II 42.5) were conducted by Vouk *et al.* (2017). After 1 day of hydration, a 7% reduction in compressive strength was obtained between M_1 and M_2, 3.5% after 3 and 7 days of hydration and finally 1% difference at 28 days. After 78 days of hydration, the compressive strength of M_2 was 7.4% lower than that of M_1. Similar results were obtained by Jamshidi *et al.* (2011) in which a 10% difference was obtained. In this study it was concluded that it is feasible to add ISSA in cement mortar by up to 20% without deteriorating cement mortar quality. It was also noted that ISSA reduced the early rate of strength gain as a result of slower hydration. However, at the later ages the rate of strength reduction was lower.

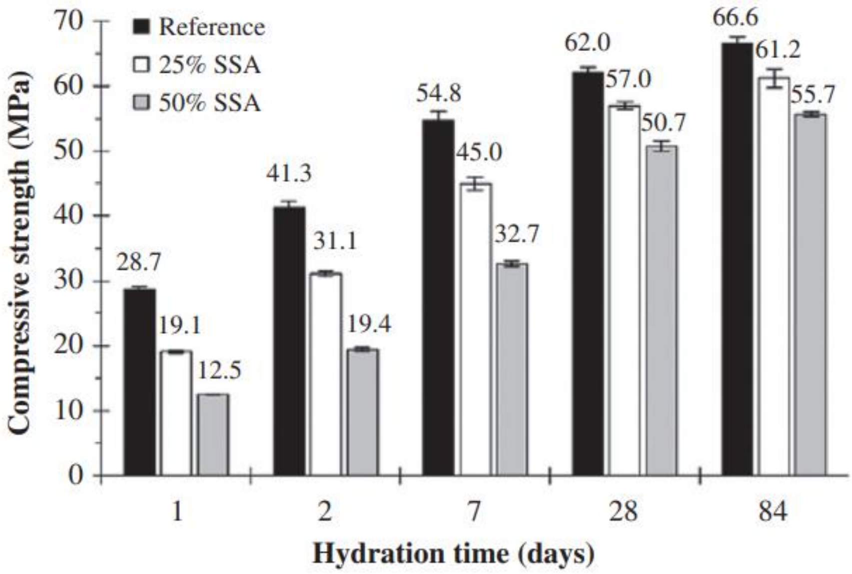

Figure 18: Compressive strength development of mortars containing 25% and 50% ISSA vs reference mortar (Cyr et al., 2007)

In a study conducted by Cyr *et al.* 2007, the effect of the curing time on the compressive strength of mortars containing ISSA at replacement levels of 25% and 50% was conducted. It was discovered that the compressive strength evolution was lower for shorter curing times, but showed improvement after 28 days of curing (Figure 18). The compressive strength of mortar containing 25% ISSA was higher than that of mortar containing 50% ISSA. Tantawy, (2012) on the other hand, also discovered that the use of ISSA in cement paste consequently reduced the build-up of pore pressure, loss of mechanical properties and crack formation.

2.5. Summary on the state of knowledge

Although many studies have been carried out on the use of ISSA as a supplementary cementitious material for cement, little attention has been given to the effect of ISSA on cement hydration and the cooling rates of ISSA post incineration on the overall performance of cement containing ISSA. The review of the state of knowledge on the topic led to the conclusion that more analysis could be done, particularly on the use of South African ISSA, to add valuable knowledge (incineration procedure/temperature, cooling rates, hydration tests, pozzolanic activity) on the use of ISSA as a partial replacement of cement.

2.6. Presented study

In the presented study, dry sewage sludge from East Rand Water (ERWAT) in Norkem Park was used. ERWAT runs a total of 19 WWTP's in South Africa. Primary and Secondary treatment of the sludge takes place following standardized procedures across all plants (Figure 6). The plant utilizes two drying methods, namely: sludge drying beds and filter belt press (FBP). The FBP method is an alternative method to the drying bed and requires less space, while offering a greater degree of operational control. In the drying bed method, digested sludge (95% water and 5% solids) is spread over an open field for drying. Whereas in the FBP method sludge conditioning using polymers takes place to improve the drainability of the sludge (Information obtained from plant visit).

Dried sewage sludge was used in this study. The sewage sludge was incinerated in a closed-lid combustion method to produce ash (material of interest). The produced sewage sludge ash was analysed for composition, morphology, pozzolanic activity, workability and compressive strength in an attempt to produce a partial replacement for Portland cement. Moreover, to add to the previous studies, the effect of cooling rates on pozzolanic reactivity of the resulting ISSA was determined. This was done to consider the effects of suppressing possible crystal formation of the silica in the ISSA to maximise the amorphous silica content, as means of improving reactivity.

References

Afrisam, 2020. The Afrisam History. [Online]. Accessed: 23 August 2020. Available at: <https://www.afrisam.co.za/about/our-history>

Aligizaki, K.K., 2005. Pore structure of cement-based materials: testing, interpretation and requirements. *CRC Press.*

Ambulkar, A., n.d. Sludge treatment and disposal. *Britannica.* Repéré à. Accessed: 16 February 2020. Available at: <https://www.britannica. com/technology/wastewater-treatment/Sludge-treatment-and-disposal.>

Anjos, M.A.S., Reis, R., Camões, A., Duarte, F. and Jesus, C., 2019. Evaluation of hydration of cement pastes containing high volume of mineral additions. *European Journal of Environmental and Civil Engineering*, *23*(8), pp.987-1002.

Anon., 2005. *Interpreting cement.* Understanding cement. Accessed: 12 February 2021. Available at: <https://www.understanding-cement.com/>

Ayub, T., Khan, S.U. and Memon, F.A., 2014. Mechanical characteristics of hardened concrete with different mineral admixtures: a review. *The Scientific World Journal*.

Ballim, Y. and Graham, P.C., 2009. Thermal properties of concrete and temperature development at early ages in large concrete elements. In: Owens, G: *Fulton's Concrete Technology*. 9th Ed, Cement and Concrete Institute, South Africa, pp. 201-236.

Barron, A.R., 2014. Chemistry of the Main Group Elements. *Rice University, Houston, USA.*

Bendapudi, S.C.K. and Saha, P., 2011. Contribution of fly ash to the properties of mortar and concrete. *International Journal of Earth Sciences and Engineering*, *4*(6), pp.1017-1023.

Bensted, J., 1983. Hydration of Portland cement. *In Advances in cement technology* (pp. 307-347). Pergamon.

Berodier, E.M.J., 2015. Impact of the supplementary cementitious materials on the kinetics and microstructural development of cement hydration. Thesis: EPFL, Lausanne. Switzerland.

Blezard, R.G., 1998. The History of Calcareous Cements. In Hewkett P.C., (Ed): *Lea's Chemistry of Cement and Concrete*, pp. 1-24.

Boualleg, S., Bencheikh, M., Belagraa, L., Daoudi, A. and Chikouche, M.A., 2017. The combined effect of the initial cure and the type of cement on the natural carbonation, the portlandite content, and nonevaporable water in blended cement. *Advances in Materials Science and Engineering*, *2017*.

Bullard, J.W., Jennings, H.M., Livingston, R.A., Nonat, A., Scherer, G.W., Schweitzer, J.S., Scrivener, K.L. and Thomas, J.J., 2011. Mechanisms of cement hydration. *Cement and Concrete Research*, *41*(12), pp.1208-1223.

Chamberlain, B., Chiesl, N., Day, J., Dowd, L., Overocker, B., Pape, D., Petrus, M., Swanson, M. and Toles, J., 1995. Concrete a material for the new stone age. Material Science and Technology Module, University of Illinois, Urbana-Champaign, USA.

Chen, M., Blanc, D., Gautier, M., Mehu, J. and Gourdon, R., 2013. Environmental and technical assessments of the potential utilization of sewage sludge ashes (SSAs) as secondary raw materials in construction. *Waste Management*, *33*(5), pp.1268-1275.

Chen, Y., He, X., Zhang, S., Tan, X. and Wan, Y., 2020. Strength and microstructure properties of solidified sewage sludge with two types of cement-based binders. *Scientific Reports*, *10*(1), pp.1-12.

Chen, Y.C. and Kuo, J., 2016. Potential of greenhouse gas emissions from sewage sludge management: a case study of Taiwan. *Journal of Cleaner Production*, *129*, pp.196-201.

Chen, Z. and Poon, C.S., 2017. Comparative studies on the effects of sewage sludge ash and fly ash on cement hydration and properties of cement mortars. *Construction and Building Materials*, *154*, pp.791-803.

Choo, L.K., 2016. Partial Replacement of Cement with Incinerated Sewage Sludge Ash (ISSA) in Mortar Brick with Natural Calcium Carbonate as Additive (Doctoral dissertation, Universiti Malaysia Pahang).

Cyr, M., Coutand, M. and Clastres, P., 2007. Technological and environmental behavior of sewage sludge ash (SSA) in cement-based materials. *Cement and Concrete Research*, *37*(8), pp.1278-1289.

David, T.K. and Nair, S.K., 2018. Compressive Strength of Concrete with Sewage Sludge Ash (SSA). In *IOP Conf. Ser. Mater. Sci. Eng* (Vol. 371, No. 1).

Dean, R.B. and Suess, M.J., 1985. The risk to health of chemicals in sewage sludge applied to land. *Waste management & research*, 3(3), pp.251-278.

Demirbas, A., Edris, G. and Alalayah, W.M., 2017. Sludge production from municipal wastewater treatment in sewage treatment plant. *Energy Sources, Part A: Recovery, Utilization, and Environmental Effects*, 39(10), pp.999-1006.

DiStefano, T.D. and Ambulkar, A., 2006. Methane production and solids destruction in an anaerobic solid waste reactor due to post-reactor caustic and heat treatment. *Water science and technology*, *53*(8), pp.33-41.

Dhir, R.K., Ghataora, G.S. and Lynn, C.J., 2017. *Sustainable Construction Materials*. Woodhead Publishing Series in Civil and Structural Engineering

Diliūnas, J., Dundulis, K., Gadeikis, S., Jurevičius, A. and Kaminskas, M., 2010. Geotechnical and hydrochemical properties of sewage sludge. *Bulletin of Engineering Geology and the Environment*, *69*(4), pp.575-582.

Donatello, S. and Cheeseman, C.R., 2013. Recycling and recovery routes for incinerated sewage sludge ash (ISSA): A review. *Waste Management*, *33*(11), pp.2328-2340.

Dyer, T.D., Halliday, J.E. and Dhir, R.K., 2001. Hydration reaction of sewage sludge ash for use as a cement component in concrete production. In *Recycling and Reuse of Sewage Sludge* (pp. 226-238). Thomas Telford Publishing.

Dyer, T.D., Halliday, J.E. and Dhir, R.K., 2011. Hydration chemistry of sewage sludge ash used as a cement component. *Journal of Materials in Civil Engineering*, *23*(5), pp.648-655.

Ekama, G.A. (ed). 1993. Sewage sludge utilization and disposal: *Information document. WRC,* Pretoria.

El-Didamony, H., Abd El-Rahman, E. and Osman, R.M., 2012. Fire resistance of fired clay bricks–fly ash composite cement pastes. *Ceramics International*, *38*(1), pp.201-209.

Escalante-Garcia, J.I., 2003. Nonevaporable water from neat OPC and replacement materials in composite cements hydrated at different temperatures. *Cement and Concrete Research*, *33*(11), pp.1883-1888.

Federal Highway Administration, 2012. User guidelines for waste and by-product materials in pavement construction.

Feenstra, L., Brouwer, J.P., Frenay, J. and Bos, S., 2003, June. Re-use of contaminated dredging sludge in a cement bound road base: Full-scale demonstration project. *In:*

Proceedings of the 5th International Conference on Science and Engineering of Recycling for Environmental Protection (Wascon 2003), p. 593.

Fontes, C.M.A., Barbosa, M.C., Toledo Filho, R.D. and Goncalves, J.P., 2004, November. Potentiality of sewage sludge ash as mineral additive in cement mortar and high-performance concrete. In *Proceedings of the International RILEM conference on the use of recycled materials in buildings and structures*, pp. 794-806.

Fu, Y.F., Wong, Y.L., Poon, C.S., Tang, C.A. and Lin, P., 2004. Experimental study of micro/macro crack development and stress–strain relations of cement-based composite materials at elevated temperatures. *Cement and Concrete Research*, 34(5), pp.789-797.

Galan, I., Andrade, C. and Castellote, M., 2012. Thermogravimetrical analysis for monitoring carbonation of cementitious materials: Uptake of CO_2 and deepening in C–S–H knowledge. *Journal of Thermal Analysis and Calorimetry*, *110*(1), pp.309-319.

Gomes, S.D.C., Zhou, J.L., Li, W. and Long, G., 2019. Progress in manufacture and properties of construction materials incorporating water treatment sludge: A review. *Resources, Conservation and Recycling*, *145*, pp.148-159.

Goni, S., Guerrero, A., Luxan, M.P. and Macías, A., 2003. Activation of the fly ash pozzolanic reaction by hydrothermal conditions. *Cement and Concrete Research*, *33*(9), pp.1399-1405.

Grobelak, A., Czerwińska, K. and Murtaś, A., 2019. General considerations on sludge disposal, industrial and municipal sludge. In *Industrial and Municipal Sludge* (pp. 135-153). Butterworth-Heinemann.

Groenewoud, W.M., 2001. CHAPTER 2-THERMOGRAVIMETRY. *Characterisation of Polymers by Thermal Analysis, Elsevier Science BV, Amsterdam*, pp.61-76.

Grieve, G., 2009. Cementitious materials. In: Owens, G. (Ed): Fulton's Concrete Technology, 9th Ed, *Cement and Concrete Institute,* South Afripp.1-16.

Halliday, J.E., Jones, M.R., Dyer, T.D. and Dhir, R.K., 2012, May. Potential use of UK sewage sludge ash in cement-based concrete. In *Proceedings of the Institution of Civil Engineers-Waste and Resource Management* (Vol. 165, No. 2, pp. 57-66). ICE Publishing.

Harison, A., Srivastava, V. and Gupta, C.B., 2013. Fly Ash as Supplementary Cementitious Material in Portland Pozzolana Cement Concrete. *International Journal of Engineering Trends and Technology (IJETT)*, *6* (3), pp.113-117.

Heikal, M., 2000. Effect of temperature on the physico-mechanical and mineralogical properties of Homra pozzolanic cement pastes. *Cement and Concrete Research*, *30*(11), pp.1835-1839.

Herselman, J.E., Wade, P.W., Steyn, C.E. and Snyman, H.G., 2005. An evaluation of dedicated land disposal practices for sewage sludge. *Water Research Commission, WRC Report*, (1209/1), p.05.

Horiguchi, T., Fujita, R. and Shimura, K., 2011. Applicability of controlled low-strength materials with incinerated sewage sludge ash and crushed-stone powder. *Journal of Materials in Civil Engineering*, *23*(6), pp.767-771.

Islam, B., 2015. Petroleum sludge, its treatment and disposal: A review. *Int. J. Chem. Sci*, *13*(4), pp.1584-1602.

Jackson, P.J., 1998. Portland cement: classification and manufacture. In: Hewlett, P.C., (Ed): *Lea's Chemistry of Cement and Concrete*, 4th Ed, Butterworth-Heinemann, pp 25-94.

Jamshidi, A., Mehrdadi, N. and Jamshidi, M., 2011. Application of sewage dry sludge as fine aggregate in concrete.

Johnson, O.A., Napiah, M. and Kamaruddin, I., 2014. Potential uses of waste sludge in construction industry: a review. *Research Journal of Applied Sciences, Engineering and Technology*, *8*(4), pp.565-570.

Khiari, B., Marias, F., Zagrouba, F. and Vaxelaire, J., 2004. Analytical study of the pyrolysis process in a wastewater treatment pilot station. *Desalination*, *167*, pp.39-47.

Khoury, G.A., 1992. Compressive strength of concrete at high temperatures: a reassessment. *Magazine of Concrete Research*, *44*(161), pp.291-309.

Kings S., 2017. *50 000 litres of sewage flow into SA's rivers every second.* Mail & Guardian. Accessed: 23 February 2020. Available at: <https://mg.co.za/article/2017-07-21-south-africas-shit-has-hit-the-fan/>

Kosior-Kazberuk, M., 2011. Application of SSA as partial replacement of aggregate in concrete. *Polish Journal of Environmental Studies*, *20*(2), pp.365-370.

Kosmatka, S.H., Kerkhoff, B. and Panarese, W.C., 2002. Fly ash, slag, silica fume, and natural pozzolans. *Design and Control of Concrete Mixtures, EB001.* , 14th Ed, Portland Cement Association, Skokie, Illinois, USA, pp 57-72.

Kruger, R.A., 2015, Coal Ash in South Africa, *World of Coal Ash (WOCA) Conference,* Nashville, Tennessee, USA

Lin, K.L., Chang, W.C., Lin, D.F., Luo, H.L. and Tsai, M.C., 2008. Effects of nano-SiO2 and different ash particle sizes on sludge ash–cement mortar. *Journal of Environmental Management*, *88*(4), pp.708-714.

Lothenbach, B., Durdzinski, P. and De Weerdt, K., 2016. Thermogravimetric analysis. *A practical guide to microstructural analysis of cementitious materials*, *1*, pp 57-72.

Lothenbach, B., Scrivener, K. and Hooton, R.D., 2011. Supplementary cementitious materials. *Cement and Concrete Research*, *41*(12), pp.1244-1256.

Manjunatha M., 2017. Use of Sewage Sludge Ash & Fly Ash in Constructions. *"International Journal of Latest Engineering Research and Applications", 8(2), pp.102-110.*

Massazza, F., 1998. Pozzolana and pozzolanic cements. In: Hewlett, P.C., (Ed): *Lea's Chemistry of Cement and Concrete,* 4th Ed, Butterworth-Heinemann, pp.471-631.

Mata-Alvarez, J., 2003. Fundamentals of the Anaerobic Digestion Process. In: Mata-Alvarez, J. (Ed): *Biomethanization of the Organic Fraction of Municipal Solid Wastes,* IWA Publishing, Amsterdam, pp.1-20.

Mejdi, M., Saillio, M., Chaussadent, T., Divet, L. and Tagnit-Hamou, A., 2020. Hydration mechanisms of sewage sludge ashes used as cement replacement. *Cement and Concrete Research*, 135, p.106115.

Mendoza, O. and Tobón, J.I., 2013. An alternative thermal method for identification of pozzolanic activity in Ca(OH)2/pozzolan pastes. *Journal of Thermal Analysis and Calorimetry*, *114*(2), pp.589-596.

Menéndez, E., Vega, L. and Andrade, C., 2012. Use of decomposition of portlandite in concrete fire as indicator of temperature progression into the material: Application to fire-affected builds. *Journal of Thermal Analysis and Calorimetry*, *110*(1), pp.203-209.

Merino, I., Arévalo, L.F. and Romero, F., 2007. Preparation and characterization of ceramic products by thermal treatment of sewage sludge ashes mixed with different additives. *Waste Management*, *27*(12), pp.1829-1844.

Monzó, J., Paya, J., Borrachero, M.V. and Córcoles, A., 1996. Use of sewage sludge ash (SSA)-cement admixtures in mortars. *Cement and Concrete Research*, *26*(9), pp.1389-1398.

Monzo, J., Paya, J., Borrachero, M.V., Bellver, A. and Peris-Mora, E., 1997. Study of cement-based mortars containing Spanish ground sewage sludge ash. In *Studies in Environmental Science* (Vol. 71, pp. 349-354). Elsevier.

Monzó, J., Payá, J., Borrachero, M.V. and Girbés, I., 2003. Reuse of sewage sludge ashes (SSA) in cement mixtures: the effect of SSA on the workability of cement mortars. *Waste Management*, *23*(4), pp.373-381.

Morsy, M.M., Shebl, S.S. and Rashad, A.M., 2008. Effect of fire on microstructure and mechanical properties of blended cement pastes containing metakaolin and silica fume.

Naamane, S., Rais, Z. and Taleb, M., 2016. The effectiveness of the incineration of sewage sludge on the evolution of physicochemical and mechanical properties of Portland cement. *Construction and Building Materials, 112*, pp.783-789.

Odler, I., 1998. Hydration, Setting and Hardening of Portland cement. In: Hewkett, P.C., (Ed):

Lea's Chemistry of Cement and Concrete, 4th Ed, Butterworth-Heinemann, pp 241-298.

Pan, S.C., Tseng, D.H., Lee, C.C. and Lee, C., 2003. Influence of the fineness of sewage sludge ash on the mortar properties. *Cement and Concrete Research*, *33*(11), pp.1749-1754.

Park, Y.J., Moon, S.O. and Heo, J., 2003. Crystalline phase control of glass ceramics obtained from sewage sludge fly ash. *Ceramics International*, *29*(2), pp.223-227.

Patil, J.V., 2017. Partial replacement of cement by fly ash in concrete mix design. *International Research Journal of Engineering and Technology (IRJET)*, *4*(11), pp.1148-1150.

Pavlík, Z., Záleská, M. and Pavlikova M., 2016. Thermally treated sewage sludge as a potential pozzolanic additive in cement-based composites. *International Multidisciplinary Scientific GeoConference: SGEM*, *2*, pp.373-380.

Payá, J., Monzó, J., Borrachero, M.V. and Soriano, L., 2019. Sewage sludge ash. In *New Trends in Eco-efficient and Recycled Concrete* (pp. 121-152). Woodhead Publishing.

PCA, Portland Cement Association., 2019. *How Cement is made.* [Online]. Accessed: 23 August 2020. Available at: <https://www.cement.org/cement-concrete-applications/howcementismade#:~:text=The%20most%20common%20way%20to,%2C%20clay%2C%20and%20other%20materials.&text=The%20crushed%20rock%20is%20combined,fed%20to%20a%20cement%20kiln.>

PCA, Portland Cement Association., 2001. Ettringite formation and the performance of concrete (No. 2166). Portland Cement Association.

Petzold, A. and Roehrs, M., 1970. Concrete for High Temperatures (Maclaren and Sons). *London.*

Piasta, W. and Lukawska, M., 2016. The effect of sewage sludge ash on properties of cement composites. *Procedia engineering*, *161*, pp.1018-1024.

PPC Pretoria Portland Cement, 2018. *Pretoria Portland Cement Integrated report*. [Online]. Accessed: 23 August 2020. Available at: <https://thevault.exchange/?get_group_doc=189/1532953157-PPCIR2018OnlineReportLORES.pdf>

Pavlík, Z., Fořt, J., Záleská, M., Pavlíková, M., Trník, A., Medved, I., Keppert, M., Koutsoukos, P.G. and Černý, R., 2016. Energy-efficient thermal treatment of sewage sludge for its application in blended cements. *Journal of Cleaner Production*, *112*, pp.409-419.

Paya, J., Borrachero, M.V., Monzo, J., Peris-Mora, E. and Amahjour, F., 2001. Enhanced conductivity measurement techniques for evaluation of fly ash pozzolanic activity. *Cement and Concrete Research*, *31*(1), pp.41-49.

Rakhimov, R.Z., Rakhimova, N.R. and Ojovan, M.I., 2015. Alternative Binders. In *Cementitious Materials for Nuclear Waste Immobilization*, 4, pp. 93

Rasmeni, Z.Z. and Madyira, D.M., 2019. A Review of the Current Municipal Solid Waste Management Practices in Johannesburg City Townships. *Procedia Manufacturing*, *35*, pp.1025-1031.

Roussel, N., Ovarlez, G., Garrault, S. and Brumaud, C., 2012. The origins of thixotropy of fresh cement pastes. *Cement and Concrete Research*, *42*(1), pp.148-157.

Roy, D.M., 1989. Fly ash and silica fume chemistry and hydration. *Special Publication*, *114*, pp.117-138.

Sahu, V. and Gayathri, V., 2014. The use of fly ash and lime sludge as partial replacement of cement in mortar. *International Journal of Engineering and Technology Innovation, 4*(1), p.30.

Screed Scientist, 2014. *Portland Cement: A Brief History. [*Online]. Accessed: 23 August 2020. Available at: <https://www.screedscientist.com/portland-cement-a-brief-history/>

Scrivener, K.L., Juilland, P. and Monteiro, P.J., 2015. Advances in understanding hydration of Portland cement. *Cement and Concrete Research*, *78*, pp.38-56.

Shi, H.S. and Kan, L.L., 2009. Leaching behavior of heavy metals from municipal solid wastes incineration (MSWI) fly ash used in concrete. *Journal of hazardous materials*, *164*(2-3), pp.750-754.

Silva, F.G.S., Fiuza, R., da Silva, J.S., de Brito, C.M.S., Andrade, H.M.C. and Gonçalves, J.P., 2014. Consumption of calcium hydroxide and formation of C–S–H in cement pastes. *Journal of Thermal Analysis and Calorimetry*, *116*(1), pp.287-293.

Sims, I. and Brown, B., 1998. Concrete aggregates. In *Lea's Chemistry of Cement and Concrete* (pp. 907-1015). Butterworth-Heinemann.

Siddique, R. and Cachim, P., 2018. *Waste and Supplementary Cementitious Materials in Concrete: Characterisation, Properties and Applications*. Woodhead Publishing.

Simpkins, D., 2005. Anaerobic Digester FAQs. *Michigan: Michigan Biomass Energy Program*.

Smol, M., Kulczycka, J., Henclik, A., Gorazda, K. and Wzorek, Z., 2015. Towards zero Waste in sewage sludge incineration. *In Proceedings Sardinia 2015, Fifteenth International Waste Management and Landfill Symposium, S. Margherita di Pula, Cagliari, Italy; 5–9 October 2015.* CISA Publisher Italy

Snyman, H.G., 2007. Management of wastewater and faecal sludge in Southern Africa. *Water Practice and Technology,* 2(4).

Stutzman, P.E., 2000, November. Scanning electron microscopy in concrete petrography. In *Materials Science of Concrete*.

Tammemagi, H.Y., 1999. The waste crisis: landfills, incinerators, and the search for a sustainable future. *Oxford university press*.

Tan, X., Chen, Y., Xue, Q., Wan, Y. and Liu, L., 2020. Conditioning of resuspension excess sludge with chemical oxidation technology: The respective performance of filtration and expression stage in compression dewatering. *Separation and Purification Technology*, *237*, p.116317.

Tantawy, M.A., El-Roudi, A.M., Abdalla, E.M. and Abdelzaher, M.A., 2012. Evaluation of the pozzolanic activity of sewage sludge ash. *ISRN Chemical Engineering*, 2012.

Tantawy, M.A., El-Roudi, A.M., Abdalla, E.M. and Abdelzaher, M.A., 2013. Fire resistance of sewage sludge ash blended cement pastes. *Journal of Engineering*, *2013*.

Tay, J.H., 1987. Sludge ash as filler for Portland cement concrete. *Journal of Environmental Engineering*, *113*(2), pp.345-351.

Tenza-Abril, A.J., Saval, J.M. and Cuenca, A., 2015. Using sewage-sludge ash as filler in bituminous mixes. *Journal of Materials in Civil Engineering*, 27(4), p.04014141.

Thomas, M.D.A., 2007. Optimizing the use of fly ash in concrete (Vol. 5420). Skokie, IL: *Portland Cement Association.*

Thomas Nutrient Solutions., 2014. *What are the Advantages and Disadvantages of Sewage Sludge Incineration*. Accessed: 27 March 2020. Available at: <https://www.thomasnutrientsolutions.com/sewage-sludge-incineration/ >

Thusi, L., 2016. *Joburg Water takes waste water treatment seriously.* Southern Courier. Accessed: 26 January 2021. Available at: <https://southerncourier.co.za/92033/joburg-water-takes-waste-water-treatment-seriously/>

Van Berg, J.D., 1993. Effects of sewage sludge disposal. *Land Degradation & Development*, *4*(4), pp.407-413.

Vimonsatit, V., Chindaprasirt, P., Ruangsiriyakul, S. and Sata, V., 2015. Influence of fly ash fineness on water requirement and shrinkage of blended cement mortars. *Engineering and Applied Science Research*, *42*(4), pp.311-316.

Vouk, D., Serdar, M., Nakić, D. and Anić-Vučinić, A., 2016. Use of sludge generated at WWTP in the production of cement mortar and concrete. *Građevinar,* 68(03.), pp.199- 210.

Vouk, D., Serdar, M. and Vučinić, A.A., 2017. Use of Incinerated Sewage Sludge Ash in Cement Mortars: Case study in Croatia. *Tehnicki vjesnik/Technical Gazette*, *24*(1).

Vu, D.D., Stroeven, P. and Bui, V.B., 2001. Strength and durability aspects of calcined kaolin-blended Portland cement mortar and concrete. *Cement and Concrete Composites*, *23*(6), pp.471-478.

Wang, K.S., Chiou, J., Chen, C.H. and Wang, D., 2005. Lightweight properties and pore structure of foamed material made from sewage sludge ash. *Construction and Building Materials*, *19*(8), pp.627-633.

Wang, H.Y., 2008. The effects of elevated temperature on cement paste containing GGBFS. *Cement and Concrete Composites*, *30*(10), pp.992-999.

Werther, J. and Ogada, T., 1999. Sewage sludge combustion. *Progress in energy and combustion science*, *25*(1), pp.55-116.

Worldometer., 2018. *South Africa Population*. Accessed: 12 February 2020. Available at: <https://www.worldometers.info/world-population/south-africa-population/>

Xu, Y., Wong, Y.L., Poon, C.S. and Anson, M., 2003. Influence of PFA on cracking of concrete and cement paste after exposure to high temperatures. *Cement and Concrete Research*, *33*(12), pp.2009-2016.

Yang, J., Zhang, S., Shi, Y., Li, C., Yu, W., Guan, R., Xiao, J., Liang, S., Hu, J., Hou, H. and Hu, J., 2017. Direct reuse of two deep-dewatered sludge cakes without a solidifying agent as landfill cover: geotechnical properties and heavy metal leaching characteristics. *RSC advances*, *7*(7), pp.3823-3830.

Ylmén, E.R., 2013. Early Hydration of Portland Cement. Thesis: Chalmers University of Technology, Gothenburg, Sweden.

Yusuf, R.O., Noor, Z.Z., Din, M.F.M. and Abba, A.H., 2012. Use of sewage sludge ash (SSA) in the production of cement and concrete–a review. *International Journal of Global Environmental Issues*, *12*(2-4), pp.214-228.

Zabielska-Adamska, K., 2020. Sewage sludge bottom ash characteristics and potential application in road embankment. *Sustainability*, *12*(1), p.39

CHAPTER 3

METHODOLOGY

This chapter details the methods carried out for the research work. These entail experimental variables, material preparation, incineration, characterization, cement paste mixture design, sample analysis, mortar preparation and testing.

3.1. Cementitious Materials

Cement pastes and mortar samples were produced using the following materials:

3.1.1. Portland cement

PC classified as CEM I, 52.5 N type was used to prepare cement pastes and mortar samples. The PC used was assumed to have a similar composition to the PC used by Ballim & Graham, 2009, as it was collected from the same source (see Table 4 below).

Table 4: Typical chemical composition of PC (Ballim & Graham, 2009)

Oxide	**% by mass**
SiO_2	22.9
Al_2O_3	4.6
CaO	64.0
Fe_2O_3	2.58
MgO	1.6
TiO_2	0.46
Mn_2O_3	0.12
Na_2O	0.12
K_2O	0.30
P_2O_5	0.06
SO_3	2.05
LOI	2.41
Total	100

3.1.2. Coal Fly ash (FA)

Coal fly ash from Eskom was used in this study. FA was used as a reference pozzolanic SCM to compare the performance of the ISSA. The FA used was assumed to have a similar composition to the FA used by Ballim & Graham, 2009, as it was collected from the same source (see Table 5 below).

Table 5: Typical chemical composition of South African coal fly ash (Ballim & Graham, 2009)

Oxide	**% by mass**
SiO_2	55.1
Al_2O_3	33.3
CaO	4.2
Fe_2O_3	3.15
MgO	1.2
Na_2O	0.0
P_2O_5	0.39
K_2O	0.69
TiO_2	1.67
Mn_2O_3	0.02
SO_3	0.12
LOI	0.45
Total	100.2

3.1.3. Dried Sewage sludge

Dried sewage sludge collected from East Rand Water (ERWAT) in Norkem Park was used in this study. To avoid inconsistent composition, all the sewage sludge was obtained from the same plant. The sewage sludge (Figure 19) was collected after being dried by the sun following treatment in the WWTP and it contained 95% solid material and 5% water.

Figure 19: Dried Sewage sludge (DSS)

The chemical composition of the dried sewage sludge (DSS) is given in Table 6 below. The sewage sludge was stored in two sealable 100 L containers to prevent contamination.

Table 6: Chemical composition of dried sewage sludge (DSS)

Oxide	% by mass
SiO_2	21.42
Al_2O_3	5.89
CaO	3.88
Fe_2O_3	4.79
MgO	1.12
TiO_2	0.44
Mn_2O_3	0.13
Na_2O	0.22
K_2O	0.51
P_2O_5	3.95
LOI	56.64
Total	98.99

3.2. Sewage sludge ash production

The sewage sludge was oven dried for 24 hours at 100ºC (Ing *et al.*, 2016) prior to incineration for better handling and removal of any excess moisture.

3.2.1. Sewage sludge incineration

Dried sewage sludge was incinerated from room temperature to produce ISSA under the three different temperature regimes shown in Table 7. A closed lid furnace was used to prevent loss of any ash. The incineration period was set at 4 hours and the heating and cooling rates measured. The heating rate was measured by recording the increase in temperature of the furnace. Three different cooling rates were assessed (see below).

3.2.1.1. Furnace cooling

Furnace cooling of the sewage sludge ash was conducted by keeping the ISSA in the furnace after incineration. The cooling rate was then measured by recording the cooling temperature of the furnace to room temperature. Once cooled to room temperature, the ISSA was removed and stored in a bag to prevent contamination.

3.2.1.2. Air cooling

Air cooling was performed by removing the ISSA from the furnace immediately after the incineration period and cooled at room temperature prior to storage. The cooling rate of the ISSA was measured and recorded using a digital thermometer. The heating and cooling profiles are given in Chapter 4.

3.2.1.3. Quenching

Quenching in water was conducted to cool the ash from the respective temperatures (see Table 7). The ISSA was removed from the furnace and immediately poured into a bucket of water for cooling. The cooling rate was not measured as it was too rapid. However, the mass of water required to cool each sample was calculated using Equation 4 (heat transfer).

$$Q = mc\Delta T \qquad (4)$$

<u>Where:</u>

Q = heat transferred

m = mass

c = specific heat

ΔT = temperature difference

Specific heat of ISSA = $0.9\ J/g$

Specific heat of water = $4.186\ J/g$

Assuming absolute values: $|Q_{Ash}| = |Q_{water}|$

Temperature of water = 20ºC

Final temperature of ISSA (y) = 25ºC

Using the mass of the produced ISSA shown in Table 12 (Chapter 4), the mass of water required to cool the ISSA from temperatures 700ºC, 800ºC and 900ºC was calculated as follows:

Mass of water required to cool ISSA incinerated at 700ºC (mass = 374 g) to 25ºC:

$$|m \times c \times \Delta T|_{water} = |m \times c \times \Delta T|_{ISSA}$$

$$|m \times 4.186 \times (y - 20)|_{water} = |374 \times 0.9 \times (700 - y)|_{ISSA}$$

$$|m \times 4.186 \times (25 - 20)|_{water} = |374 \times 0.9 \times (700 - 25)|_{ISSA}$$

$$m = 10855.47\ g$$

$$m = 10.86\ kg$$

The same calculation was carried out to determine the mass of water required to cool ISSA from 800ºC (11.66 kg) and from 900ºC (12.45 kg). An increase in the mass of water was observed with an increase in the incineration temperature.

Table 7: Sample runs

Incineration Temp (ºC)	**Furnace cooling (F_{ISSA})**	**Air cooling (A_{ISSA})**	**Quenching in water (Q_{ISSA})**
700 ºC (7)	$7F_{ISSA}$	$7A_{ISSA}$	$7Q_{ISSA}$
800 ºC (8)	$8F_{ISSA}$	$8A_{ISSA}$	$8Q_{ISSA}$
900 ºC (9)	$9F_{ISSA}$	$9A_{ISSA}$	$9Q_{ISSA}$

3.2.2. Incinerated sewage sludge ash

The incinerated sewage sludge ash shown in Figure 20 (a) was ground using a pulverizer (0068I Fact east model) for a duration of 20 minutes to produce the fine ISSA shown in Figure 20 (b).

(a) (b)

Figure 20: Incinerated sewage sludge ash (a) and pulverized incinerated sewage sludge ash (b)

3.2.3. Particle size analysis of ISSA

Particle size analysis was carried out using a Malvern Mastersizer (MS2000) to determine the particle size distribution of PC, FA and ISSA. The Mastersizer accomplished this by using the laser diffraction technique that measures the intensity of the scattered light as a laser beam passed through a dispersed particulate sample (Particle Technology Labs, n.d). Particle size distribution was an important analysis to conduct as it affects the rate and extent of hydration, as well as the workability of cement paste and mortar.

3.3. Dried sewage sludge /Incinerated sewage sludge ash characterization

Dried sewage sludge and incinerated sewage sludge ash were characterized using atomic absorption spectroscopy (AAS), x-ray fluorescence (XRF) and scanning electron microscopy (SEM) equipped with energy dispersive spectroscopy (EDS).

3.3.1. Digestion and Atomic Absorption Spectroscopy (AAS) Analysis of DSS/SSA

A 200 Series (Agilent Technologies) AAS was used to analyse the elemental composition/concentration of DSS and ISSA's to determine the effect of the incineration, incineration temperature and cooling rates. AAS is often used to determine the concentration of over 62 different metal elements in material (Hoffman *et al.*, 2010). The compositions of the DSS/ISSA's were an important aspect in an attempt to measure the concentrations of valuable elements for use as a SCM. A microwave digester was used to convert pulverized DSS/ISSA into a measurable and soluble form prior to the analysis. To achieve this, 1 g of ground samples of DSS/ISSA's were suspended in a solution of 3 mL HCl and 10 mL HNO_3 standard solutions for extraction. The samples were then digested for 20 minutes and filtered as shown in Figure 21 (standard operating procedure of the Multiwave GO, Anton Paar microwave digestion system).

Figure 21: DSS/ISSA filtration

As a result of the high concentrations of nitric acid (HNO_3) and hydrochloric acid (HCl), 2 mL of the digested mixture was diluted with water to produce a standard solution of 25 mL to achieve a suitable concentration level and reliable results as shown in Figure 22. The digested samples were then analysed using the AAS. Acetylene was used to fuel the AAS and air as the oxidiser to detect each element through hollow cathode lenses.

Figure 22: Diluted standard solutions (25 mL) of SS/ISSA prior to AAS analysis

3.3.2. Characterization of ISSA (SEM and XRF)

Microscopic analysis was performed using a Jeol JSM 6400 Scanning Electron Microscope (SEM). The analysis was used to obtain information on the surface morphology of the ISSA's in powder form along with EDS analysis to identify the composition of some of the particles that were observed in the ISSA's. The ISSA's were also characterized for chemical composition using XRF analysis. XRF is a non-destructive method used to obtain the elemental composition of material. (XRF Technology, *n.d*). XRF is widely used in modern cement production companies to test the quality and consistency of the cement.

3.3.3. Determination of the relative density of ISSA

The pycnometer method was used to measure the relative density of the ISSA (ASTM D 854-00). This method is commonly used to measure the relative density of soil solids. The weight of a dry clean empty pycnometer was determined and recorded as W_p. The pycnometer was then filled with dry ISSA and the total weight measured and recorded as W_{ps}. The pycnometer was then filled with distilled water, left to soak for 10 minutes and its total weight measured as W_B (see Figure 23, a). The pycnometer was then emptied and cleaned. The emptied pycnometer was then filled with water only (Figure 23, b) and its weight measured as W_A. The weights recorded were then used to calculate the relative density of the ISSA using the equation below.

$$\rho_{rd} = \frac{W_0}{W_0 + (W_A - W_B)} \quad \text{.....................(relative density)} \qquad (5)$$

Where: W_0 = weight of dry ISSA = $W_{ps} - W_p$

W_A = weight of pycnometer filled with water only

W_B = weight of pycnometer filled with ISSA and water

(a) (b)

Figure 23:Pycnometer filled with ISSA and water (a) and pycnometer filled with water only (b)

3.4. Preparation of cement paste mix

A total of 33 cement paste samples were prepared to study the hydration and reactivity of cement paste containing 30% ISSA as PC replacement compared to a 100% PC paste sample (primary reference mix) and cement paste containing 30% fly ash (secondary reference mix containing a common pozzolanic material). The sewage sludge ashes incinerated and cooled at the rates described in Table 7 were used to prepare cement paste samples at a replacement level of 30%. The proportions of each mix are shown in Table 8 below.

Table 8: Compositions of cement pastes

Mixture	PC %	FA %	ISSA %	W/B
C100	100	0	0	0.45
FA30	70	30	0	0.45
ISSA30	70	0	30	0.45

3.4.1. Casting and curing of specimens

Cement paste samples were manually mixed on a steel bowl at a constant water/binder ratio of 0.45 and cast on wooden moulds of 100 mm length, 17 mm width and 10.5 mm depth. Non-stick foil was used to cover the inside of the containers to prevent sticking, loss of any cement paste or difficulty in removing. The samples were cured at room temperature for analysis after 6 hours, 7 days and 28 days of hydration. Fractured surfaces of each of the specimens were analyzed using SEM and crushed using a pestle and mortar to fine powder for TGA analysis.

3.4.2. Hydration arrest of specimens

Hydration arrest is carried out to maintain the age of samples for analysis and for preserving the microstructure of fresh cement paste samples. There are different cement hydration arrest methods such as direct drying, microwave drying, solvent, oven, vacuum drying etc. For the purpose of this study the microwave drying method investigated by Luz & Pandolfelli, (2011) was used. After each curing age (6 hours, 7 days and 28 days) the samples were dried in a microwave operating at low power mode until the samples reached a constant mass (this occurred at approximately 20 minutes). The samples were thereafter kept in a vacuum desiccator to prevent absorption of moisture and to preserve the dryness.

3.5. Reactivity and hydration studies

3.5.1. SEM analysis to assess cement paste hydration

SEM was used to analyze the hydration progress of cement paste samples containing 30% ISSA incinerated at 800ºC compared to the primary reference mix (100% PC) and secondary reference mix (30% FA and 70% PC). The analysis was performed on fresh fractured surfaces after 6 hours and 7 days of hydration. All samples were mounted on aluminium microscope stubs using carbon tape as shown in Figure 24 (a). The samples were then coated (immediately before observation to prevent contamination and moisture absorption) with both carbon and palladium gold to enhance clear imaging of samples as shown in Figure 24 (b). The initial use of carbon only resulted in poor coating and poor imaging. More focus was given to the progress of the hydration at early ages (6 hours and 7 days), where a clear indication of the growth of hydrates on the surface of grains is often observed (Scrivener *et al.*, 2018). The micrographs were used to study the hydration process of each cement paste sample to determine the effect of ISSA on the hydration of cement paste.

(a)

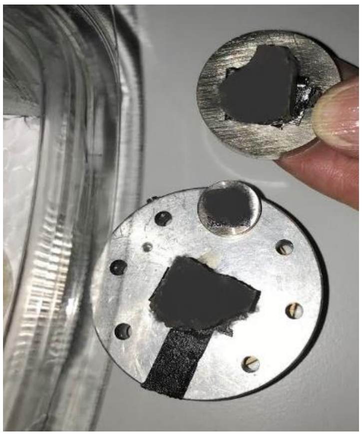

(b)

Figure 24: Fractured cement paste samples mounted on stubs (a); coated cement paste samples prior to SEM analysis(b)

3.5.2. Pozzolanic activity of cement paste samples using TGA technique:

TGA/DSC analysis provides insight into the chemical reaction mechanisms of cementitious materials during heating (Trník *et al.*, 2015). The primary products of the cement hydration process are calculated by using mass loss data from TGA/DSC curves. The decomposition of $Ca(OH)_2$ to produce $CaO + H_2O$ is denoted by the weight loss between the temperature range of 425ºC and 550°C.

In this study a TA Q600 Simultaneous TGA/DSC consisting of a vertical tubular oven with alumina crucibles that hold 10 mg of sample and can be heated to a maximum temperature of

1200ºC was used. Cement pastes were analyzed after 6 hours, 7 days, and 28 days of hydration to prevent an overlap of free water evaporation with the loss of chemically bound water. The pastes were ground using a pestle and mortar until they passed through a 75 µm sieve. The TGA was operated under the parameters shown in Table 9 to provide an appropriate environment for the test (ASTM, 2003; Jamshidi *et al.*, 2012; Asim & Sutan, 2015).

Table 9: TGA Parameters

Parameter	**Value**
Crucible material	Alumina
Sample particle size	200 microns
Sample weight	10 mg
N_2 gas flow rate	100 mL/min
Max temperature	1000ºC
Heating rate	20ºC/min
Total test time	49 min

The analysis was conducted to determine the reactivity of cement paste samples by measuring the mass loss at elevated temperatures and the derivative (dm/dT) using differential scanning calorimetry (DSC). Figure 25 shows a typical TGA/DTG (Derivative thermogravimetry) analysis of Portland cement paste after 7 days of hydration. The first peak of the derivative trend shows the removal of free and absorbed water. The second peak shows calcium hydroxide dehydroxylation (Equation 6) and the third and fourth peaks illustrate the decarbonation of calcium carbonate that takes place according to the reaction shown in Equation 7 below (Anjos *et al.*, 2019).

$$Ca(OH)_2 = CaO + H_2O \qquad (6)$$

$$CaCO_3 = CaO + CO_2 \qquad (7)$$

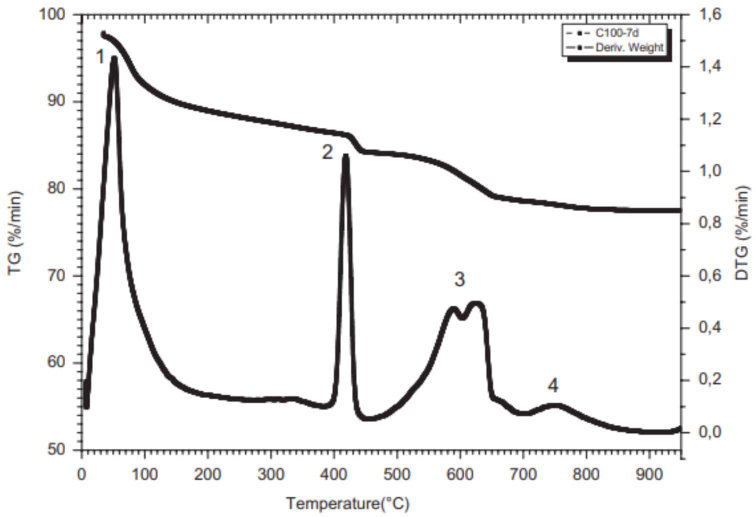

Figure 25: Typical TGA/DTG analysis of PC after 7 days of hydration (Anjos et al., 2019)

The reactivity of cement is often measured using $Ca(OH)_2$ content that can be obtained through TGA analysis at 400°C – 450°C (second peak in Figure 25). A method introduced by Baert *et al.* (2008) was used to determine the reactivity of ISSA blended cement pastes using the mass losses obtained from the TGA curves. Equation 8 was used to calculate the calcium hydroxide after the analysis, based on the mass loss related to its decomposition. Equation 9 was used additionally to determine the calcium carbonate ($CaCO_3$) content formed. This content was based on the mass loss related to its decomposition which was then used to determine the $Ca(OH)_2$ that converted to $CaCO_3$, from absorption of CO_2 according to the equation: $Ca(OH)_2 + CO_2 = CaCO_3 + H_2O$. Equation 10 was used to determine chemically combined water as a measure of the overall hydration (Baert *et al.,* 2008; Anjos *et al.,* 2019).

$$CH[\%] = ML_{Ca(OH)_2}[\%].\frac{MM_{Ca(OH)_2}}{MM_{H_2O}} \quad (8)$$

$$CaCO_3[\%] = ML_{CaCO_3}[\%].\frac{MM_{CaCO_3}}{MM_{CO_2}} \quad (9)$$

$$H_2O_{Q.comb} = Mass(loss\%)_{1000ºC} - Mass(loss\%)_{100ºC} \quad (10)$$

Where:

$CH[\%]$ = Calcium hydroxide content produced during the hydration of the binder.

$ML_{Ca(OH)_2}$= Mass loss of calcium hydroxide from the TGA curve

$MM_{Ca(OH)_2}$= Molecular weight of calcium hydroxide

MM_{H_2O} = Molecular weight of water

$CaCO_3[\%]$ = Calcium carbonate formed based on the mass loss related to its decomposition.

ML_{CaCO_3}= Mass loss of calcium carbonate from the TGA curve

MM_{CaCO_3}= Molecular weight of calcium carbonate

MM_{CO_2} = Molecular weight of carbon dioxide

$H_2O_{Q.comb}$ = Chemically combined water

$Mass(loss\%)_{1000ºC}$ = Mass loss from 0ºC to 1000ºC (total)

$Mass(loss\%)_{100ºC}$ = Mass loss of free water from 30ºC to 100ºC

3.6. Compressive strength tests

Cement mortars were prepared to study the effect of ISSA on the compressive strength of mortar at a PC replacement level of 30%. To compare the effectiveness of ISSA, reference mixes containing 100% PC and one containing 30% FA/70% PC were prepared. These samples were used to the compare the workability and compressive strength of the mortar mixtures containing ISSA.

3.6.1. Number of specimens

A total of 11 mortar mixes were prepared (reference mix 100% PC, 30% FA / 70% PC and 30% ISSA / 70% PC) using all the ISSA's described in Table 7. For each given mix, nine cubes measuring 50 × 50 × 50 mm each were prepared. Three cubes of each mix were used to test compressive strength after 3, 7 and 28 days of hydration. The average failure load (kN) obtained from the tests of each three set of cubes at the respective ages was used to calculate the compressive strength result (MPa) (see Section 3.6.6).

3.6.2. Mortar mix design

A mortar mix design was established by using a standard mix of 1 m^3 as a basis to calculate the mass of each constituent in the volume of the cubes used.

Assumption: (1 m^3 requires 250 kg water)

Table 10: Standard mortar mix design for 1 m^3 volume cube

1 m^3 basis		**Mix 1 (100% PC)**		**Mix 2 (70%/30% PC/FA)**		**Mix 3 (70%/30% PC/ISSA)**	
Material	Density(kg/m^3)	Mass (kg)	Volume (m^3)	Mass (kg)	Volume (m^3)	Mass (kg)	Volume (m^3)
Water	1000	250	0,250	250	0,250	250	0,250
PC	3150	500	0,159	350	0,111	350	0,111
Fly ash	2300	-	-	150	0,0652	-	-
ISSA	2285	-	-	-	-	150	0,0656
Sand	2850	1685	0,591	1635	0,574	1633	0,573

A total of 9 cubes were used for each of the 11 mixes. The total volume of the cubes was calculated using the dimensions of the cubes and a total volume of 0,00124 m^3 was obtained:

Volume of 1 cube = 0,000125 m^3

Volume of 9 cubes = 0,000125 × 9 = 0,001125 m^3

+ 10% wastage = 0,0001125 m^3

Total volume = volume of 9 cubes + 10% allowance for wastage

= 0,00124 m^3

Table 11: Mortar mix proportions and selected mortar properties

Mix Design (9 cubes = 0,00124 m3)	**Mix 1 (100 PC)**	**Mix 2 (70/30 PC/FA)**	**Mix 3 (70/30 PC/ISSA)**
Material	Mass (g)	Mass (g)	Mass (g)
Water	310	310	310
PC	620	434	434
Fly ash	-	186	-
ISSA	-	-	186
Sand	2089	2027	2025
Water/binder ratio	0.5	0.5	0.5

3.6.3. Flow test

Flow tests were conducted for all mortar samples to measure and compare the workability of all the mixtures. A standard test (ASTM C1437-07) was used to assess the flow of mortar samples prior to casting. The mould was placed on the flow table (see Figure 26) and filled with two layers of mortar. Tamping was done 20 times after each layer to ensure sufficient filling. Upon filling, the mortar was cut off to a plane surface flush with a sawing motion across the top of the mould. The table and mould were then cleaned around the edges and the mould removed from the mortar for testing. The table was then immediately dropped 25 times in 15 seconds and the measurements recorded. Equation 11 was used to calculate the flow percentage.

$$Flow\ \% = \frac{Diameter\ of\ flow\ (cm) - diameter\ of\ cone}{diameter\ of\ cone} \times 100 \qquad (11)$$

Figure 26: Flow table and mould

3.6.4. Casting of specimens

Steel moulds were modified to facilitate 9 cubes per mix as shown in Figure 27. The set of moulds was lubricated to prevent adhesion of mortar to mould surfaces and to ease demoulding. Four screws were used to fix the moulds on the steel bar during casting. The cubes were filled by two layers of mortar to the brim and the surfaces cut off with a sawing motion to obtain a flat top surface across each mould as shown in Figure 28. A vibration table was used for compaction. The moulds were then covered with a plastic to prevent drying and left to cure at room temperature (24 ± 2ºC) for 24 hours.

Figure 27: Empty 50×50×50 mm cube moulds

Figure 28: Cube moulds filled with cement mortar

3.6.5. Curing of specimens

After casting and setting had taken place, the specimens were demoulded (24 hours after casting) and cured in a water bath of 22 ± 2ºC until each test age (3, 7 and 28 days). This enabled adequate strength gain prior to compressive strength testing.

3.6.6. Compressive strength test of mortar containing ISSA:

Compressive strength tests were carried out to measure the strength of the mortar samples containing ISSA, compared to the reference samples. Tests were performed after 3, 7 and 28 days of curing. The compressive strength tests were determined by destructive testing on a compression test machine following a standard procedure (ASTM C109). Progressive loading was applied at a rate of 54 kN/min to 108 kN/min. Figure 29 shows the mortar samples before and after the test. The compressive strength was calculated using Equation 12:

$$R_c = \frac{F_c}{A} \text{ (MPa)} \qquad (12)$$

Where: R_c = Compressive strength (MPa)

F_c = Applied load (N)

A = Area (mm^2)

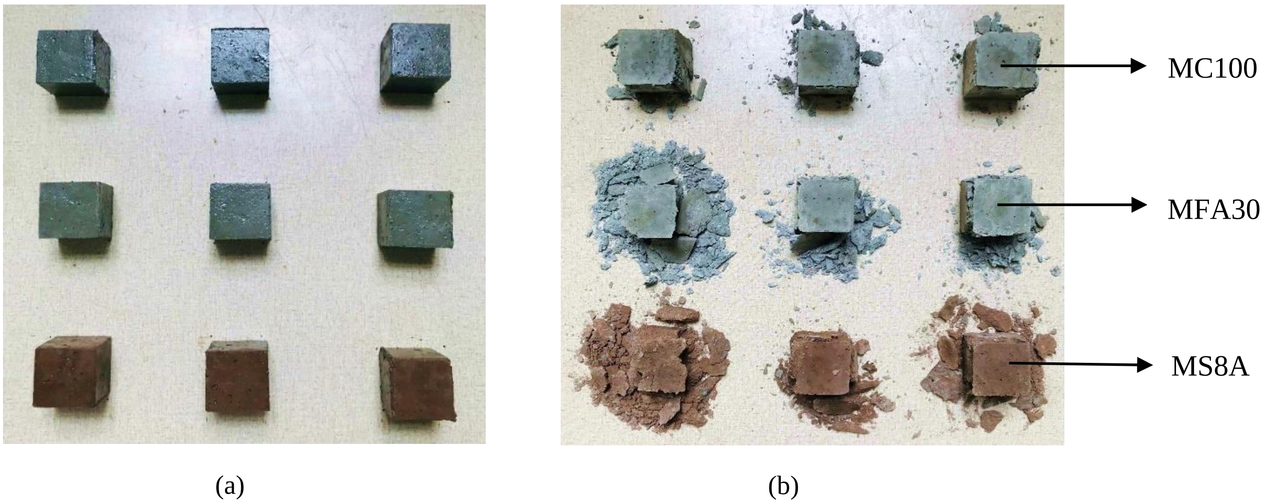

Figure 29: Mortar cubes (50 mm) before (a) and after (b) compressive strength testing

3.7. Summary of the methodology

A summary of the various tests procedures of the work is presented in the schematic diagram shown in Figure 30 below.

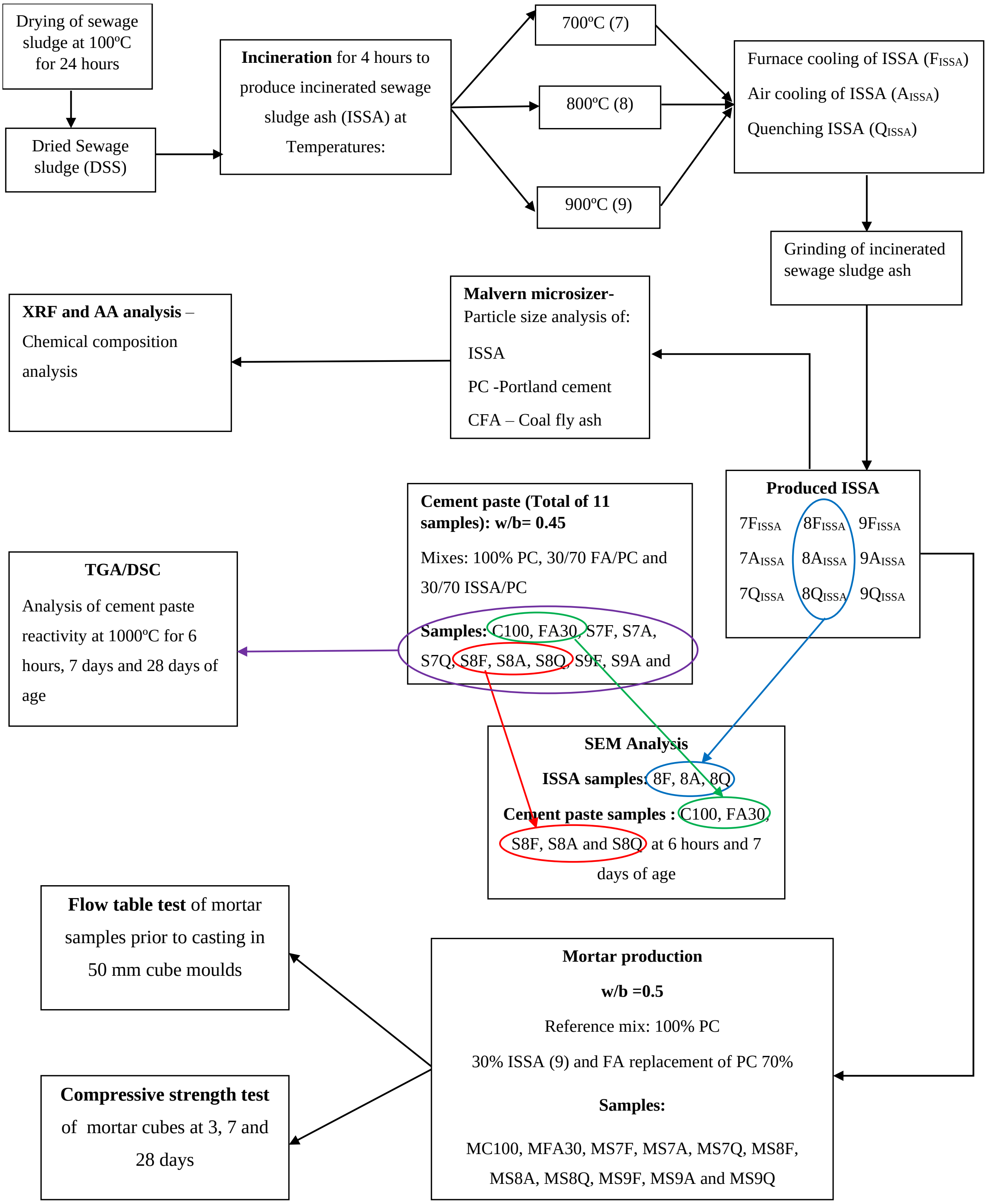

Figure 30: Schematic flow chart of methodology

References

Anjos, M.A.S., Reis, R., Camões, A., Duarte, F. and Jesus, C., 2019. Evaluation of hydration of cement pastes containing high volume of mineral additions. *European Journal of Environmental and Civil Engineering*, *23*(8), pp.987-1002.

Asim, F.Z.A. and Sutan, N.M., 2015. Thermal Characterization of Pozzolanic Activity of Hydrated Cement System Modified by Silica Based Industrial Waste. *Journal of Applied Science & Process Engineering*, *2*(1), pp. 1-7.

ASTM, International, 2003. ASTM E 1131-03: Standard test method for compositional analysis by thermogravimetry. In Annual book of ASTM standards 2003, American Society for Testing and Materials, West Conshohocken, Pennsylvania, USA.

ASTM, International, 2000. ASTM D 854-00: Standard test method for specific gravity of soil solids by water pycnometer. In Annual book of ASTM standards 2000, American Society for Testing and Materials, West Conshohocken, Pennsylvania, USA.

ASTM, International, 2007. ASTM C 1437-07: Standard test method for flow of hydraulic cement mortar. In Annual book of ASTM standards 2007, American Society for Testing and Materials, West Conshohocken, Pennsylvania, USA.

Baert, G., Hoste, S., De Schutter, G. and De Belie, N., 2008. Reactivity of fly ash in cement paste studied by means of thermogravimetry and isothermal calorimetry. *Journal of Thermal Analysis and Calorimetry*, *94*(2), pp.485-492.

Ballim, Y. and Graham, P.C., 2009. The effects of supplementary cementing materials in modifying the heat of hydration of concrete. *Materials and Structures*, *42*(6), pp.803-811.

Grieve, G., 2009. Cementitious materials. In Owens, G. (Ed): *Fulton's Concrete Technology,* 9^{th} Ed, Cement and Concrete Institute, South Africa, pp.1-16.

Hoffmann, G., Schingnitz, D. and Bilitewski, B., 2010. Comparing different methods of analysing sewage sludge, dewatered sewage sludge and sewage sludge ash. *Desalination*, *250*(1), pp.399-403.

Ing, D.S., Chin, S.C., Guan, T.K. and Suil, A., 2016. The use of sewage sludge ash (SSA) as partial replacement of cement in concrete. *ARPN Journal of Engineering and Applied Sciences,* 11(6), pp. 3771-3775.

Jamshidi, M., Jamshidi, A. and Mehrdadi, N., 2012. Application of sewage dry sludge in concrete mixtures. *Asian Journal of Civil Engineering*, pp. 365-375.

Li, H., Liu, G. and Cao, Y., 2014. Content and distribution of trace elements and polycyclic aromatic hydrocarbons in fly ash from a coal-fired CHP plant. *Aerosol and Air Quality. Research*, 14(4), pp.1179-1188.

Luz, A.P. and Pandolfelli, V.C., 2011. Halting the calcium aluminate cement hydration process. *Ceramics International*, *37*(8), pp.3789-3793.

Musa, N.M., 2014. Thermal analysis of cement paste partially replaced with Neem Seed Husk Ash. Int J Sci Eng Res, 5(1), pp.1101-1105.

Particle Technology Labs, n.d. Malvern Panalytical Mastersizer 2000 Laser Diffraction Analysis Sample Report. Accessed: 03 November 2020.

Scrivener, K., Bazzoni, A., Mota, B., and Rossen, J.E., 2018, Electron Microscopy. In: Scrivener, K., Snellings, R., and Lothenbach, B. (Eds): *A Practical Guide to Microstructural Analysis of Cementitious Materials*, CRC Press, p.351.

XRF Technology., n.d. *How Does XRF Work?* ThermoFisher Scientific. Accessed: February 2020. Available at: https://www.thermofisher.com/za/en/home/industrial/spectroscopy-elemental-isotope-analysis/spectroscopy-elemental-isotope-analysis-learning-center/elemental-analysis-information/xrf-technology.html#:~:text=XRF%20is%20an%20acronym%20for,a%20primary%20X%2Dray%20source.

CHAPTER 4

RESULTS and DISCUSSION

This chapter outlines the findings from all the experimental work carried out to evaluate the feasibility of ISSA as a partial replacement of PC. The chapter begins by detailing the production of ISSA from dried sewage sludge. Results on the characteristics of ISSA compared to PC and FA from XRF, AAS and SEM/EDS tests are then presented. Furthermore, results of the performance of ISSA used as a partial replacement of PC in cement paste are covered. For this purpose, SEM was carried out to evaluate the development of hydration products and TG/DSC to analyse the reactivity of ISSA and to quantify the amount of calcium hydroxide and the chemically combined water generated during the hydration process of cement paste samples. Lastly, flow tests and compressive strength tests results of mortar specimens are presented and discussed.

4.1. Incineration

Dried sewage sludge (DSS) was incinerated at temperatures of 700ºC, 800ºC and 900ºC for a period of four hours to produce incinerated sewage sludge ash (ISSA). On average 43.92% ash was produced from the DSS that was fed into the furnace as shown in Table 12. As expected, the mass produced decreased with an increase in the incineration temperature. During the process, the organic fraction of sewage sludge was decomposed, leaving behind solid residue known as sewage sludge ash. The ash was then collected for use in this study.

Table 12: Mass of ISSA produced

Incineration Temperature (ºC)	Mass of DSS into furnace (g)	Mass of ISSA produced (g)	Percentage yield (%)
700ºC	800	374	46.75
800ºC	800	350	43.75
900ºC	800	330	41.25

The decomposition of sewage sludge occurred at different stages. The four stages are described below:

- The loss of moisture and absorbed water at 50ºC - 130ºC
- The emission of volatile organic matter at 200ºC - 320ºC

- The combustion of non-organic content due to the varying boiling points of hydrocarbons in the sewage sludge at 330ºC - 390ºC
- The thermal decomposition of fixed carbon captured by inorganic matter, loss of structural water of the clay mineral in the sewage sludge and the elimination of carbonaceous matter in the sewage sludge at 400ºC - 670ºC (Tantawy *et al.*, 2012).

4.1.1. Heating and cooling rate curves

The graphs illustrated in Figure 31–32 show the temperature profiles (heating rates and cooling rates) for the incineration process. Furnace cooling, air cooling and quenching were carried out to study the effect of cooling rate on the effectiveness of ISSA as a partial replacement of PC. The different cooling rates were studied for all the incineration temperatures shown in Table 12. A total of nine ISSA's were produced. The heating and cooling rates increased with an increase in the incineration temperature. It took approximately 40 minutes for the furnace to reach the temperature of 700ºC, 62 minutes to reach 800ºC and 94 minutes to reach 900ºC. (All temperatures were held for a period of 4 hours).

4.1.1.1. Furnace cooling curves

Figure 31 shows the heating and furnace cooling rate curves of the incineration of ISSA at the studied temperatures of 700ºC, 800ºC and 900ºC.

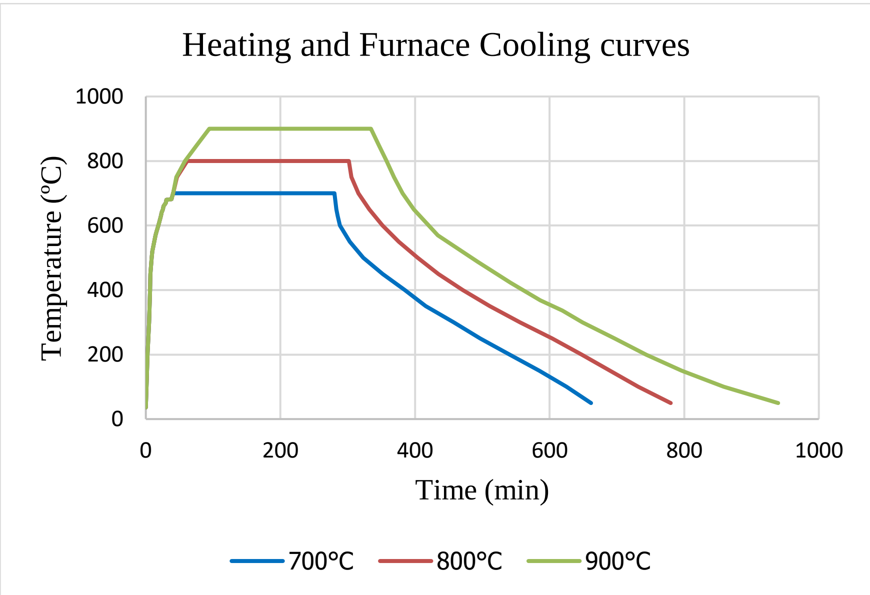

Figure 31: Heating and furnace cooling rate (Incineration temperatures; 700ºC, 800ºC and 900ºC)

An increase in the cooling time was recorded with an increase in maximum temperatures. It took approximately 6 hours to cool ISSA from 700ºC to room temperature, 8 hours to cool ISSA from 800ºC and 10 hours to cool ISSA from 900ºC.

4.1.1.2. *Air cooling curves*

Figure 32 shows the heating and air-cooling rate curves of the incineration of ISSA at 700ºC, 800ºC and 900ºC. Air cooled samples generally took less time to cool to room temperatures. It took approximately 2.7 hours to cool the ISSA from 700ºC to room temperature, 3 hours to cool ISSA from 800ºC and 3.4 hours to cool ISSA from 900ºC.

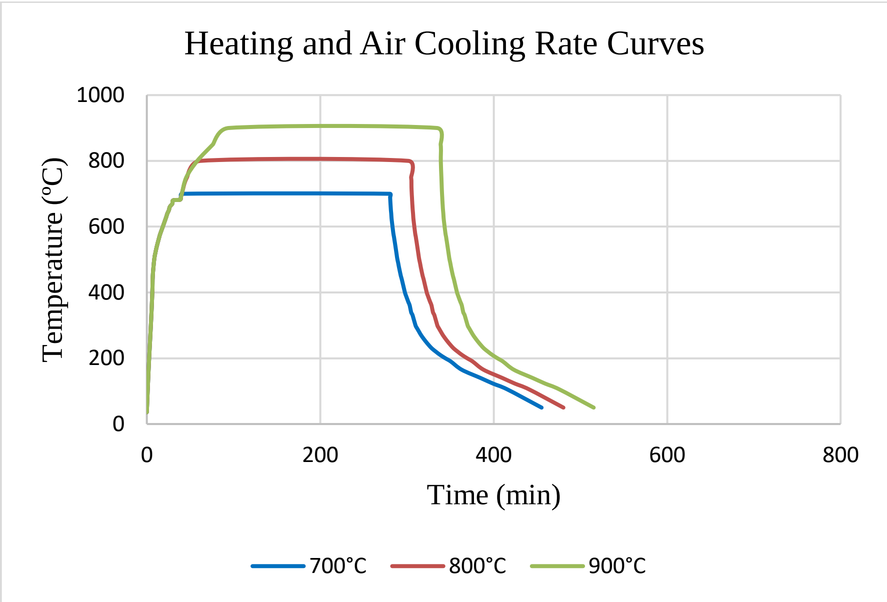

Figure 32: Heating and air-cooling rate (Incineration temperatures; 700ºC, 800ºC and 900ºC)

4.1.1.3. *Water Quenching*

The heating temperature profiles of the quenched ISSA's were similar to the ones observed above. However, the cooling rates of the quenched ISSA's were not measured as they were too rapid.

4.2. Characterization of sewage sludge/ash

4.2.1. The colour effect on cement containing ISSA.

The red colour in the ISSA is shown in Figure 20 while the effect on mortar containing ISSA can be seen in the cube moulds in Figure 28. In Figure 29, the colour difference between the ISSA mortar and the MC100 and MFA30 can be clearly seen. In practical terms, the colour effect will have an impact on the potential use of ISSA in concrete from an aesthetic perspective which may result in a limit on the possible percentage substitution of ISSA in cement (Kappel *et al.*, 2017).

4.2.2. Particle size distribution curves

Figure 33 shows the particles size distribution of PC, FA and ISSA. FA particles were in the range of 1.7 µm to 180 µm. According to Li *et al.* (2014) the particle sizes of FA can range from 0.3 to 250 µm with the major fraction in the range of 20-25 µm. PC particle sizes ranged from 0.48 µm to 630 µm. These results may be due to possible agglomeration of particles during analysis. ISSA particles ranged from 1.7 µm to 180 µm with a secondary small curve on the ISSA volume density curve in which an unusually small amount of larger particles in the size range of 180 µm to 1250 µm were measured. This result is attributed to the variability and irregularity of the ISSA particles (see Section 4.2.5) or may be a representation of a fraction of the ISSA that was harder to grind.

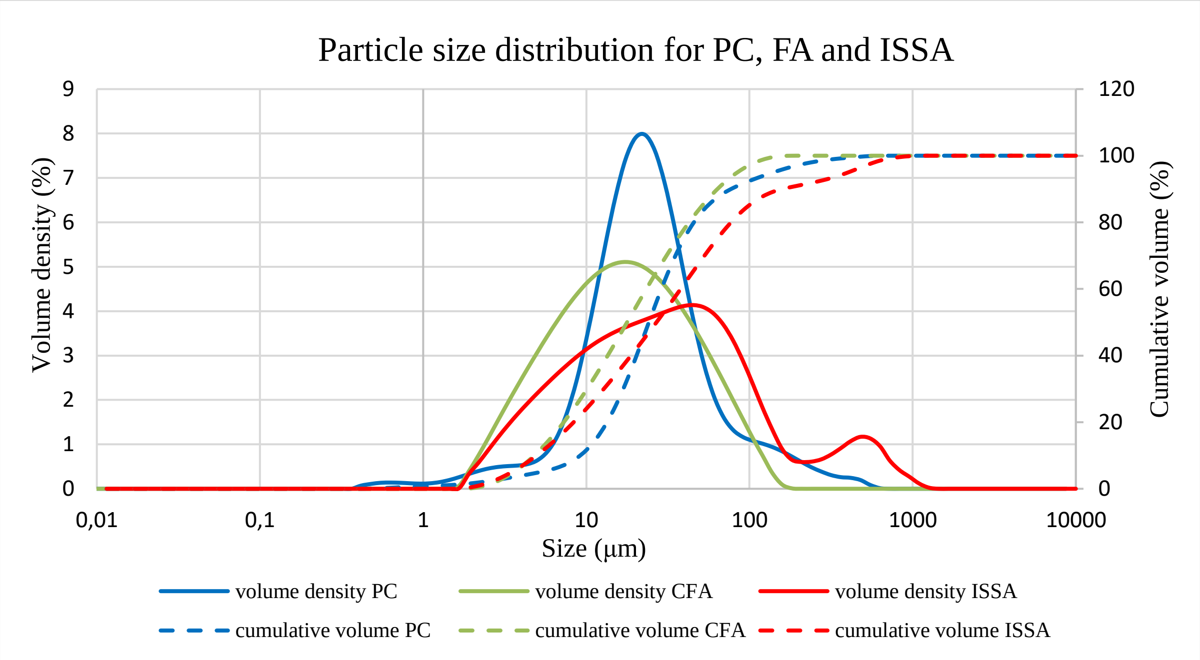

Figure 33: Particle size distribution of PC, FA and ISSA

The cumulative volume percentage (Figure 33) was also calculated from the volume density percentage results to enable the determination of median particle sizes also known as the D_{50}. Results of the analysis showed that the D_{50} of FA was the lowest with a value of 17.37 µm. The D_{50} of PC obtained was 24.60 µm and that of ISSA, 28.3 µm. These results indicate that there were 50% FA particles smaller than 17.37 µm, 50% PC particles smaller than 24.60 µm and 50% ISSA particles smaller than 28.30 µm. These results indicate that the largest quantity of small particles obtained were those of FA, followed by PC and lastly ISSA which exhibited the lowest quantity of small particles. In a study conducted by Coutand *et al.* (2006) a maximum size of 100 µm of ISSA particles was reported, whereas Halliday *et al.* (2012) reported a maximum size of 600 µm and Garcés *et al.* (2008) reported a particle size below 250 µm. The overall comparison between the particle size distribution of PC, FA and ISSA shows that the ISSA had coarser particles.

The particle size of cement has a major impact on the rate of hydration when exposed to water. Some researchers have indicated that particles exceeding 50 μm are unlikely to be entirely hydrated, even if the water availability is not rate limiting (Pekmezci & Akyuz, 2004). This suggests that during the curing stage, the smallest particles react first and at near proximity, resulting in the deposition of hydration products. Similarly, when ISSA was used as a partial replacement of cement, its smallest particles are considered to have been the most reactive and thus acted as a binder, whereas the larger particles which are considered less reactive primarily acted as a filler.

4.2.3. Density of ISSA

The relative density of ISSA was calculated using the pycnometer method described in Section 3.3.3. Table 13 shows the results of the analysis.

Table 13: Density of ISSA results

Pycnometer measurements	**Mass obtained (g)**
W_p	47.58 g
W_{ps}	97.58 g
W_A	147.71 g
W_B	175.83 g
Relative density	2.29
Density	2285 kg/m^3

The density of the ISSA was found to be 2285 kg/m^3 which is lower than the density of PC that has a value of 3150 kg/m^3 and fly ash with a value of 2350 kg/m^3. In previous studies, similar densities of ISSA were obtained. Halliday *et al.* (2012) reported densities of ISSA in the range of 2160 kg/m^3 to 2280 kg/m^3 and Coutand *et al.* (2006) reported a density of 2640 kg/m^3. These slight differences are attributed to the differing origins of the ISSA and preparation methods of the ISSA.

4.2.4. Atomic Absorption Spectroscopy (AAS) of ISSA

4.2.4.1. The effect of incineration temperature and cooling rate on the elemental composition of ISSA

Table 14 shows the elemental composition of DSS and ISSA. AAS analysis was used to determine the elemental composition and to determine the effect of incineration on the composition DSS by observing the changes in the concentration of elements.

Table 14: AA results of DSS and the 9 ISSA's produced in mg/L

Test	DSS	S7F	S8F	S9F	S7A	S8A	S9A	S7Q	S8Q	S9Q
Fe	275.23	396.48	378.72	372.32	415.14	425.20	359.14	427.68	419.58	363.05
Ca	134.89	211.81	228.02	292.31	244.23	251.10	257.77	219.78	232.14	317.86
Al	112.07	269.02	298.18	383.79	447.17	426.32	370.68	414.21	413.74	358.83
Mg	28.21	42.10	39.36	41.11	43.07	44.36	39.08	46.10	44.68	78.61
Si	166.20	236.70	234.30	274.10	205.50	241.30	230.70	276.30	283.70	288.80
P	6.11	7.54	8.26	8.02	9.14	8.52	8.65	9.52	9.78	9.85
K	106.57	27.62	20.89	9.98	25.75	24.80	8.01	24.57	22.48	10.38
Ti	5.10	22.40	20.80	12.30	11.30	9.73	9.25	8.29	8.78	6.12
Na	3.81	16.71	16.34	17.28	15.68	17.82	16.39	15.78	16.75	17.11
Zn	16.31	13.36	10.94	8.54	13.54	12.84	9.16	13.53	12.66	8.70
Mn	5.92	10.08	9.74	9.46	10.24	10.67	6.58	10.52	11.23	9.33
V	3.14	4.39	4.31	4.27	4.20	5.21	5.19	5.15	6.41	5.55
Cr	3.33	3.96	3.03	3.18	4.00	3.83	3.20	4.01	3.87	3.18
Co	5.98	3.59	3.15	2.75	3.23	3.23	2.94	3.17	3.27	2.69
Cu	6.35	3.45	3.15	1.76	3.24	2.94	1.53	2.45	2.96	1.38
Pb	24.51	3.35	2.69	1.31	3.49	2.51	0.93	3.29	2.82	1.47
Ni	1.98	2.76	2.22	1.77	2.45	2.48	1.60	2.40	2.66	1.57

Figure 34 shows a graphical presentation of results. The results show that DSS had a significant amount of the elements found in PC (Ca, Si, Al, Fe, Mg and Na). The incineration temperature had an immense impact on the resultant concentration of elements in the ISSA. A notable increase in the concentration of these elements after incineration was observed. Similar observations were obtained in previous studies (Halliday *et al.*, 2012; Chen & Lin, 2006; Coutand *et al.*, 2006), although in varying quantities due to the origins of the DSS. Potassium and phosphorus were also detected in small amounts in both the DSS and the ISSA's. Potassium was reduced as a result of incineration, whereas phosphorus showed a slight increase after incineration. The concentrations of most elements in the ISSA's increased with a reduction in the incineration temperature from 900°C to 700°C.

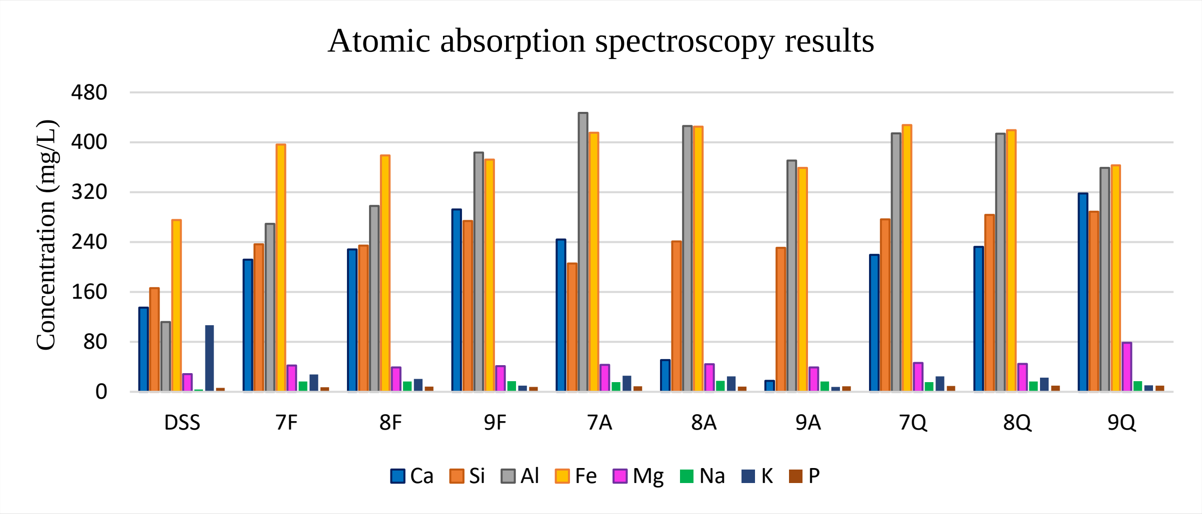

Figure 34: AA results of DSS and the 9 ISSA's produced in mg/L

The presence of heavy metals; lead (Pb), chromium (Cr), copper (Cu), nickel (Ni) zinc (Zn), cobalt (Co), Titanium (Ti), vanadium (V) and manganese (Mn) were also detected in the ISSA as shown in Figure 35. Notable increases in concentrations of Ti and Mn were observed after incineration. However, incineration had a low impact on the concentrations of Ni, V and Cr with slight changes in the concentration observed after incineration.

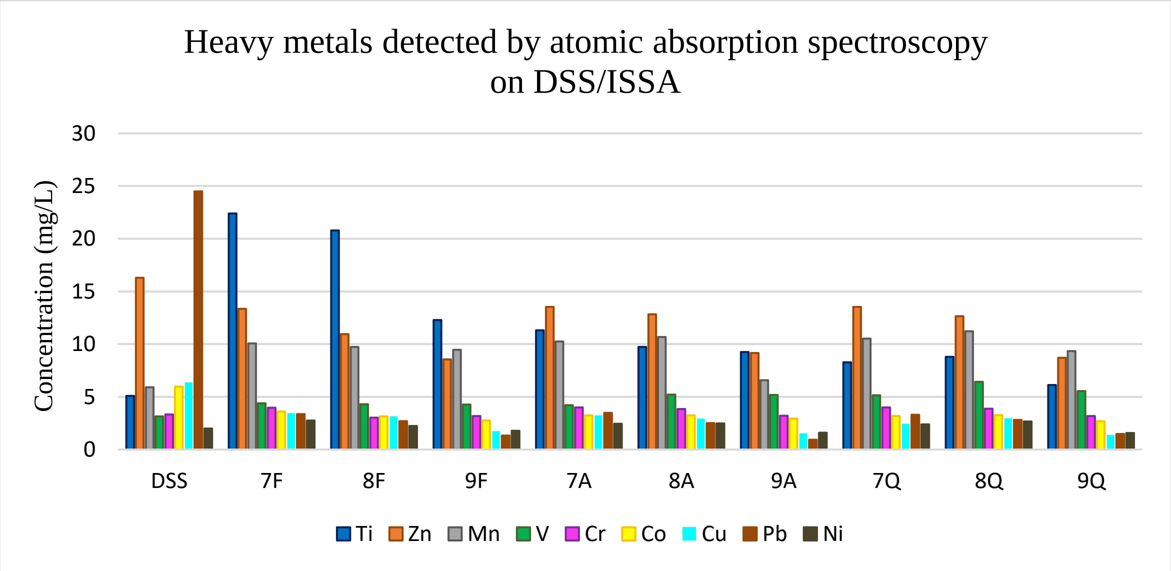

Figure 35: Heavy metals detected in DSS and ISSA

Considerable reductions in concentrations of Pb, Zn, Cu and Co were observed after incineration. The presence of heavy metals in DSS tends to limit its use in various industries. Hence, the reduction in the concentration of these elements reduces exposure problems and potential release to the environment during utilization, making it suitable to use the ISSA as a partial replacement of PC. It was also noted that the concentration of most elements increased in the order: air cooled (A_{ISSA}) > quenched (Q_{ISSA}) > furnace cooled (F_{ISSA}) of the cooling rates. Furthermore, the high content of silicon (Si) obtained showed that the ISSA can also substitute a slight portion of sand in mortar or concrete mixtures.

4.2.5. XRF analysis of ISSA

To further determine the composition of ISSA, XRF oxide compound analysis was conducted. The results of the analysis are shown in Table 15. A graphical presentation of these results is shown in Figure 36.

Table 15: XRF results of DSS and the 9 ashes produced in mass percentage

Test	DSS	S7F	S7A	S7Q	S8F	S8A	S8Q	S9F	S9A	S9Q
SiO_2	21.42	49.08	50.50	52.55	52.57	53.88	50.19	52.47	52.31	49.67
Al_2O_3	5.89	14.34	13.34	13.16	14.84	13.26	14.88	15.13	13.55	14.13
CaO	3.88	7.77	8.21	7.06	7.43	6.89	8.24	7.97	7.68	7.79
Fe_2O_3	4.79	10.94	11.10	10.25	10.98	10.19	11.03	11.38	11.28	10.78
MgO	1.12	2.82	2.49	2.40	2.78	2.65	2.77	2.80	2.15	2.63
TiO_2	0.44	0.99	1.01	0.93	1.00	0.90	1.00	1.03	0.99	0.99
Mn_2O_3	0.13	0.28	0.28	0.25	0.28	0.24	0.28	0.28	0.28	0.27
Na_2O	0.22	0.69	0.64	0.52	0.68	0.62	0.71	0.75	0.53	0.62
K_2O	0.51	1.01	1.04	0.94	0.99	0.90	1.05	1.08	1.03	1.01
P_2O_5	3.95	8.69	8.84	8.07	8.94	7.74	8.94	9.24	8.34	8.74
LOI	56.64	4.36	3.36	5.90	2.42	2.59	3.58	1.16	1.16	1.19
Total	98.99	100.97	100.81	102.03	102.91	99.86	102.67	103.29	99.30	97.82

4.2.5.1. Pozzolanic properties of ISSA according to XRF analysis

The main compounds found in the ISSA were SiO_2 with values in the range of 49.08% to 53.88%, CaO in the range of 6.89% to 8.24%, Al_2O_3 in the range 13.16% to 15.13% and Fe_2O_3 in the range 10.19% to 11.38%, these are the major compounds found in PC (Table 4). The proportion of SiO_2 found in the ISSA was higher than in PC and comparable with that of FA (see Figure 36). The CaO obtained was also comparable with that of FA. The significant amounts of Al_2O_3, Fe_2O_3 and CaO observed are attributed to the use of ferric salts, aluminium sulphate and lime used as flocculators in the conditioning of secondary sludge in WWTP's (Tantawy *et al.*, 2012; Halliday *et al.*, 2012), as well as the oxidation of the elements during incineration.

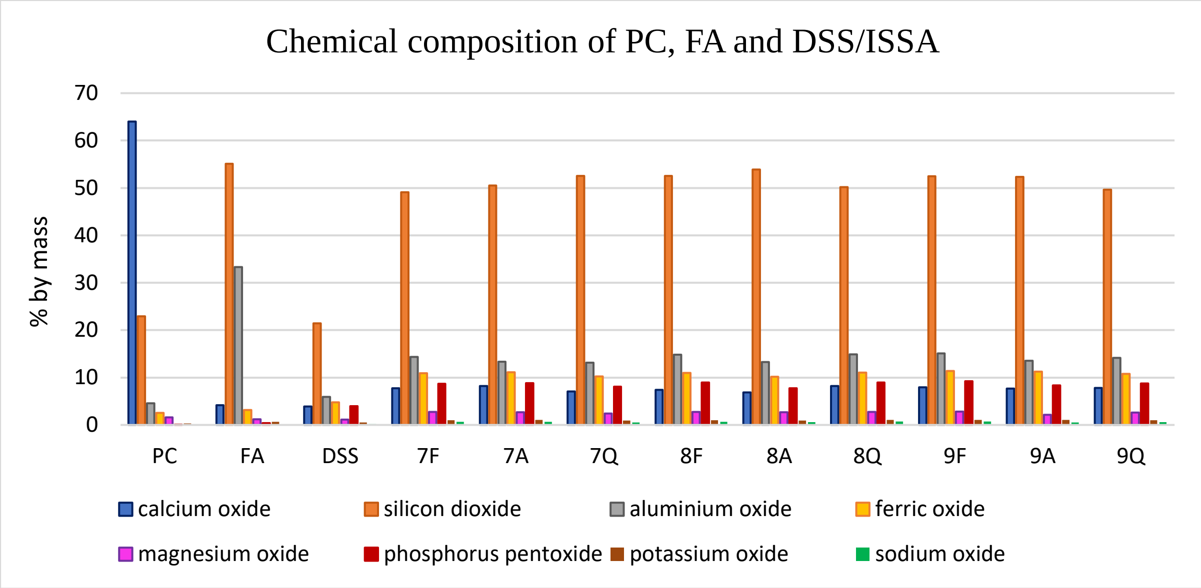

Figure 36: X-ray fluorescence results of PC and FA compared to DSS and ISSA

These results are similar to those obtained in previous studies (shown in Table 3), while also taking into account the fact that the composition of ISSA varies with WWTP's which accounts for the slight differences observed. According to Naamane *et al.* (2016), the aforementioned compounds increase in concentration with an increase in incineration temperature, due to the reaction with oxygen to form oxides during the incineration process. The same trend was observed in this study. Sewage sludge ash incinerated at 900ºC showed the highest increase in concentrations for a majority of the compounds. However, this was not the case for all the compounds and the changes in the composition observed were not high. A relation between the cooling rates of the ISSA and the composition of the compounds could not be established as the values varied with the incineration temperature. However, it was observed that an increase in the concentration of the compounds occurred after the incineration of sewage sludge.

The cementitious compounds found in the ISSA were comparable to those found in FA, making ISSA a possible supplementary material for Portland cement. A slightly higher MgO content was obtained on the ISSA. According to Yin, (2011) a mass fraction of MgO in the range of 1-5% can help enhance the strength of cement. A considerable amount of P_2O_5 ranging from 3.95% to 9.24% was also obtained in the dried sewage sludge and all the sewage sludge ashes. This may be due to the presence of domestic detergents used in WWTP inflow. LOI values in the range of 1.16% – 5.90% were also identified in the ISSA's, possibly as a result of absorbed water and incomplete incineration in the descending order 700ºC > 800ºC > 900ºC. This trend was common for all cooling rates, F_{ISSA}, A_{ISSA} and Q_{ISSA}. The highest cooling rate (Q_{ISSA})

exhibited the highest LOI. Similar LOI values were obtained in previous research. Halliday *et al.* (2012) reported a value of 2.2% and Garcés *et al.* (2008) reported a value of 5.1%.

The CaO/SiO_2 (C/S) ratios of the ISSA's were calculated and compared to those of FA and PC using the chemical compositions in Table 4 and 5. The C/S was found to be variable and seemed to be independent of the incineration temperature and the cooling rate of the ISSA. The C/S ratios obtained for the ISSA's were in the range of 0.13 - 0.16 as shown in Table 16. The ratios were substantially lower than the ratio of PC with a value of 3, and higher than that of FA with a ratio of 0.08. According to Massazza, (1998), the variability of the C/S ratio can be attributed to the non-stoichiometry of C-S-H that is dependent on the material.

Table 16: CaO/SiO_2 ratio of PC, FA and ISSA

Material	**C/S ratio**
PC	3
FA	0,08
S7F	0,16
S7A	0,14
S7Q	0,15
S8F	0,16
S8A	0,13
S8Q	0,15
S9F	0,13
S9A	0,16
S9Q	0,16

4.2.6. ISSA SEM/EDS results

SEM micrographs and EDS results are shown below (Figures 37 – 39) for the different ISSA produced at a temperature of 800ºC then furnace cooled, air cooled and quenched in water.

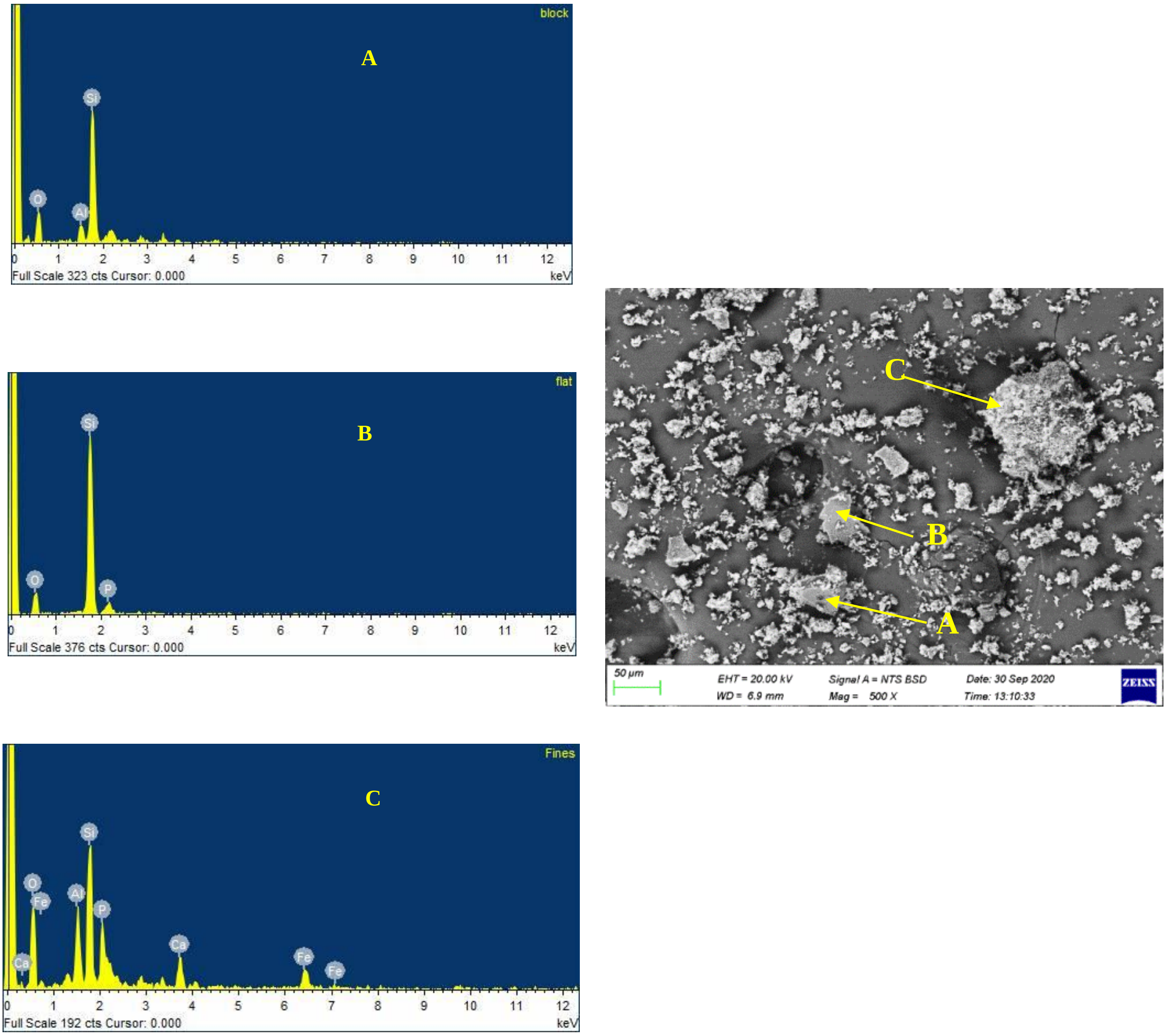

Figure 37: Micrographs (500X magnification) and EDS of ISSA incinerated at 800°C and furnace cooled ($8F_{ISSA}$)

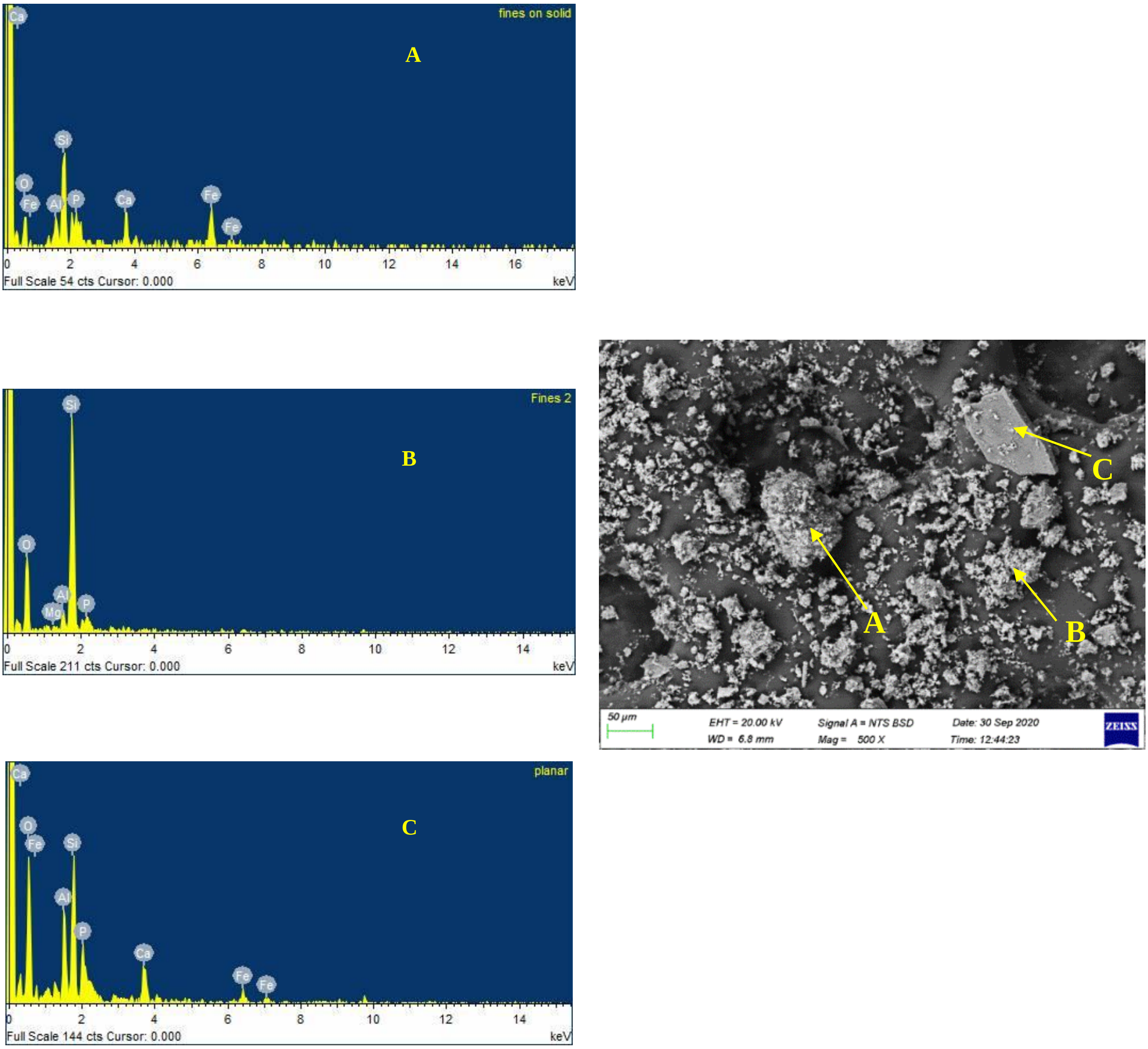

Figure 38: Micrographs (500X magnification) and EDS of ISSA incinerated at 800°C and air cooled ($8A_{ISSA}$)

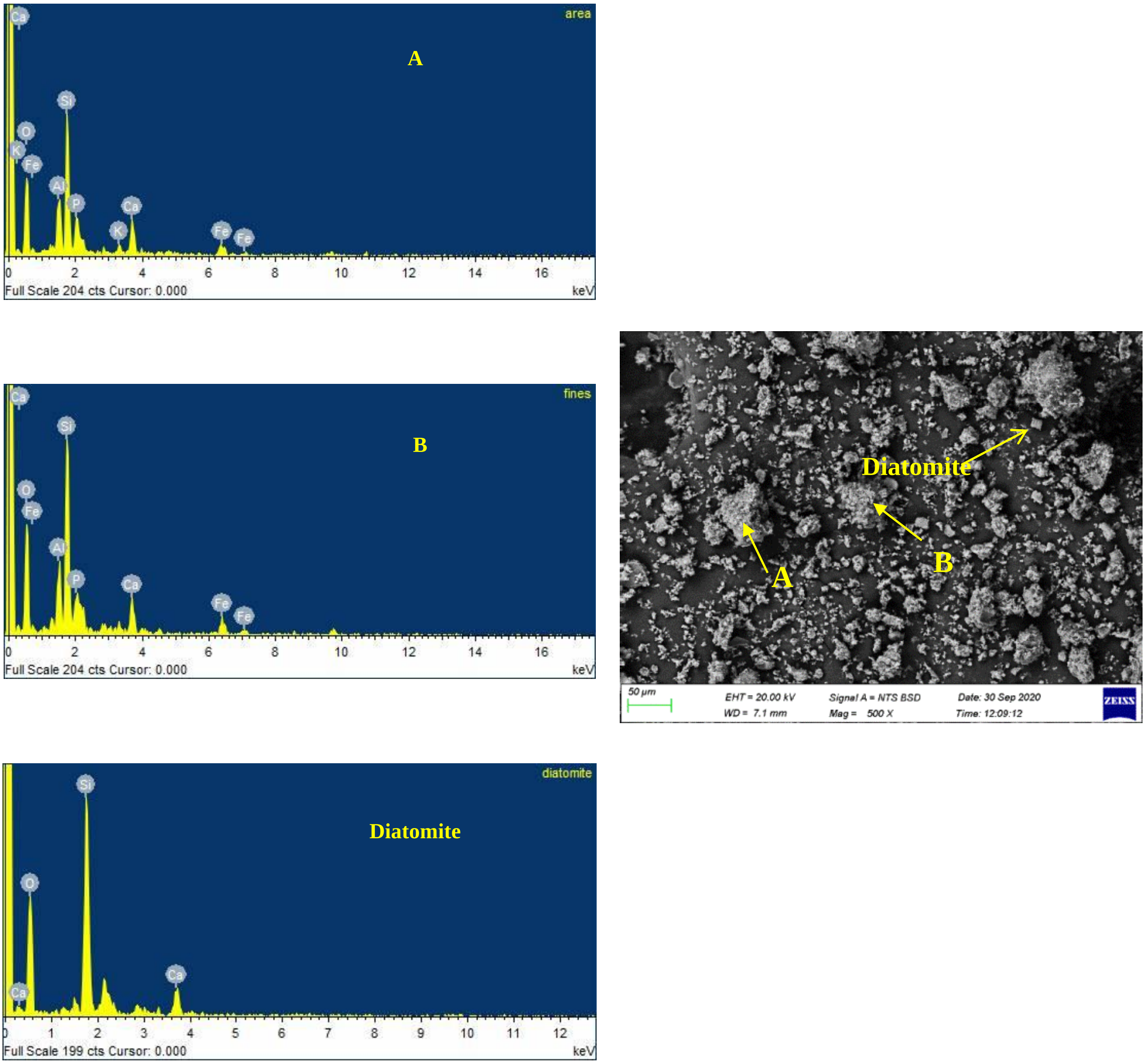

Figure 39: Micrographs (500X magnification) and EDS of ISSA incinerated at 800°C and quenched in water ($8Q_{ISSA}$)

The SEM results of ISSA showed an irregular morphology of grains with strongly developed surfaces and a few traces of rectangular or spherical grains. A closer look at the morphology of the ISSA is shown in Figure 40 (a – c). These results are similar to previous research findings by (Monzo *et al.*, 2003; Tantawy *et al.*, 2012; Horiguchi *et al.*, 2011; Kosior-Kazberuk, 2011; Naamane *et al.*, 2016; Zabielska-Adamska, 2020). The ISSA was made up of particles that varied in shape and size with a heterogeneous distribution of particles.

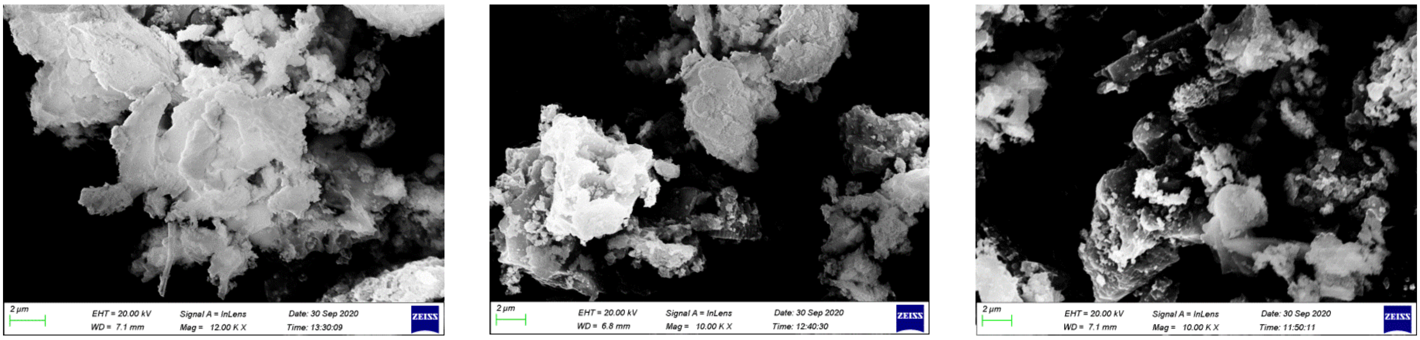

(a) **(b)** **(c)**

Figure 40: Micrographs of ISSA incinerated at 800°C, (a) Furnace cooled, (b) Air cooled and (c) Quenched in water

Fine particles were also observed in all ashes incinerated at different temperatures. Larger particles fused with fine particles were observed as seen in Figure 37, point C, Figure 38, point A and Figure 39, point A and B. This resulted in a porous structure which, when coupled with the irregular morphology was found to increase the water demand and cause difficulties in terms of workability when used to replace PC in mortar. These findings were similar to previous studies (Halliday *et al.*, 2012; Monzo *et al.*, 1997, 2003). Furnace cooled and air cooled ISSA (Figures 37 and 38) also exhibited some prismatic particles with sharp edges indicated as points B and C respectively. Particles of these kind were described as a rare trace in previous research works (Tantawy *et al.*, 2012; Naamane *et al.*, 2016).

Figures 37 - 39 also show the EDS analysis of the particles observed on the SEM micrographs. High peaks of silicon (Si) as the major constituent of the particles were observed with some parts of the ash showing evidence of iron (Fe) and aluminium (Al). These results were related to the chemical composition of the ISSA as analysed using AA and XRF techniques. Figure 41 shows some traces of artificial diatomaceous earth (diatomite) from the wastewater treatment of the sludge. Diatomite is a low-cost material with a variety of properties and is commonly used as an adsorbent in WWTP's (Zhang *et al.*, 2009).

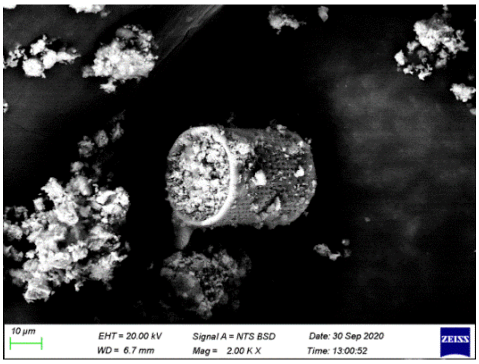

Figure 41: Micrograph (2000X magnification) of a diatomite particle on ISSA incinerated at 800°C

Diatomite is mainly composed of quartz (SiO_2). The comprehensive chemical composition of diatomite is shown in Table 17. The compounds found in the diatomite are valuable components in making ISSA a good pozzolanic material hence, it can also be deduced that this material contributed to the high amount of SiO_2 found in the ISSA. The effect of diatomite on the hydration of ISSA blended cement paste is discussed further in Section 4.3.2.1.

Table 17: Chemical composition of diatomaceous earth (Wypych, 2016)

Component	**% by mass**
SiO_2	85.5 - 91.8
Al_2O_3	3.2 – 4.5
CaO	0.3 – 0.6
Fe_2O_3	1.0 – 1.4
K_2O	0.0 – 1.2
Na_2O	0.5 – 3.6
TiO_2	0.1 – 0.2

4.3. Hydration and reactivity studies of cement paste containing ISSA

4.3.1. Cement paste

Cement paste samples were prepared with a w/b ratio of 0.45 with an aim of assessing the effect of ISSA on the reactivity of cement. When the mixing was conducted, a reduction in the workability of cement paste was obtained with an increase in the difficulty of mixing when 30% of PC was replaced with ISSA. The reduction in workability of cement paste containing ISSA can be attributed to the irregular morphology of ISSA illustrated on the SEM micrographs of ISSA in Section 4.2.5, which showed a variety of particles ranging from large to fine sized particles (Figures 37-39). This result was expected due to the irregular morphology of ISSA that reduced the flow of the cement paste. According to Yusuf *et al.* (2012), the high demand for water is also attributed to the mismatch in permeability and the bulk specific gravity of ISSA that differs from those of natural inorganic silt.

4.3.2. SEM observations of cement paste samples after 6 hours of hydration

Figures 42 - 46 show the SEM micrographs of cement pastes after 6 hours of hydration. Compositional and microstructural changes in the cement paste samples were determined by SEM analysis. The micrographs enabled tracking of possible hydration of ISSA compared to PC and FA grains while also providing an understanding of the deposition of C-S-H hydrates within fractured cement paste specimens. According to Scrivener *et al.* (2018), morphological assessments of cement paste are only useful at the early stages of hydration. The SEM micrographs below show the hydration analysis of 100% PC paste in Figure 42, 30% FA/70% PC cement paste in Figure 43 and 30% ISSA/70% PC cement pastes (ISSA incinerated at 800ºC), S8F (furnace cooled) in Figure 44, S8A (air cooled) in Figure 45 and S8Q (quenched) in Figure 46.

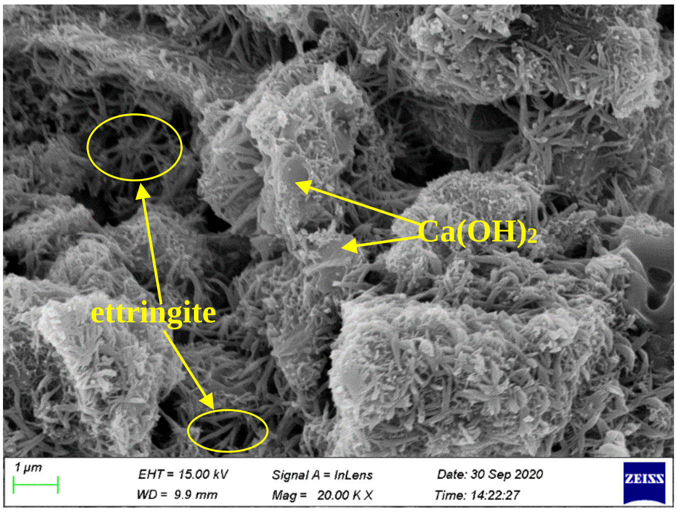

Figure 42: SEM micrograph of 100% Portland cement paste (C100) after 6 hours of curing

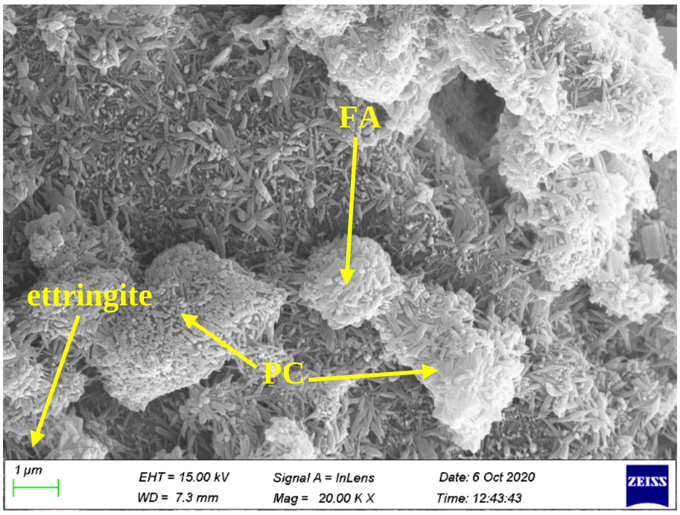

Figure 43: SEM micrograph of FA cement paste after 6 hours of hydration

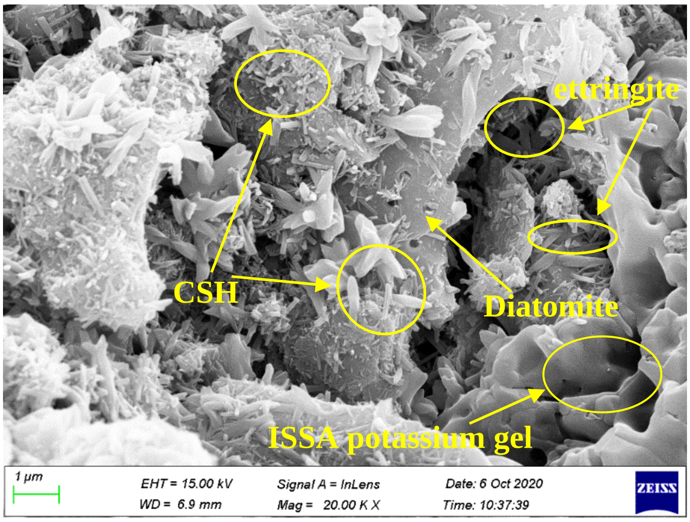

Figure 44: SEM micrograph of S8F cement paste after 6 hours of hydration

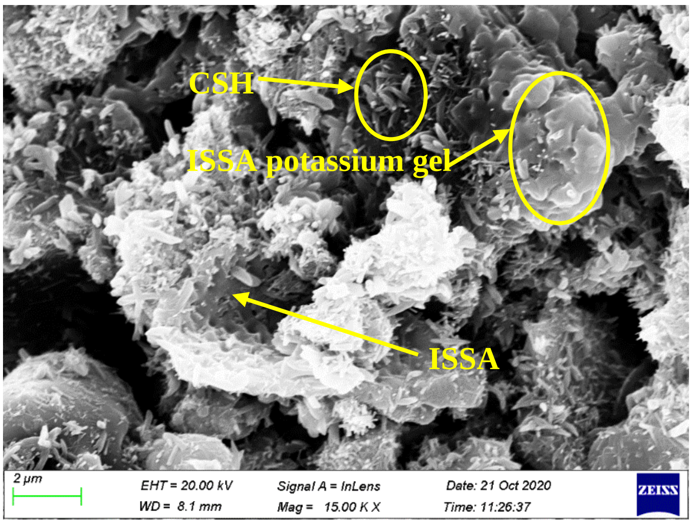

Figure 45: SEM micrograph of S8A cement paste after 6 hours of hydration

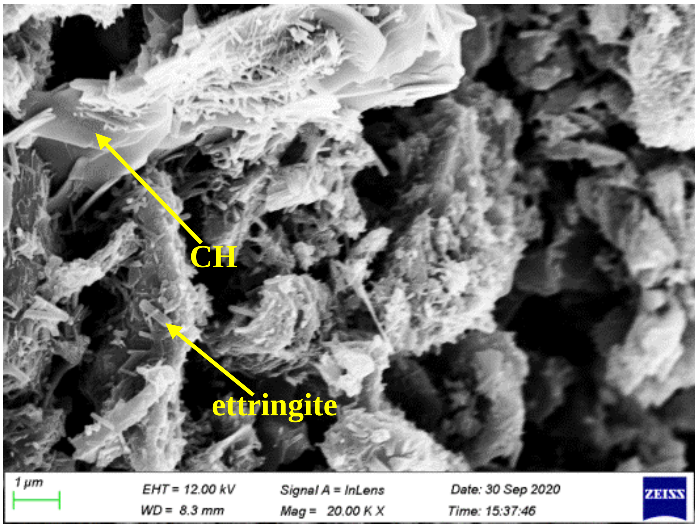

Figure 46: SEM micrograph of S8Q cement paste after 6 hours of hydration

4.3.2.1. Effect of ISSA on the hydration of cement paste after 6 hours of hydration

SEM analysis (Figure 42 to 46) uncovered the products of the hydration of the cement pastes. Figure 42 shows the micrograph of the reference sample (100% PC paste) which showed more hydration products, such as ettringite (a primary constituent of early hydration of cement), C-S-H (calcium silicate hydrates) and $Ca(OH)_2$ (calcium hydroxide) than the blended cement pastes. This result was expected due to the high amount of C_3S and C_2S in PC. Notable hydration products were also observed in FA and ISSA blended cement paste in Figures 43 - 46. This was indicated by the growth of ettringite, C-S-H fibrils and $Ca(OH)_2$ crystal planes on the surfaces of grains.

Calcium hydroxide is an essential product of the cement hydration process. As mentioned in the literature, it can be distinguished by its layered crystal plates morphology that tend to form small patches in cement grains. Calcium hydroxide crystal growth formation results from the reaction of calcium silicates with water according to the reactions shown in Equations 2 – 3, Chapter 2. Although the $Ca(OH)_2$ is an important constituent during PC hydration, the main cementing compound during curing is the C-S-H gel distinguished by its crystalline and thin layers of fibrils attached to the surface of large cement particles. C-S-H contains both free water and chemically bound water (see Section 4.5). Both $Ca(OH)_2$ and C-S-H are produced as hydrated products from the major reaction of C_3S and C_2S with water (Equations 2 and 3, Chapter 2). Traces of C-S-H were found visibly on ISSA blended cement paste samples S8F and S8A in Figure 44 and 45 respectively.

$Ca(OH)_2$ crystal growth increases with the water content and cement content, hence a lower quantity of $Ca(OH)_2$ plates was observed on ISSA blended cement paste (Figures 44 – 46).

However, it is also important to note that this reduction in $Ca(OH)_2$ can be related to the progression in hydration reactions and to the pozzolanic activity of ISSA. According to Figures 44 and 45, a potassium gel forming part of the ISSA was observed after 6 hours of hydration in S8F and S8A cement pastes. As seen in the Figures, the gel seemed to have retarded the hydration reactions with its components exhibiting a solid morphology with little to no hydration products observed on its surfaces. The gel was surprisingly not observed in S8Q blended cement paste. It is also important to note that the morphology of hydration products seen in S8Q is more fibrous. This result can be linked to the hydration in the paste. It was also noted that the extent of the hydration of ISSA blended cement pastes showed an increase in the order $F_{ISSA} < A_{ISSA} < Q_{ISSA}$ of the ISSA cooling rates. The diatomite used during sewage sludge treatment interestingly also served a good purpose in the hydration of the paste. Figure 47 shows traces of diatomite on all ISSA blended cement pastes observed after 6 hours of curing. Visible hydration products were observed on its surfaces with some traces of ettringite needles.

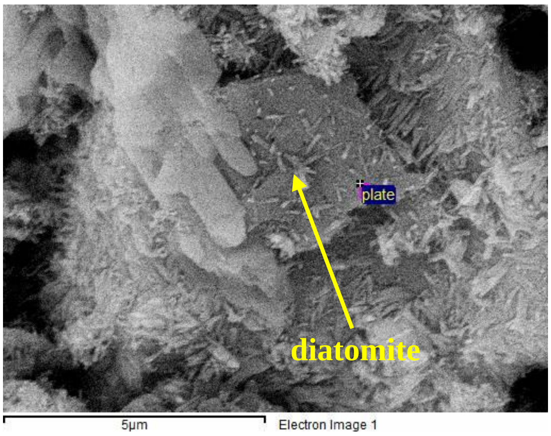

(a)

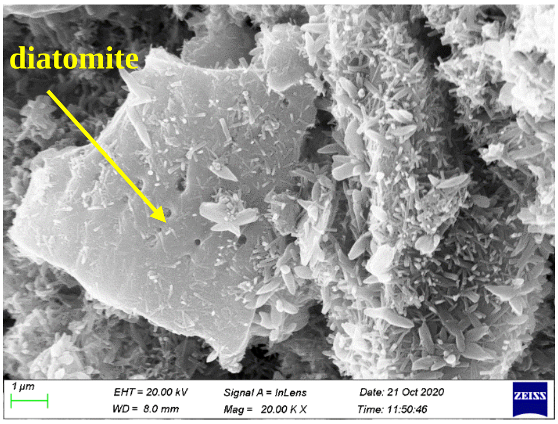

(b)

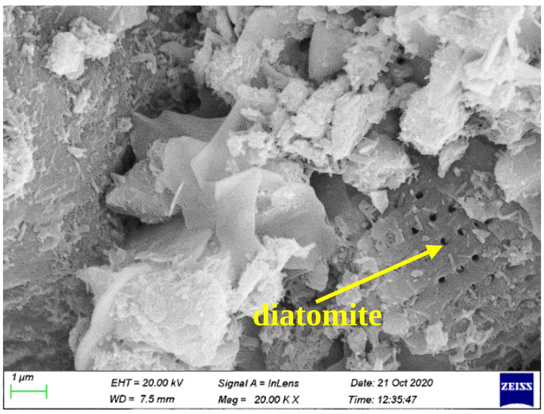

(c)

Figure 47: SEM micrographs showing traces of diatomite particles in cement paste samples (a) S8F, (b) S8A and (c) S8Q

4.3.3. SEM observations after 7 days of hydration

SEM analysis was also conducted after 7 days of hydration to analyse the hydration progress of ISSA blended cement paste mixtures compared to PC paste mix and FA blended cement paste mix. Results of the observations made are illustrated in the Figures 48 - 52 below.

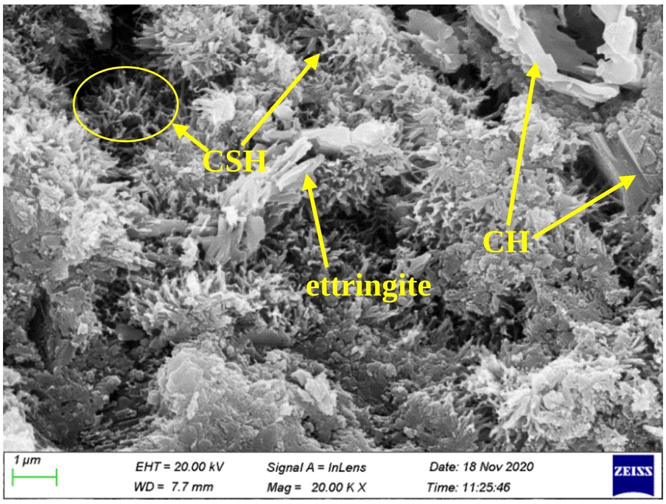

Figure 48: SEM micrograph of 100% PC paste (C100) after 7 days of hydration

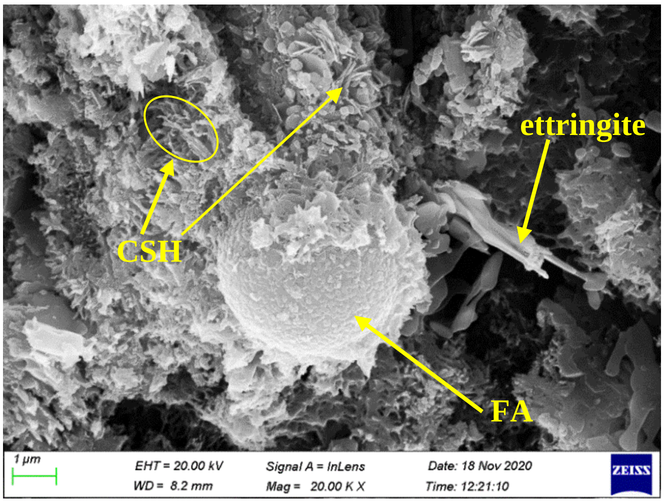

Figure 49: SEM micrograph of FA cement paste after 7 days of hydration

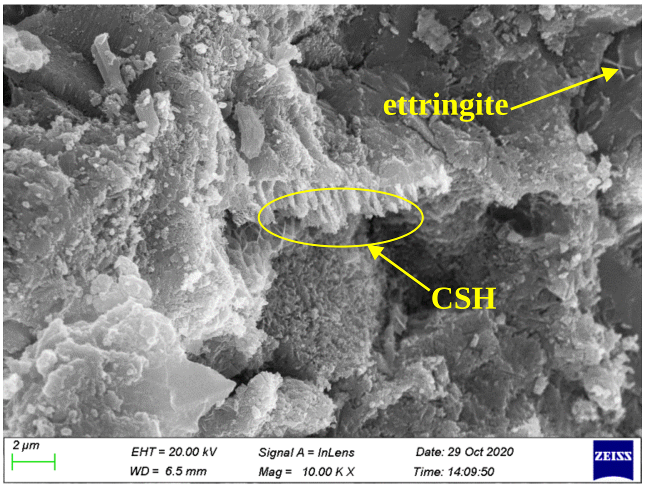

Figure 50: SEM micrograph of S8F cement paste after 7 days of hydration

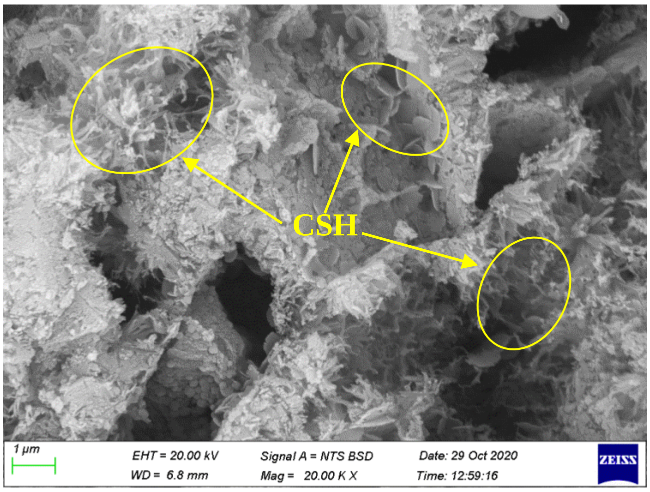

Figure 51: SEM micrograph of S8A cement paste after 7 days of hydration

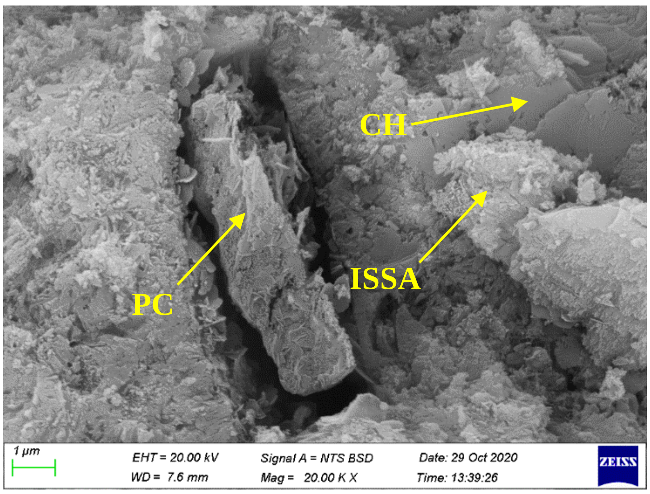

Figure 52: SEM micrograph of S8Q cement paste after 7 days of hydration

4.3.3.1. Effect of ISSA on the microstructure of cement at seven days

Analysis of cement paste samples after 7 days of hydration showed that an increase in the curing age resulted in more uniformly hydrated surfaces observed for all cement paste samples. According to Scrivener *et al*, (2018), as the degree of hydration progresses the surfaces of grains become covered which tends to make everything look the same. To explain this Van Beek & Hilhorst, (1999), used a theory of growing spheres to describe the formation of cement paste microstructure as shown in Figure 53. Cement grains illustrated as spheres grow in an outward direction, and as they start to interconnect, the development of strength commences, and the pores eventually become blocked. This effect was observed when comparing the micrographs after 6 hours and after 7 days of hydration. The differences in the microstructure of reference cement paste and ISSA blended cement paste were distinctively evident. Hydration products were observed with a reduction in ettringite needles due to the progression of hydration.

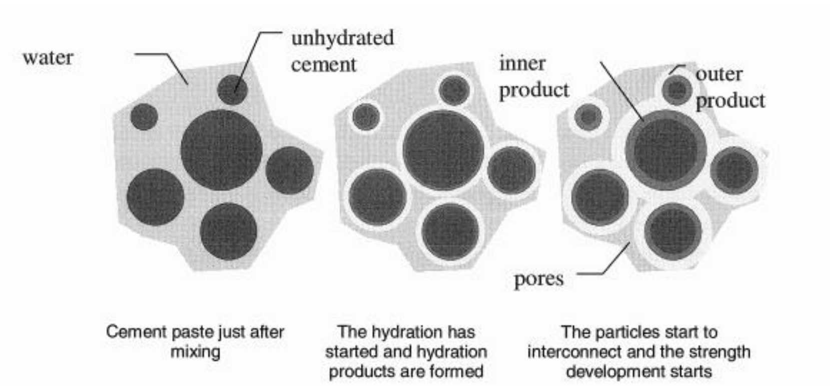

Figure 53: Microstructure formation illustrated by growing spheres (Van Beek & Hilhorst, 1999)

Figure 48 shows the SEM micrograph of the reference sample C100 without PC displacement. Visible traces of C-S-H, ettringite and $Ca(OH)_2$ after 7 days of hydration were traced. Several hydration products were also observed on ISSA blended cement pastes as shown in Figures 49 – 52. Ettringite needles were observed on Figures 48, 49 and 50; however, in smaller amounts compared to the observations made after 6 hours. With the use of EDS analysis, traces of PC and ISSA were distinguished as shown in Figure 50 (S8Q). However, due to the progression of the reactions in the paste, the surfaces of the grains were more covered and looked almost the same. It was also noted that fewer traces of $Ca(OH)_2$ were observed, especially on the FA and ISSA blended cement paste samples as shown in Figures 49 – 52. This result is attributed to possible pozzolanic reactions that consumed the calcium hydroxide as hydration progressed.

4.4. Thermal analysis of cement paste containing ISSA

Figures 54 - 56 show TGA/ DSC curves of ISSA blended cement past samples compared to reference cement paste samples after 6 hours, 7 days and 28 days of hydration. Thermal analysis is one of the techniques commonly used to analyse the hydration stages of cement – water systems (Bhatty & Reid, 1985). The TGA/DSC method was used to determine the effect of ISSA on mass loss, chemically bound water and calcium hydroxide content of PC pastes at high temperatures. During hydration, the reactions shown in Equations 2 and 3 (Chapter 2) occurred. The extent of hydration was determined using these reactions. The reactions, however, are highly dependent on the hydration temperature, water-cement ratio and surface areas of starting materials (Beaudoin & Odler, 2019). The same operation procedure was used for the TGA (see Table 9).

4.4.1. DSC curves

The DSC curves were used to determine the notable changes in weight loss that occurred during the thermal process. The DSC graphs (54 - 56, a2, b2 and c2) show mass loss peaks at 0 – 100°C, 100 – 200°C, 400 – 450°C and 600 – 710°C at all ages.

4.4.1.1. Effect of ISSA on initial peak

Figure 54 (a2, b2 and c2) shows a high mass loss peak for all cement pastes obtained at a temperature range of 30ºC to 100ºC, where the removal of free and absorbed water occurred. According to Scrivener *et al.* (2018), the heating rate set for TGA has a strong influence on the temperature at which the main mass loss is observed for a sample. Hence, the same heating rate (20ºC/min) was used for analysis of the samples and the mass loss occurred at the same temperature for all the samples tested. A reduction in the peak intensity was observed with an increase in curing age from 6 hours to 28 days. This change can be observed by comparing Figure 56 (a2, b2 and c2), Figure 55 (a2, b2 and c2) and Figure 54 (a2, b2 and c2). The reduction in the intensity of the first peak on the DSC curves was also noted with the addition of 30% ISSA in cement paste along with an increase in the curing age for all cement paste samples. This result is attributed to the reduced reactivity caused by ISSA. The first peak of the reference sample C100 was higher than the peak of FA30 cement paste and even higher than that of the ISSA blended cement pastes due to the more strongly absorbed water in sample C100.

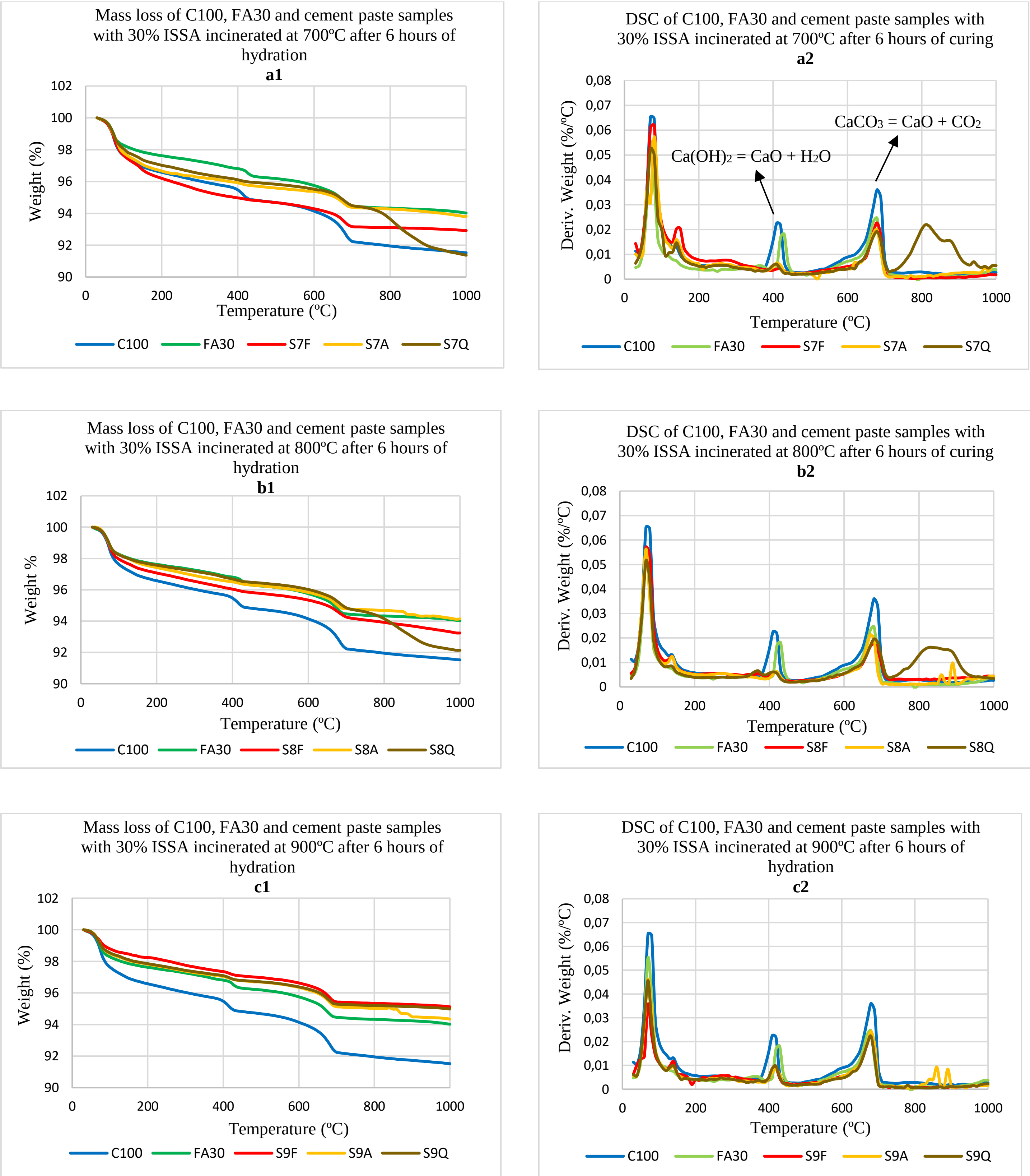

Figure 54: TGA mass loss profiles of cement pastes C100 (100% PC paste), FA30 (cement paste containing 30% replacement of PC by FA) and S7F/S7A/S7Q, S8F/S8A/S8Q and S9F/S9A/S9Q (cement paste containing 30% ISSA) after 6 hours of hydration.

The reduction in the intensities of the first peaks observed with the addition of ISSA to the cement paste can also be linked to the increased water absorption that was observed during mixing. According to previous studies, the increased water absorption is caused by significant amounts of P_2O_5 and SO_3 found in the ISSA (Vouk *et al.,* 2016; Naamane *et al.,* 2016). Similarly, in the present study significant amounts of P_2O_5 with values in the range of 7.74% to 9.24% were discovered in the ISSA (see Table 15). The water present in the cement paste can be distinguished in accordance with the ease with which it can be extracted from the cement paste. Hence it is classified into the forms: capillary, adsorbed, interlayer and chemically combined water (Neville, 1997; Mehta & Monteiro, 2014; Anjos *et al.,* 2019). Chemically combined water (Section 4.5.1) was calculated and used as a measure of the extent of the hydration of the pastes.

4.4.1.2. Second and third peaks

The second mass loss peaks were observed at 100ºC – 200ºC for all the cement pastes, as shown in Figures 54 – 56 (a2, b2 and c2). These peaks are related to the dehydration of the bound water from the C-S-H phase as well as calcium sulpho-aluminate or carbo-aluminate hydrates (Scrivener *et al.,* 2018). The peaks were higher for all ISSA blended cement paste compared to the reference samples. This result is related to the impact of the slow formation of hydration products. The third peaks were observed at 400°C – 450°C as a result of calcium hydroxide dehydroxylation. Reductions in the peak intensities were observed with the addition of ISSA in the cement pastes. This observation is attributed to the consumption of $Ca(OH)_2$ suggesting that pozzolanic reactions took place due to the ISSA that was present in the cement pastes.

Slight shifts of $Ca(OH)_2$ peaks to a higher temperature range of samples S9F, S9A and S9Q were observed after 6 hour and 7 days of hydration compared to C100. This observation showed that the $Ca(OH)_2$ content of these samples was unstable at high temperatures. The total calcium hydroxide $Ca(OH)_2$ content was calculated from the TGA curves between 400ºC and 450ºC to measure reactivity of the ISSA blended cement pastes compared to the reference cement pastes. Calcium carbonate ($CaCO_3$) content was also calculated and added as the $Ca(OH)_2$ that converted to $CaCO_3$ during sample preparation (see Section 4.5.2).

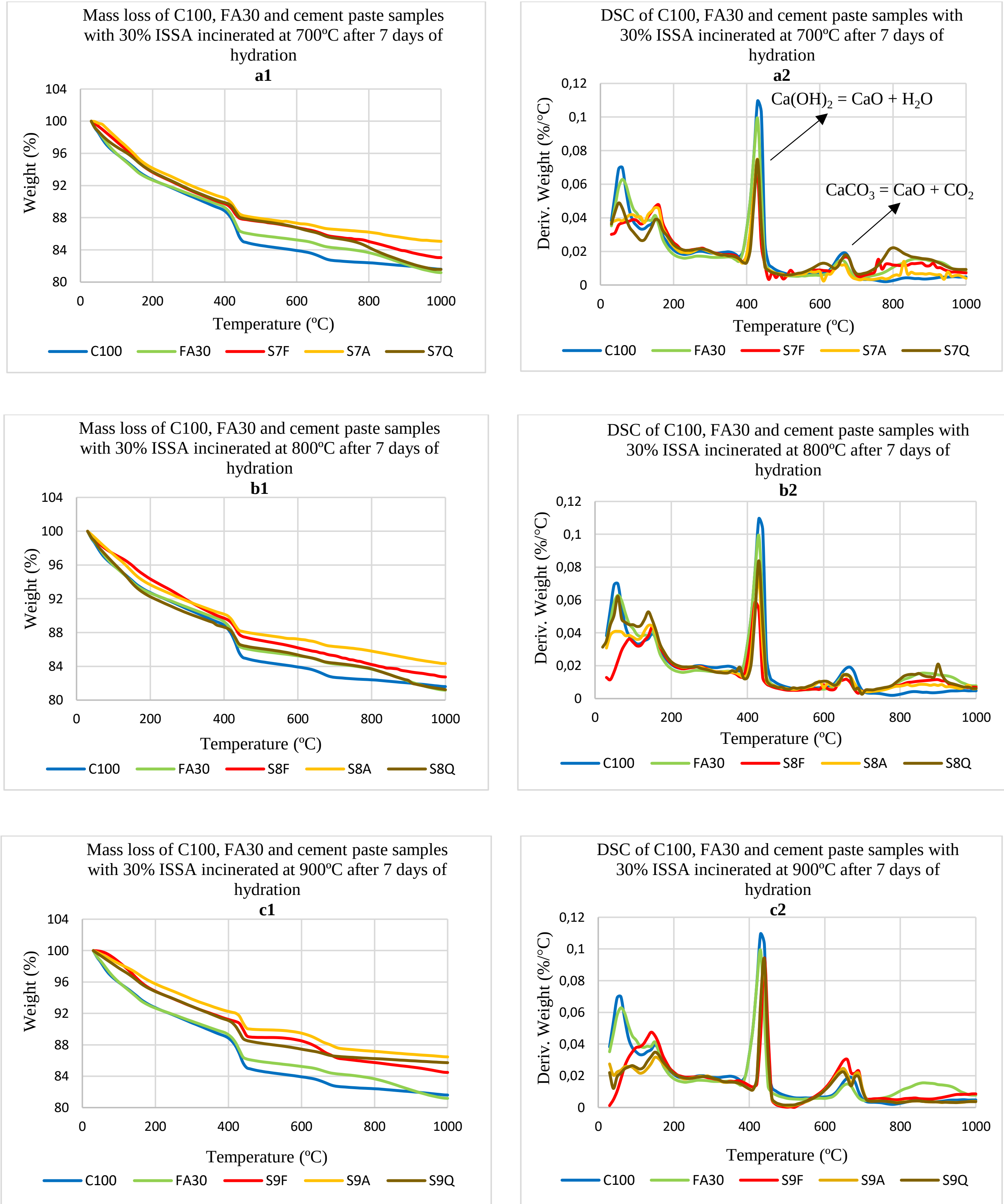

Figure 55: TGA weight loss profiles of cement pastes C100 (100% PC paste), FA30 (cement paste containing 30% replacement of PC by FA) and S7F/S7A/S7Q, S8F/S8A/S8Q and S9F/S9A/S9Q (cement paste containing 30% ISSA) after 7 days of hydration.

4.4.1.3. *Fourth and fifth peaks*

Furthermore, fourth peaks were observed at 600°C– 710°C in Figure 54 – 56 (a2, b2 and c2). These peaks are related to the decarbonation of calcium carbonate that took place according to the reaction shown in Equation 7. (Scrivener *et al.,* 2018). It was noted that the intensities of these peaks were reduced with the addition of ISSA after 6 hours of curing. However, they began to show comparable intensities after 7 and 28 days of curing. Some exothermic effects beyond 840°C up to 1000°C were observed on ISSA blended cement pastes particularly, S7Q and S8Q after 6 hours of curing. These peaks were also observed after 7 days of hydration for cement paste samples S7Q, S8Q and FA30. Interestingly, these peaks were only observed on the reference samples C100 and FA30 after 28 days and not on ISSA blended cement pastes. These peaks are related to the recrystallization of wollastonite ($CaSiO_3$) in the cement paste mixtures (Khan *et al.,* 2019). The peaks observed on S7Q and S8Q were linked to the rapid mass loss of S7Q and S8Q samples seen in the TGA curves at elevated temperatures (Figure 54, a1 and b1). These observations suggest that the ISSA (quenched) blended cement pastes were more reactive at early ages. The microscopic analysis of cement pastes containing quenched ISSA incinerated at 800ºC also showed better hydration characteristics (see Section 4.3.2/ 4.3.3).

4.4.2. The effect of ISSA on cement paste TGA mass loss

In general, the exposure to high temperatures led to moisture loss of the cement paste samples. This was mainly due to the evaporation of bound water and the dehydration of hydration products. The mass loss increased with an increase in the temperature. TGA results showed a reduction in mass loss of the cement pastes with the addition of ISSA (Figures 54 - 56, a1 - c1). This suggests that partially replacing some of the cement with ISSA and FA made the hydration process slower. According to Boualleg *et al.* (2017), this observation may be attributed to the following:

- Reduction in calcium silicates and aluminates contents of cement paste;
- Consumption of calcium hydroxide due to the pozzolanic reaction of ISSA especially at early ages;
- Reduction of the calcium hydroxide (a compound that is most vulnerable to external attacks) due to a lower amount of PC in the paste;
- The slow reactivity of ISSA which slowed down the hydration due to less C-S-H production, and consequently resulted in reduced mass loss.

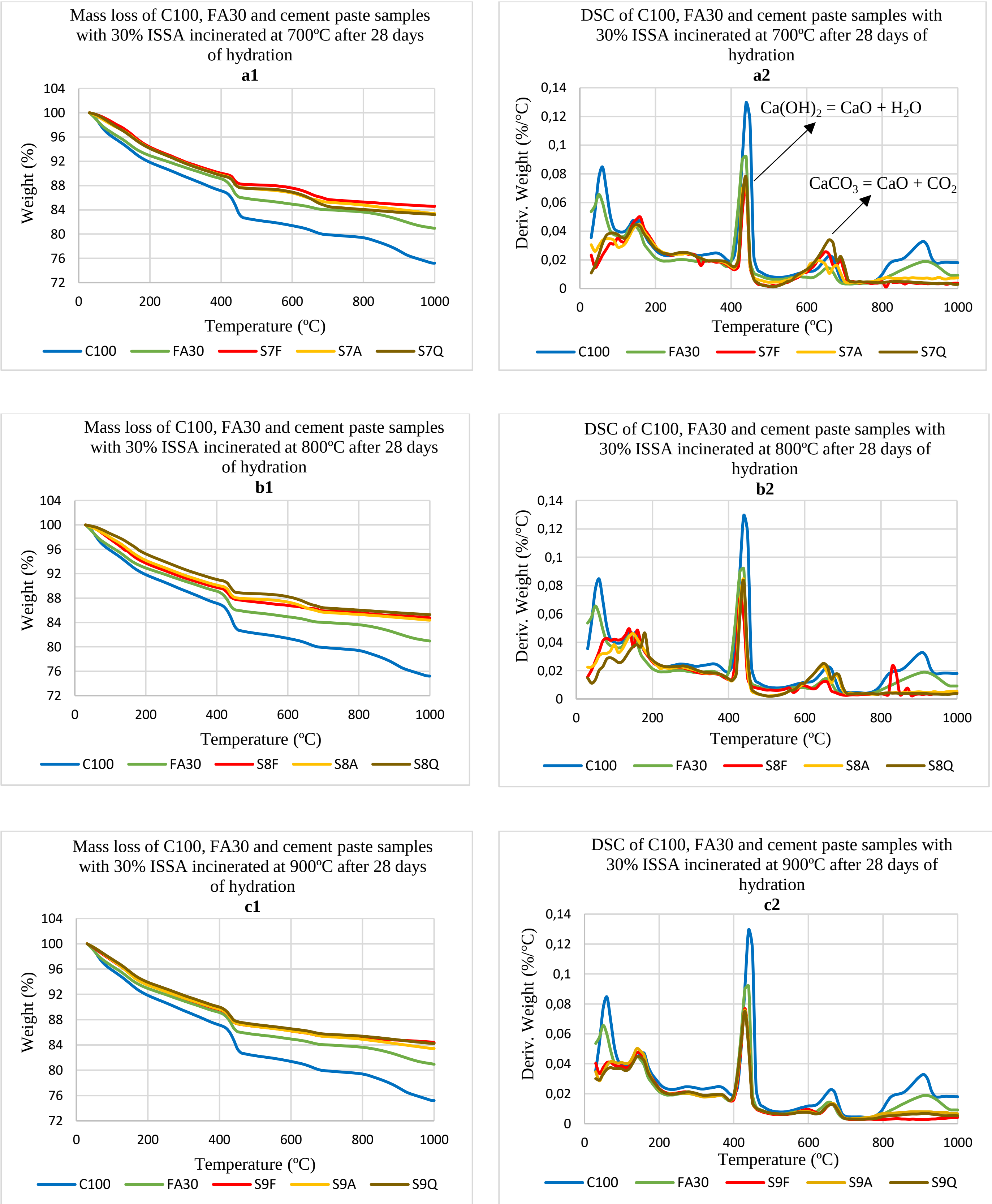

Figure 56: TGA weight loss profiles of cement pastes C100 (100% PC paste), FA30 (cement paste containing 30% replacement of PC by FA) and S7F/S7A/S7Q, S8F/S8A/S8Q and S9F/S9A/S9Q (cement paste containing 30% ISSA) after 28 days of hydration..

4.4.2.1. *Effect on the mass loss after 6 hours*

Figure 54 (a1 – c1) shows the TGA mass loss curves obtained after 6 hours of hydration. The overall mass loss obtained for each sample (initial – final) was calculated from the curves. Figure 57 shows a presentation of the overall mass losses obtained for all the cement paste samples after 6 hours of hydration (plotted separately for clear scaling). A fluctuating trend was observed on ISSA blended cement pastes. A total mass loss of 8.48% was obtained for the reference C100. These results were comparable with ISSA blended cement. Interestingly, a slightly higher mass loss was obtained for sample S7Q with a total mass loss of 8.63%, followed by S8Q with total mass loss of 7.97% and S7F with a mass loss of 7.09%. These results can also be linked to a high thermal reactivity of the ISSA at elevated temperatures, particularly the quenched ISSA.

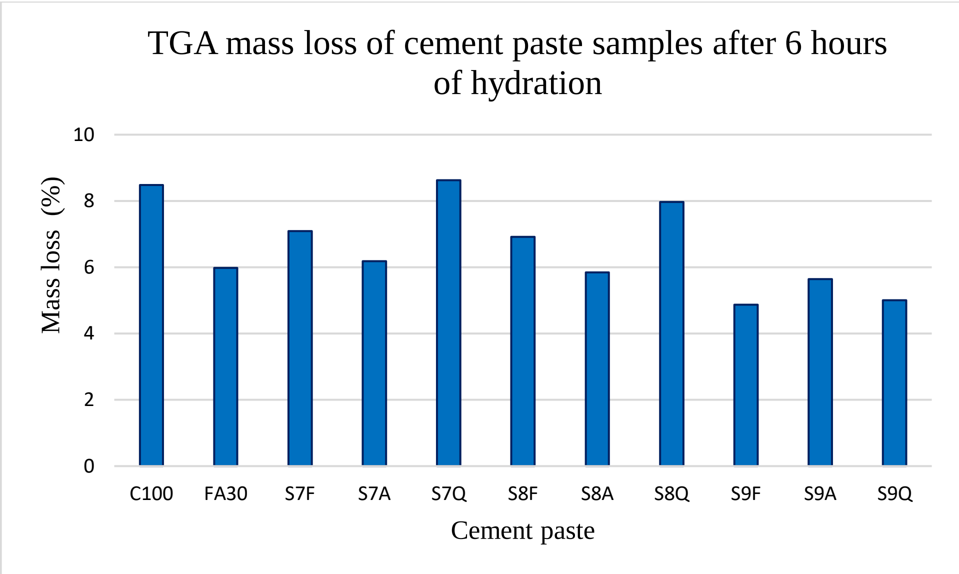

Figure 57: Mass loss of cement paste samples after 6 hours of hydration

A total mass loss of 5.98% was obtained for FA blended cement paste (FA30) suggesting a reduction in the reactivity due to the displacement of cement in the paste. Figure 54, b1 and c1 shows the mass loss curves of samples containing ISSA incinerated at 800ºC and 900ºC respectively. Figure 57 shows that the overall mass loss decreased with an increase in the incineration temperature of the ISSA used in the cement pastes, after 6 hours of hydration. Mass loss percentages of 6.92%, 5.85% and 7,97% were reported for S8F, S8A and S8Q and 4.87%, 5.64% and 5.01% were reported for samples S9F, S9A and S9Q respectively.

4.4.2.2. *Effect on the mass loss at 7 days*

Figure 55 (a1 – c1) shows the TGA mass loss curves obtained after 7 days of hydration. The overall mass loss percentage of each sample is shown in Figure 58. A total mass loss of 18.4% was obtained for the reference sample and 18.82% for the FA blended cement paste sample. It is important to note that FA30 cement paste showed a higher mass loss compared to the reference sample at 7 days. These results are attributed to the heterogeneous nucleation effect produced by FA that tends to accelerate the hydration of cement consequently resulting in more mass loss (Zeng *et al.,* 2012). The results also show that both S7Q and S8Q went as far as surpassing the total mass loss of the PC mix at high temperatures. The results of these samples were highly comparable to those of the FA blended cement paste with values of 18.43% and 18.76% being reported for S7Q and S8Q respectively.

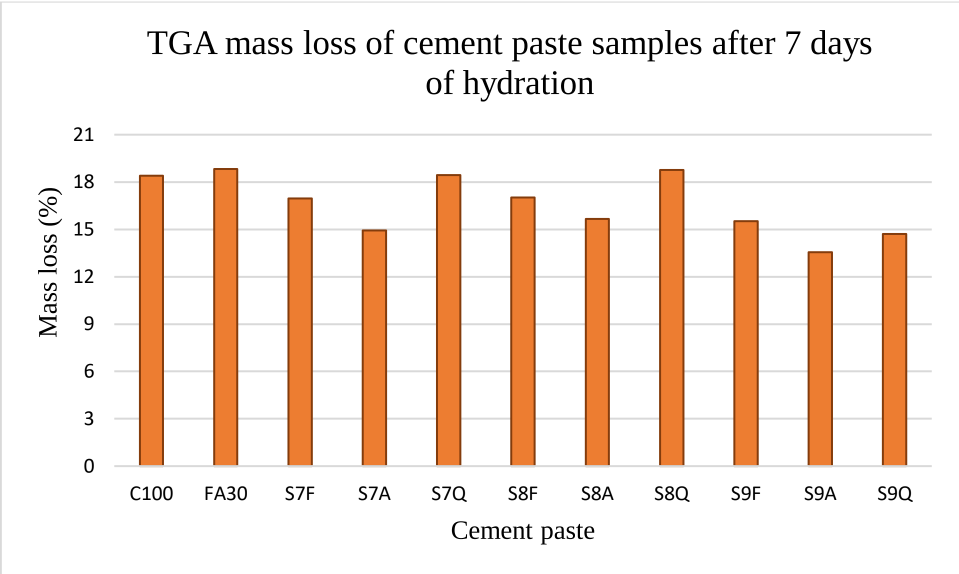

Figure 58: Mass loss of cement paste samples after 7 days of hydration

According to literature, mixing PC with ISSA can also influence the kinetics of hydration and more notably the alite dissolution (Tantawy *et al.,* 2013). Thus, the rapid mass loss of S7Q and S8Q at high temperatures (700ºC - 1000ºC) can also be linked to the hydration reactions in the pastes. According to Mejdi *et al.* (2020), increased hydration in ISSA blended cement paste is attributed to orthophosphate ions (PO_4^{3-}) released by ISSA. In conjunction with the characterization and observations made during the cement paste preparation, these results can also be linked to i) the irregular shape of ISSA particles that gave rise to an interlocked structure on the unreacted particles; ii) reduced influence of the w/c ratio due to absorption of water in ISSA particles; and iii) the slow water removal of ISSA which enabled complete cement hydration.

Reductions in mass loss were obtained with the addition of ISSA for samples S7F and S7A with values of 16.95% and 14.93% respectively, S8F and S8A with values of 17.03% and 15.66% and S9F, S9A and S9Q with values 15.52%, 13,55% and 14.71% respectively. Overall, the lowest mass losses were obtained for cement pastes containing air cooled ISSA (A) for all incineration temperatures after 7 days of hydration. These results suggest that the quenched (Q) ISSA showed better performance in terms of thermal reactivity and mass loss.

4.4.2.3. Effect on the mass loss at 28 days

Figure 56 (a1 – c1) showed the TGA curves obtained at 28 days of curing. The overall mass loss of each sample is shown in Figure 59. After 28 days, a total mass loss of 24.8% was obtained for the reference sample C100 and 19.05% for FA30 cement paste. The total mass loss of the reference sample and FA30 cement paste showed an increase with an increase in curing time, indicating an increase in the degree of hydration over time (see Figure 59). Slight increases in the mass losses of ISSA blended cement pastes were also observed with an increase in curing time. Values of 15,43%, 16,61% and 16,79% for samples S7F, S7A and S7Q, 15.24%, 15,62% and 14,72% for samples S8F, S8A and S8Q and lastly 15.6%, 16.57% and 15.78% for S9F, S9A and S9Q were obtained, respectively.

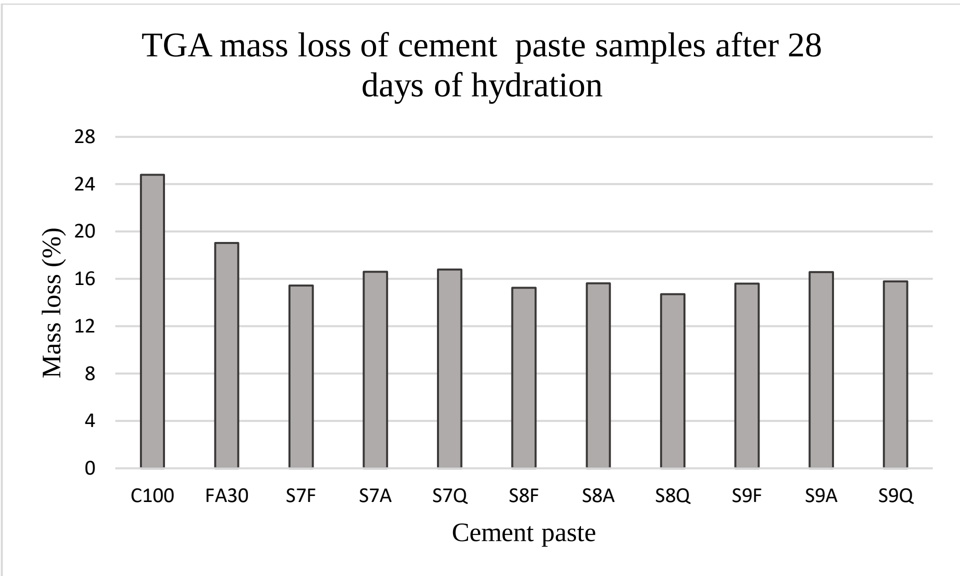

Figure 59: Mass loss of cement paste samples after 28 days of hydration

It is also important to note that the mass loss curves of ISSA blended cement pastes were more closely related to each other than to the FA30 cement paste and the reference sample resulting in closely packed curves (Figure 56, a1-c1). These results indicate that at later ages the differently cooled ISSA's investigated started showing the same reactivity. As a result, the relation between the cooling rate of ISSA and the mass loss varied with the incineration temperatures of the ISSA.

4.4.2.4. The effect of curing age on the mass loss

A distinct increase in mass loss with curing time was observed for all the cement pastes analysed. As shown in Figure 60, this relation proceeded up to 28 days of curing for the reference mix (8.48% after 6 hours to 18.4% after 7 days and 24.8% after 28 days of hydration) and FA30 cement paste (5.98% after 6 hours, 18.82% after 7 days and 19.05% after 28 days). However, for ISSA blended cement pastes an increase in the mass loss was observed more distinctively from 6 hours to 7 days. From 7 days to 28 days, a fluctuating trend was observed with a majority of the samples showing slight increases in the mass loss.

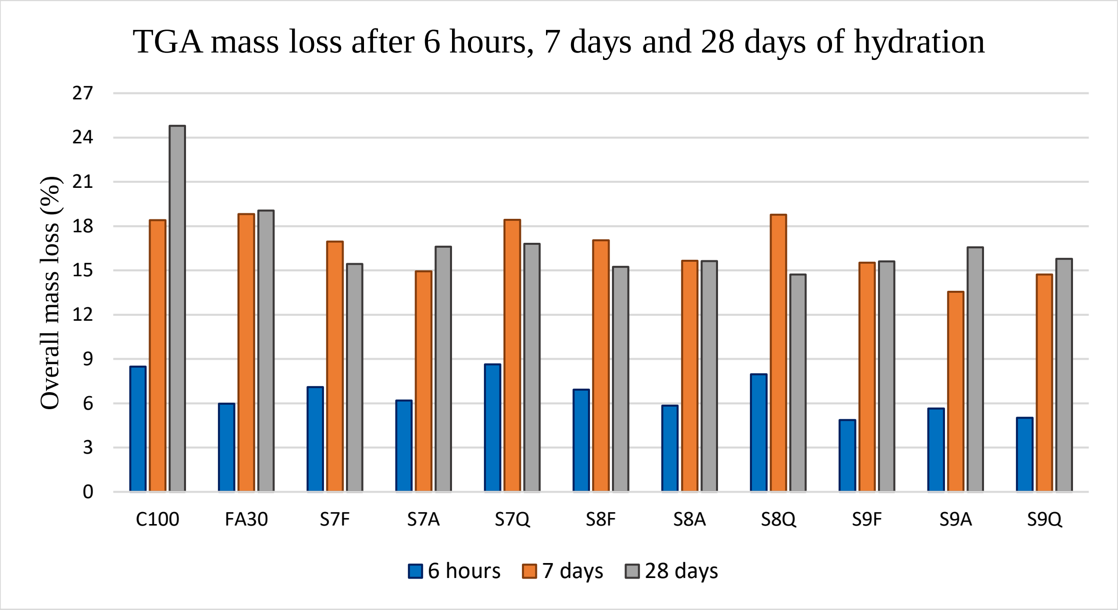

Figure 60: Mass loss of cement paste samples after 6 hours, 7 days and 28 days of hydration

Sample S9F increased from 4.87% after 6 hours to 15.52% after 7 days and only increased to a value 15.6% after 28 days of hydration. A reduction in mass loss was also observed for samples S7F, S7Q, S8F and S8Q from 7 days to 28 days and since a lower endothermic effect coincides with a lower activation energy (de Souza *et al.*, 2014), these results suggest that the $Ca(OH)_2$ crystallinity was low at later ages. An increase in mass loss with an increase in curing time is related to progressive hydration over time. These results also suggest that the hydration of ISSA blended cement paste took place at a slower rate than the C100 and FA30 cement paste samples at later stages.

4.4.2.5. The effect of incineration temperature and cooling rate of ISSA on the TGA mass loss

Although the mass loss of differently cooled ISSA blended cement pastes varied with the curing ages, it was noted that in most instances more mass loss was obtained for ISSA blended cement paste containing quenched ISSA. A relationship was also established between the ISSA incineration temperature and the mass loss of ISSA blended cement paste at all the respective ages. An increase in the ISSA incineration temperature resulted in a reduced mass loss of the cement paste. As a result, the lowest mass loss percentages were obtained for cement paste samples containing ISSA incinerated at 900ºC. In terms of energy, incineration temperatures below 900ºC are better from an economic standpoint.

4.5. Hydration and reactivity analysis studies

Chemically combined water ($H_2O_{Q.comb}$) and calcium hydroxide contents were calculated based on the TGA results illustrated in Figures 54 - 56 (a1 - c1). The techniques described in Section 3.5.2 were used to evaluate the effect of ISSA at a 30% replacement level of PC on the hydration of cement paste. The objective of this analysis was to determine the level of hydration and pozzolanic activity of ISSA blended cement pastes. Calcium hydroxide was used as a performance and durability indicator of the cement paste mixtures. Calcium hydroxide is known as the basicity reserve of cementitious material and it maintains a high pH level of 12.6 (Boualleg *et al.*, 2017). The decomposition of calcium hydroxide occurred in the temperature range of 400ºC to 450ºC. This was followed by the decomposition of calcium carbonate at 600ºC -710ºC.

The total amount of calcium hydroxide produced in each sample indicates the moisture and pozzolanic reaction (Boualleg *et al.*, 2017). Often, the overall calcium hydroxide content is lowered by pozzolanic material in blended cement products (PC + pozzolana) (Massazza, 1998). However, after 28 days it may be higher, lower, (Abdul-Maula & Odler, 1981; Diamond *et al.*, 1988; Barry, 1988) or the same (Costa & Massazza, 1983; Diamond *et al.*, 1988). As a result, a lower amount of CO_2 is required to react with calcium hydroxide in order to absorb the entire calcium hydroxide. This would allow the pH of the cement paste water to drop more quickly (Roziere *et al.*, 2009), and possibly initiate corrosion of the reinforcing steel.

4.5.1. Chemically combined water

Figure 61 illustrates the chemically combined water ($H_2O_{Q.comb}$) of C100, FA30 cement paste and ISSA blended cement pastes after 6 hours, 7 days and 28 days of hydration. It was noted that the amount of $H_2O_{Q.comb}$ showed a reduction with the displacement of PC by FA and ISSA. These results indicated that at early ages the amount of chemically combined water was related to the compressive strength. The substitution of 30% PC with ISSA led to the reduction of C_2S and C_3S. These are main the compounds responsible for strength development in the early and late stages of cement hydration (Bougara *et al.*, 2010; Boualleg *et al.*, 2017). Figure 61 also shows that a radical increase in $H_2O_{Q.comb}$ was obtained from 6 hours to 7 days for all cement paste samples.

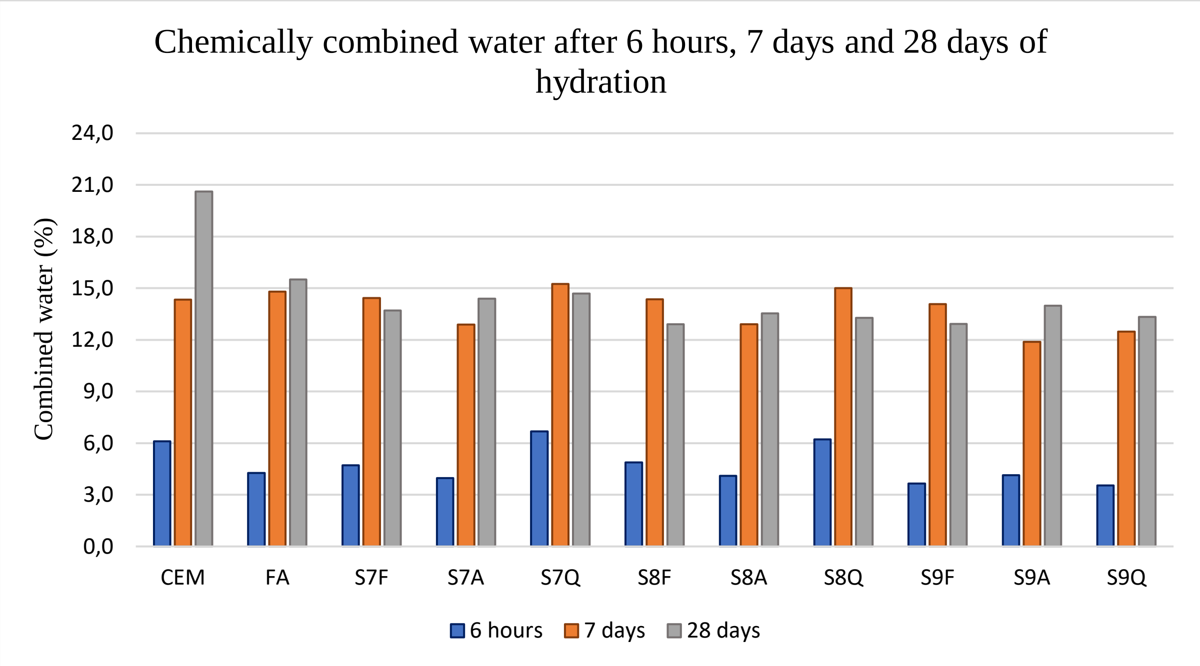

Figure 61: Chemically combined water content of cement paste samples after 6 hours, 7 days and 28 days of hydration

The highest value of $H_2O_{Q.comb}$ obtained after 6 hours of curing was found to be that of S7Q with a percentage of 6.7%. From 7 to 28 days, the $H_2O_{Q.comb}$ of cement paste containing ISSA increased at a lower rate than the reference pastes, with some samples showing a reduction in the $H_2O_{Q.comb}$ particularly from 7 to 28 days. This result is attributed to the lower amount of PC and the pozzolanic reaction effect of ISSA. The rate of increase or decrease was dependent on the cooling rate and the incineration temperature of the ISSA. From 7 to 28 days, the reference sample showed the highest percentage increase of 44.6% of $H_2O_{Q.comb}$ compared to percentage increases of 4.7% for FA30, 11.6% for S7A, 4.7% for S8A, 17.6% for S9A and 6.4% for sample S9Q. The reduced $H_2O_{Q.comb}$ obtained for ISSA blended cement pastes can be related to the high-water absorption of ISSA consequently producing a smaller amount of hydration products.

FA blended cement paste had the second highest amount of $H_2O_{Q.comb}$ after 28 days of hydration. This result can be attributed to the high surface area of fly ash that tends to accelerate the hydration of cement pastes by its reaction with liberated $Ca(OH)_2$. This reaction results in the production of supplementary hydration products as well as higher combined water contents. Reductions in $H_2O_{Q.comb}$ of 4.9%, 3.9%, 10.4%, 11.3% and 8.5% were obtained for samples S7F, S7Q, S8F, S8Q and S9F with an increase in hydration age from 7 days to 28 days. These reductions can be related to the pozzolanic reactions that took place resulting in $Ca(OH)_2$ depletion in the cement pastes and the polymerization of C-S-H gel that results in delayed hydration reactions due to the presence of supplementary additions (Boualleg *et al*, 2017).

4.5.1.1. The effect of incineration temperature and cooling rate on chemically combined water

Fluctuations of $H_2O_{Q.comb}$ of the ISSA blended cement pastes at the different cooling rates (F_{ISSA}, A_{ISSA} and Q_{ISSA}) and temperatures of 700°C, 800°C and 900°C were observed (see Figure 61). Based on these fluctuations, direct relations between the $H_2O_{Q.comb}$ content and incineration temperature or $H_2O_{Q.comb}$ and cooling rate were not established. This is due to the fact that $H_2O_{Q.comb}$ is most commonly related to the water/binder ratio. The cement pastes were all prepared using the same water/binder ratio. As a result, the observed fluctuations are assumed to be related to the varying compositions of the ISSA's obtained through XRF analysis, for all the cooling rates.

4.5.2. Evolution of calcium hydroxide

Figure 62 shows the amounts of calcium hydroxide content of the cement pastes after 6 hours, 7 days and 28 days of hydration. The results obtained for ISSA blended cement paste were compared with C100 and FA30 cement pastes. Cement paste produces calcium hydroxide as early as 6 hours of age as a result of the C_2S and C_3S hydration reactions which constitutes 80% of the cement matrix (Sisomphon & Franke, 2011). Cement paste samples containing pozzolanic material tend to have their pozzolanic reaction initiated simultaneously with the cement reaction. The main outcome observed on the TGA/DSC curves at the different ages was the mass loss that corresponded to the dehydroxylation of calcium hydroxide at 400ºC to 450ºC (DSC peak of 420ºC) and the decomposition of $CaCO_3$ at 600ºC to 710ºC.

The starting and ending temperature of calcium hydroxide dehydroxylation and the decomposition of $CaCO_3$ varies with the enthalpy of the reaction taking place (Anjos *et al.,* 2019). This effect is dependent on the age, type, amount of cement, w/c ratio and material used to replace cement in the paste (Anjos *et al.*, 2019; Pane & Hansen, 2005; Alarcon Ruiz *et al.*, 2005; El-Shimy *et al.*, 2000; Dweck *et al.*, 2000).

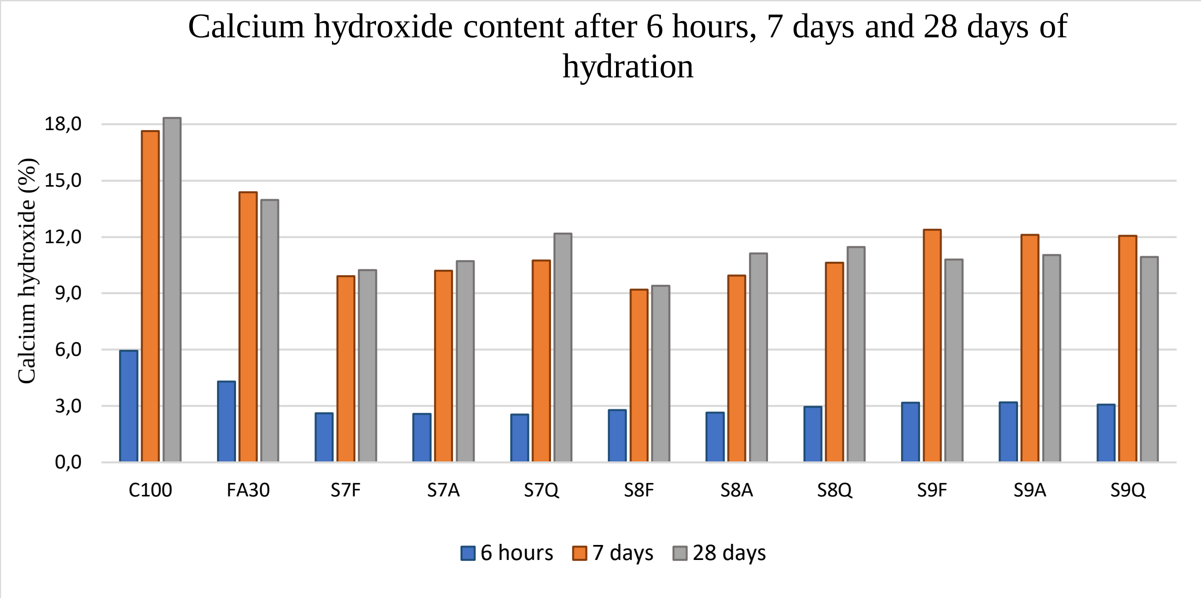

Figure 62: Calcium hydroxide content of cement paste samples after 6 hours, 7 days and 28 days of hydration

4.5.2.1. *Effect of ISSA on calcium hydroxide content after 6 hours of hydration*

Figure 62 shows a reduction of $Ca(OH)_2$ content with the addition of FA and ISSA, particularly with the addition of ISSA blended cement paste at all the ages. This is mainly attributed to the effect of pozzolanic material which significantly lowered the hydration reaction especially at early ages, compared to sample C100. A value of 5.9% was obtained for C100 and 4.3% for FA30 resulting in a 27% reduction of $Ca(OH)_2$ with the addition of FA after 6 hours of curing. The results obtained after each age were also plotted separately for clear scaling (see Figure 63). Calcium hydroxide reductions of over 50% on average were observed with the addition of ISSA into the cement paste. However, it should also be noted that the $Ca(OH)_2$ content increased with an increase in the incineration temperature at this age.

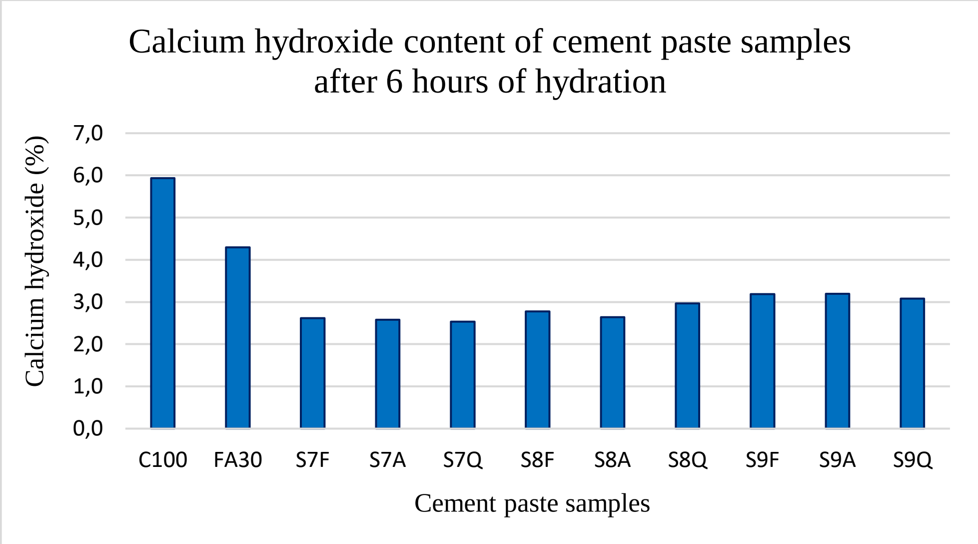

Figure 63: Calcium hydroxide of PC and FA/ISSA blended cement paste samples after 6 hours of hydration

Cement paste containing ISSA incinerated at 900ºC showed an average reduction of 46.32% in $Ca(OH)_2$ content with values of 3.2%, 3.2% and 3.1% having been reported for samples S9F, S9A and S9Q respectively. In comparison, average reduction percentages of 52.54% and 55.37% were obtained for cement pastes containing ISSA incinerated at 800ºC and 700ºC respectively. Although the $Ca(OH)_2$ content showed a notable reduction with the addition of ISSA, there was, however, an increase with an increase the ISSA incineration temperature from 700ºC to 900ºC. A reduction in $Ca(OH)_2$ content is often used an indication of the pozzolanicity of supplementary materials in cement. Thus, these results indicate that ISSA had a certain level of pozzolanicity.

4.5.2.2. Effect of ISSA on calcium hydroxide content after 7 days of hydration

Analysis after seven days of hydration showed that the $Ca(OH)_2$ content was increased in comparison to the $Ca(OH)_2$ content after 6 hours of hydration for all cement paste samples, as a result of the hydrolysis of C-S-H. The calcium hydroxide content obtained at 7 days on ISSA blended cement was lower than that of FA30 cement (14.4%) which was lower than that of C100 (17.6%). The reduction of the amount of PC in the ISSA blended cement paste led to the reduction of C-S-H which consists of the main binding properties. In comparing the performance of ISSA blended cement pastes, S9F exhibited the highest amount of $Ca(OH)_2$ with a value of 12.4% followed by S9A and S9Q with a value of 12.1% for both samples (see Figure 64).

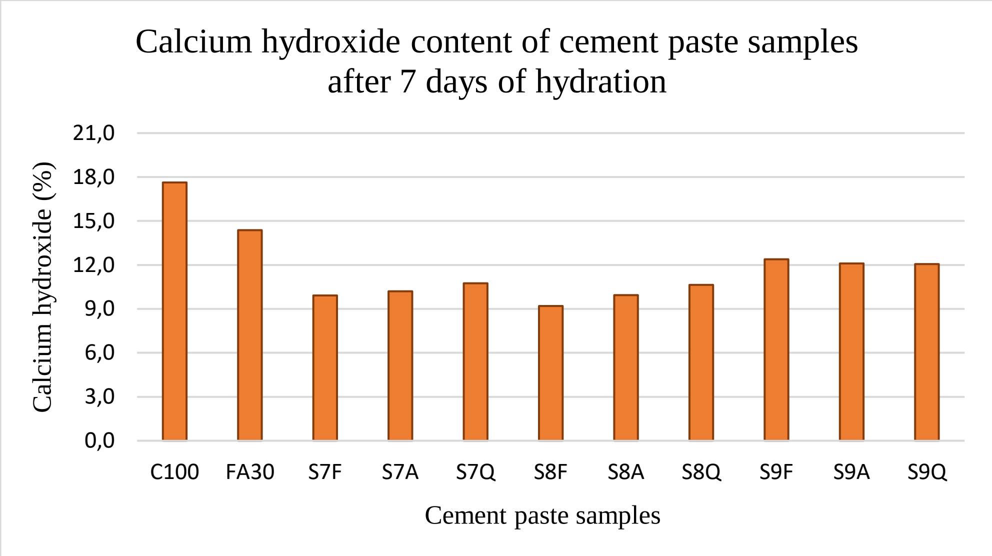

Figure 64: Calcium hydroxide content of PC and FA/ISSA blended cement paste samples after 7 days of hydration

Furthermore, values of 9.2%, 9.9%, 10.6%, 9.9%, 10.2% and 10.7% were obtained for samples S8F, S8A, S8Q, S7F, S7A and S7Q respectively. From these results it was established that the $Ca(OH)_2$ content increased with an increase in the incineration temperature of ISSA. After 7 days of hydration, the reduction percentage of $Ca(OH)_2$ content was lower compared to the reduction percentage after 6 hours (Figure 62). These results are related to accumulation of $Ca(OH)_2$ released from the hydration process in the pore solution of the cement paste. At a later stage, this accumulation triggered a slow pozzolanic reaction of the ISSA with $Ca(OH)_2$ thus resulting in the formation of additional hydration products (Tantawy *et al.*, 2013). The cooling rate also played a role in this effect. The $Ca(OH)_2$ content showed an increase in the order $F_{ISSA} < A_{ISSA} < Q_{ISSA}$ of the cooling rates for cement paste containing ISSA incinerated at 700ºC and 800ºC. For cement paste containing ISSA incinerated at 900ºC, the highest $Ca(OH)_2$ content was obtained for furnace cooled ISSA.

4.5.2.3. Effect of ISSA on calcium hydroxide content after 28 days of hydration

Figure 65 shows the $Ca(OH)_2$ content that was obtained in the cement paste samples after 28 days of hydration. It was noted that the $Ca(OH)_2$ content increased in the order $F_{ISSA} < A_{ISSA} < Q_{ISSA}$ of the ISSA cooling rates. With the exception of cement paste containing ISSA incinerated at 900ºC, in which approximately the same content of $Ca(OH)_2$ was obtained for S9A and S9Q. However, based on the overall results it was deduced that the percentage increase in $Ca(OH)_2$ content was significantly high for the cement pastes samples containing quenched ISSA after 28 days of curing, similar to the results obtained after 6 hours and 7 days of hydration.

A reduction of $Ca(OH)_2$ is often expected at later ages on blended cement especially if the material used as a partial replacement is pozzolanic (Massazza, 1998). However, in Figure 65, a fluctuating trend was obtained at 28 days of age for cement paste samples containing ISSA. Some of the ISSA blended cement pastes samples showed a reduction in $Ca(OH)_2$ content, whereas the majority of the samples showed an increase in $Ca(OH)_2$ content. The reductions occurred due to the progress of the pozzolanic reaction and the changes in the composition of hydrates as the hydration progresses. According to Massazza, (1998); fluctuations in calcium hydroxide content of cement paste containing pozzolanic materials are caused by:

- Impediments to the progression of reactions;
- Pozzolanic reaction;
- Changes in the hydrated phases compositions;
- Quickening of the clinker calcium silicates hydrolysis.

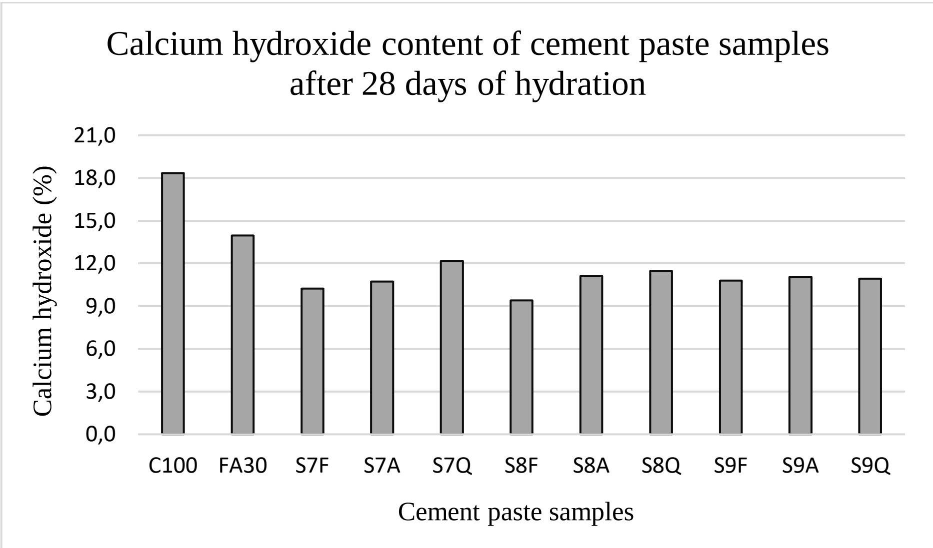

Figure 65: Calcium hydroxide content of PC and FA/ISSA blended cement paste samples after 28 days of hydration

It is often stated that the $Ca(OH)_2$ content is highly dependent on the w/c ratio and the nature of the pozzolan. In this case, the same water cement ratio was applied on all ISSA blended cement paste samples. Thus, the observed changes can be attributed to the incineration temperatures of 700ºC, 800ºC and 900ºC as well as the cooling rates of the ISSA (F_{ISSA}, A_{ISSA} and Q_{ISSA}) that make up the nature of the ISSA. Figure 62 showed that an increase in $Ca(OH)_2$ content occurred from 7 days to 28 days for samples S7F, S7A, S7Q, S8F, S8A and S8Q with increases of 3.03%, 4.90%, 14.01%, 2.17%, 12.12% and 8.49% respectively. This observation can be related to the increase in the degree of hydration, which means that the ISSA's used in these pastes could not reduce the $Ca(OH)_2$ content after 28 days of hydration. According to Anjos *et al.* (2019) the absence of $Ca(OH)_2$ is often expected in cement paste containing pozzolanic material. This is due to the consumption of $Ca(OH)_2$ by the pozzolanic material to produce C-S-H in this case ISSA up to 28 days. Thus, the remaining $Ca(OH)_2$ may be a result of the pozzolanic material behaving as a filler.

The increase in $Ca(OH)_2$ observed also suggests that although 30% of PC was replaced, the ISSA material still resulted in an increase in the production of $Ca(OH)_2$ and thus could not reduce the $Ca(OH)_2$ content after 28 days of hydration. The increase in the $Ca(OH)_2$ content also indicates that the pozzolanic reaction kinetics of these ISSA's were slower than the cement paste reaction. This also suggests that an increase in the replacement level could enhance the pozzolanic reaction. When considering these blended cement pastes, it is important to also note the fast effect of the cement reaction. The excess $Ca(OH)_2$ in these samples can also be explained by the following:

i) The ISSA was yet to react with the $Ca(OH)_2$ in excess over 28 days of curing;
ii) Use of these materials increased the cement hydration although at a lower rate than the reference sample;
iii) The material was depleted prior to the consumption of $Ca(OH)_2$.

A reduction in calcium hydroxide content was obtained for sample FA30 and for ISSA blended cement paste samples S9F, S9A and S9Q as expected. The $Ca(OH)_2$ content obtained for these samples was lower than the reference samples after 28 days of hydration. Figure 62 shows that samples FA30, S9F, S9A and S9Q had reductions of 2.78%, 12.9%, 9,09% and 9.92% from 7 days to 28 days. These results suggest that pozzolanic reactions took place and consumed the calcium hydroxide content. As a result, the cementitious matrices of these pastes are considered more durable due to the reduction of calcium hydroxide after 28 days, a compound that can easily be susceptible to harmful agents.

The reduction in $Ca(OH)_2$ also showed the capability of ISSA to react with the $Ca(OH)_2$ derived from the reaction of cement. This reaction took place when the pozzolanic material in the blended cement paste started hydrating. The PC simultaneously released calcium hydroxide ions Ca^{++} and OH^-, and as the reaction proceeded the pozzolanic material captured the Ca^{++} ion to produce C-S-H or aluminate hydrates. In this case, the cement reaction was slower than the pozzolanic reaction, hence the reduction in calcium hydroxide. These findings are similar to previous research work on cement pastes containing pozzolanic materials by Anjos *et al.*

(2019). In a similar study conducted by Tantawy *et al.* (2013), the addition of ISSA in cement paste resulted in an enhanced pozzolanic reaction, thus contributing to the formation of crosslinked fibrous calcium silicate with a low Ca/Si ratio. From a pragmatic point of view, the low calcium hydroxide content is also linked to the effectiveness of ISSA as pozzolanic material.

4.6. The use of ISSA as a partial replacement of cement in mortar

4.6.1. Flow test results of mortar containing ISSA

The effect of ISSA on the workability was studied on mortar samples. The flow table test described in Section 3.6.3 was used. In this study, ISSA was used to replace 30% of PC in the preparation of mortar to assess its possible contribution to strength development. Figure 66 shows the results of the tests. A number of reports from literature have described the reduction in the workability of ISSA blended cement mixtures (Vouk *et al.*, 2016; Naamane *et al.*, 2016; Pan *et al.*, 2003; Monzo *et al.*, 1996). Similarly, in the presented work, the workability of ISSA blended cement was found to be in the range of 19.8% to 27.2%, considerably lower than that of reference mix (MC100) and FA30 cement mortar for which values of 38% and 34.5% were reported, respectively.

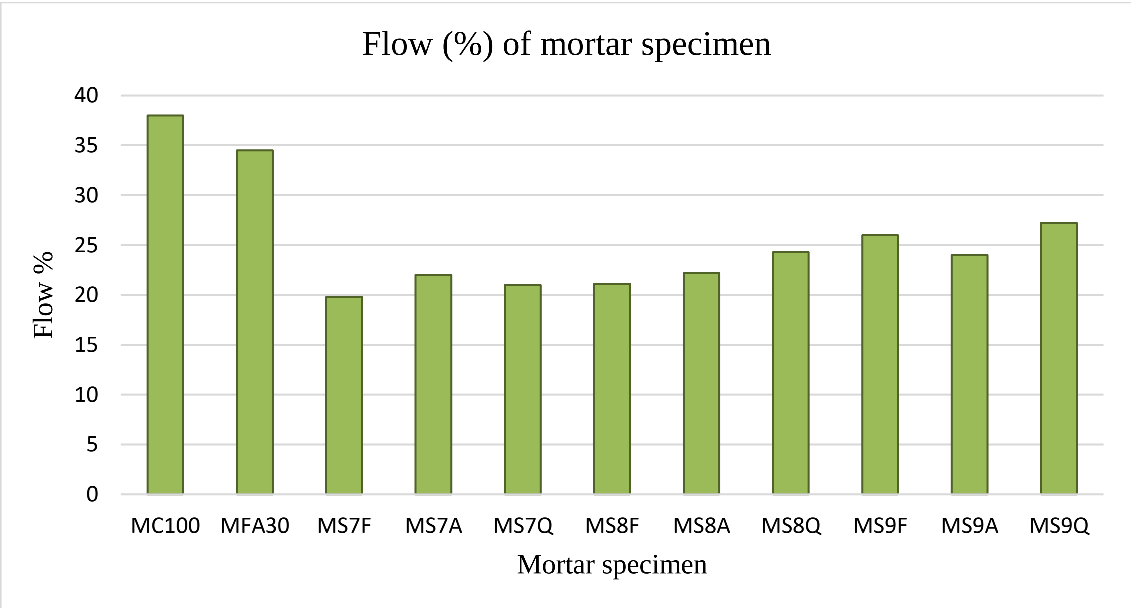

Figure 66: Flow of mortar samples

The reduction in mortar workability is attributed to the irregular morphology of ISSA particles (Figures 37 – 39). The reduction in workability of the cement mortar can also be attributed to the increased water absorption caused by ISSA. These results were also similar to previous research results in which using ISSA as a SCM in mortar was found to increase the water absorption. The increased water absorption simultaneously resulted in longer setting time and the reduction of mortar workability due to the high amounts of phosphorus pentoxide (P_2O_5) and sulphur trioxide (SO_3) found in the ISSA (Vouk *et al.,* 2016; Naamane *et al.,* 2016).

Figure 66 also shows a reduction of mortar workability on ISSA blended mortar compared to the reference sample. However, the increase in incineration temperature of ISSA from 700ºC to 900ºC was found to improve the workability. The F_{ISSA}, A_{ISSA} and Q_{ISSA} cooling rates had a varying influence on the flow percentage. Samples containing ISSA incinerated at 700ºC showed an increase in workability in the order: MS7F < MS7Q < MS7A, whereas for ISSA incinerated at 800ºC the increase observed was in the order: MS8F < MS8A < MS8Q and MS9A < MS9F < MS9Q for ISSA incinerated at 900ºC. As a result, the highest cooling rate (Q_{ISSA}) showed the highest workability results with the exception of sample MS7Q that was exceeded by sample MS7A.

4.6.2. Compressive strength test results

Figure 67 shows the compressive strength development of all mortar samples after 3, 7 and 28 days. The compressive strength showed an increase with the curing ages due to the hydration process that took place over time. The rate of increase in the compressive strengths of ISSA blended mortars between the ages was comparable to that of the reference sample MC100 and even higher for some samples, especially between 7 to 28 days. According to Neville, (2008), the increase in the formation of hydration products over time leads to an increase in the strength of mortar. In addition to this, the gradual increase in the hydration products in the mortar with curing time, enables the filling up of pores and development of a compact microstructure.

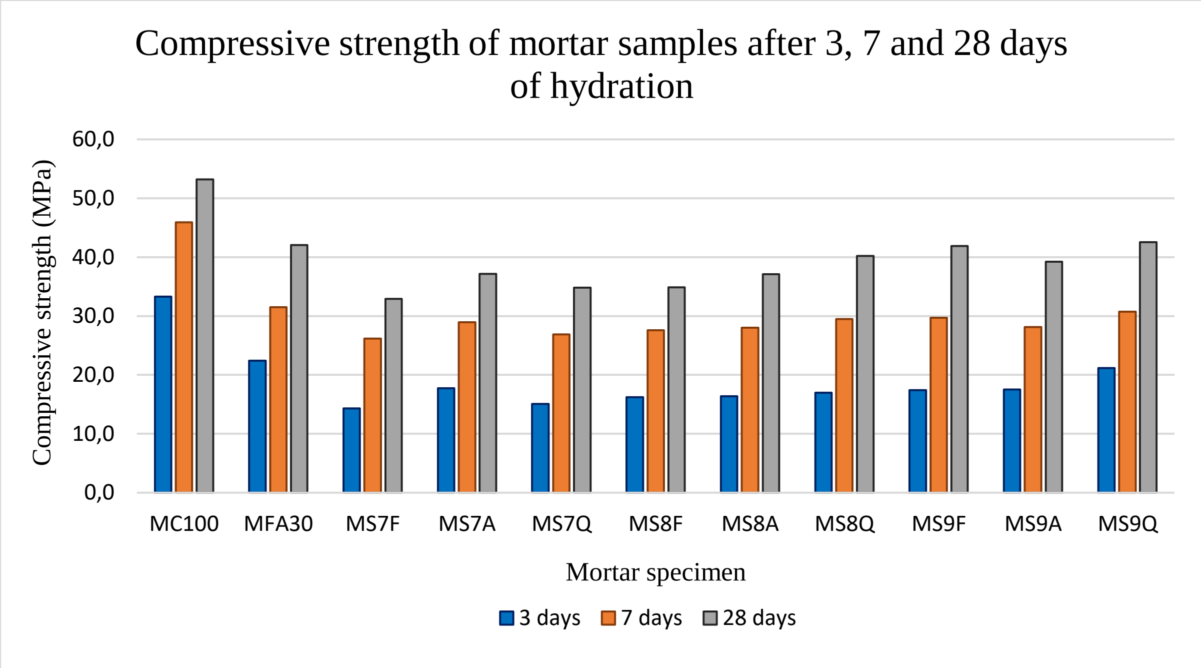

Figure 67: Compressive strength test results of mortar samples after 3 days, 7 days and 28 days of hydration

In Figure 67, it can be observed that a reduction in compressive strength occurred with the addition of ISSA and FA as a replacement of PC at all ages. These results were linked to the reduced rate of hydration reactions as a result of the displaced PC. Similarly, the hydration products formed in FA and ISSA blended cement pastes (see Section 4.3.2 and 4.3.3) were reduced compared to the reference sample C100 and the size of the products was smaller. The reduced amount of hydration products is assumed to have contributed to the ineffective binding of ISSA particles which results in the low strength of solidified ISSA blended mortar. However, it is also important to note that the compressive strengths of ISSA blended mortar were highly comparable to that of MFA30. Thus, it can be deduced that ISSA showed some effectiveness as a partial replacement of PC.

4.6.2.1. Effect of ISSA on compressive strength at 3 days of hydration

Figure 68 shows the compressive strength development of mortar samples after 3 days of curing (plotted separately for clear scaling). The highest percentage reduction in compressive strength was reported for sample MS7F with a reduction rate of 57.1% relative to the reference sample. The lowest strength reduction was observed for sample MS9Q with a reduction of 36.6% reported relative to the reference mortar.

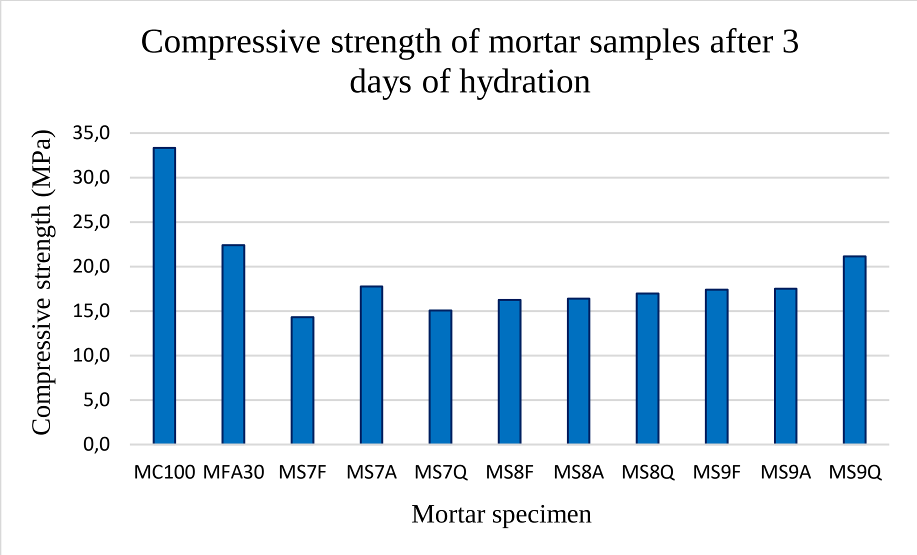

Figure 68: Compressive strength of mortar samples after 3 days of hydration

The percentage reduction of MFA30 was slightly lower with a reduction of 32.7%, which may be related to the rapid cementation and hydration properties of the fly ash. Approximately 50% reduction in compressive strength on average was obtained for the remainder of the ISSA blended mortars. These results are attributed to the irregular morphology of the ISSA which is assumed to have enabled a reduced packing density of the mortar thus resulting in reduced compressive strength. The large particles observed through SEM analysis of the ISSA may have also reduced the ability of the ISSA to fill up pores which resulted in a reduced compaction of the mortar.

The incineration temperatures and cooling rates played a vital role in the compressive strength trend. It can be observed that the compressive strength increased with an increase in the incineration temperature of ISSA from 700ºC to 900ºC. Samples: MS8Q, MS9F and MS9A had approximately the same compressive strength after 3 days of curing, with values of 17, 17.4 and 17.5 MPa respectively. The highest compressive strength on the ISSA blended mortar was that of sample MS9Q with a value of 21.1 MPa. Thus, it was deduced from these results that the highest cooling rate (Q_{ISSA}) reduced the weakening effect of ISSA related to its low cementing properties. These results can also be related to the amount of calcium hydroxide obtained in S9Q blended cement paste (Section 4.5.2).

4.6.2.2. Effect of ISSA on compressive strength after 7 days of hydration

Figure 67 showed that an increase in compressive strength occurred for all cement paste samples from 3 days to 7 days of curing. The increase in compressive strength of MFA30 and ISSA blended cement, although at a lower rate compared to the reference sample, is attributed to the conversion of $Ca(OH)_2$ into C-S-H as a result of pozzolanic reactions. Figure 69 shows that a reduction in compressive strength was obtained with the addition of FA and ISSA in the mortar after 7 days of hydration.

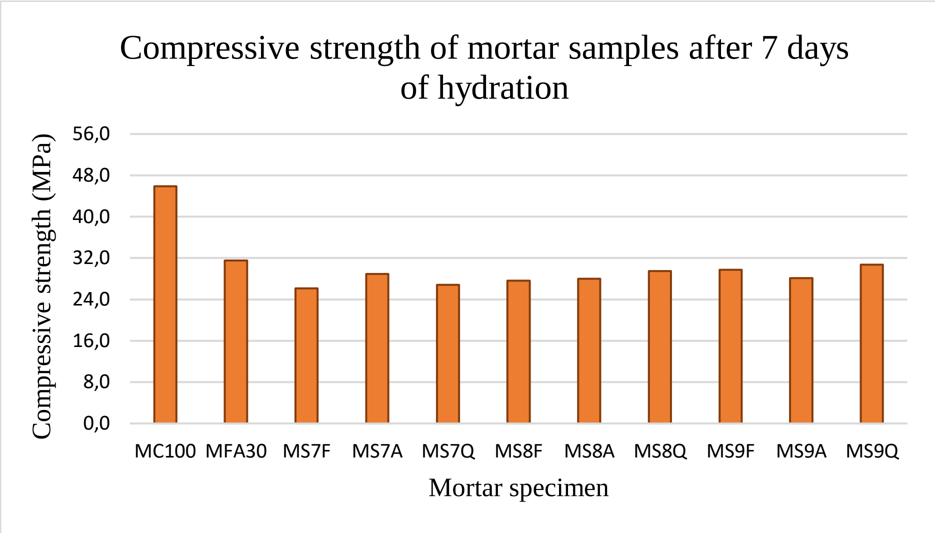

Figure 69: Compressive strength of mortar samples after 7 days of hydration

A compressive strength value of 45.9 MPa was obtained for the reference sample after 7 days of curing, resulting in a percentage increase of 37.8% compared to the compressive strength after 3 days of hydration (see Figure 68). MFA30 had the second highest strength obtained after 7 days with a value of 31.5 MPa. The results also showed that the compressive strength results of ISSA blended mortar samples obtained were comparable to the MFA30 samples with values of 30.7 MPa, 29.7 MPa, 29.5 MPa and 28.9 MPa reported for samples MS9Q, MS9F, MS8Q and MS7A respectively. The trend in these results was related to the contribution of free calcium hydroxide (Section 4.5.2). Although a reduction in $Ca(OH)_2$ was obtained, samples that had the highest $Ca(OH)_2$ at 7 days also exhibited the highest compressive strength.

The reduction in compressive strength with the addition of ISSA was also related to the fineness of the ISSA. In a study conducted by Halliday *et al.* (2012), it was established that coarser ISSA tends to contribute to the reduction in compressive strength. According to Section 4.2.2 of this study (particle size distribution), ISSA possessed the largest quantity of big particles compared to PC and FA. Section 4.2.5 also shows that the ISSA had an irregular morphology. The reduction in the compressive strength is thus partially related to the particle size distribution of the ISSA.

4.6.2.3. Effect of ISSA on compressive strength after 28 days of hydration

Figure 70 shows the compressive strength development of the mortar samples after 28 days of hydration. Low strength reduction rates were obtained for MFA30 and ISSA blended mortars compared to the reference sample at this age. A compressive strength result of 53.2 MPa was obtained for the reference sample C100. Sample MS9Q showed a slightly better performance than MFA30 (42 MPa) at 28 days of age with a value of 42.5 MPa (compressive strength reduction of 20.1% relative to the reference sample). These results were expected due to the high reactivity of quenched ISSA thus far, related to a higher degree of hydration. According to Chen & Poon (2017), the slow water removal of ISSA can enhance complete cement hydration to some extent, hence the performance of this sample. These results are also linked to the $Ca(OH)_2$ conversion and production of C-S-H as a result of pozzolanic reaction.

Figure 62 showed a substantial reduction in $Ca(OH)_2$ content for cement paste samples S8Q and S9Q compared to C100, thus the high compressive strength gain obtained for samples MS8Q and MS9Q was related to the contribution of C-S-H that seemingly outweighed the contribution of $Ca(OH)_2$. According to Mehta & Monteiro, (2014), C-S-H has a higher surface area and contributes largely to the strength development. The rate of increase in compressive strength of MS9Q and MFA30 was comparable to that of the reference sample although the overall compressive strength results were lower.

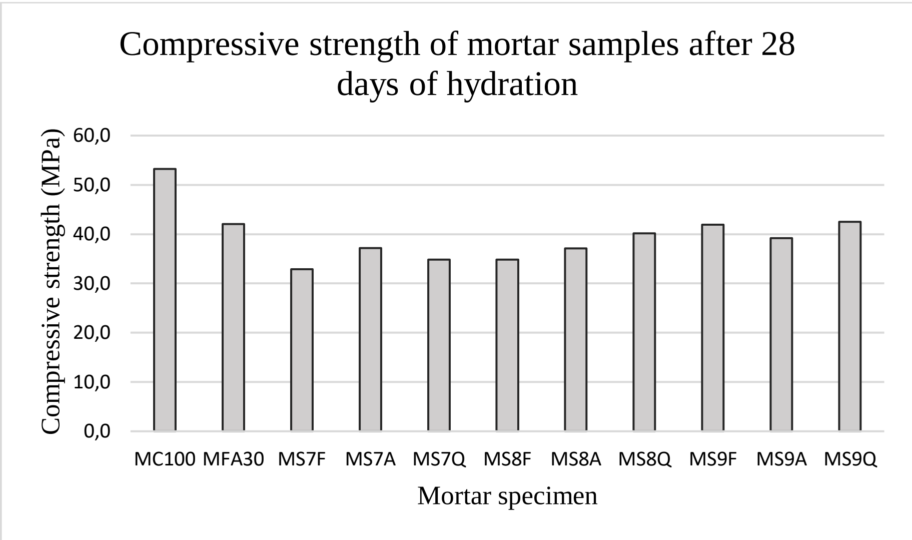

Figure 70: Compressive strength of mortar samples after 28 days of hydration

Furthermore, a value of 41.9 MPa was obtained for sample MS9F and values of 40.2 MPa, 39.2 MPa, 37.1 MPa, 37.1 MPa, 34.9 MPa, 34.8 MPa, 32.9 MPa were obtained for samples MS8Q, MS9A, MS8A, MS7A, MS8F, MS7Q and MS7F respectively. These results indicate that the compressive strength increased with an increase in the incineration temperature of the ISSA. High compressive strengths were obtained with the use of quenched ISSA in the mortar as a partial substitution of PC. These findings were expected as they can be related to reactivity of quenched ISSA compared to furnace or air-cooled ISSA thus far. Analysis of calcium hydroxide (Section 4.2.5) also showed the same trend indicating a high degree of hydration with the use of quenched ISSA, thus resulting in considerable compressive strength.

Overall, the results obtained at 28 days were closely related to MFA30 mortar and the reference mortar as compared to the early ages. According to Manjunatha, (2017), a lower pozzolanic activity is the source of strength reduction in cement mixtures containing ISSA. Different results were obtained in the current study. Although the fly ash is considered to have higher pozzolanicity than ISSA, the compressive strength obtained for ISSA blended mortar was comparable to that of MFA30 blended mortar and slightly higher for sample MS9Q after 28 days. To add to this, the rate of increase in compressive strength of MS9Q (45.5% increase from 3 days to 7 days and 38.4% increase from 7 to 28 days) between these ages was higher than that of MFA30 (40.6% increase from 3 days to 7 days and 33.3% increase from 7 to 28 days) and also higher than MC100 (37.8% increase from 3 days to 7 days and 15.9% increase from 7 to 28 days) (see Figure 67). These results suggest that the highest cooling rate (Q_{ISSA}) and the highest incineration temperature (900ºC) were the best methods to be considered when preparing ISSA for partial substitution in cement products. Differing from the findings of Tantawy *et al.* (2012) who recommended temperatures below 800ºC.

4.7. Correlations

4.7.1. Correlation between chemically combined water and calcium hydroxide

Figure 71 shows the trend curve between chemically combined water and calcium hydroxide content at 28 days of age for all cement paste samples studied. The trend curve shows a good correlation (R^2 = 0.92). Variations can be seen with ISSA blended cement paste samples. The chemically combined water content was high for the reference sample followed by the FA blended cement paste due to the degree of C-S-H gel polymerization (Boualleg *et al.*, 2017). These results were also a reflection of the C-S-H content produced as a result of hydration (Boualleg *et al.*, 2017). The calcium hydroxide content, on the other hand, reflected the progress of the hydration. The reduced $Ca(OH)_2$ content in ISSA blended cement paste also reflects the pozzolanic reaction of ISSA that resulted in the consumption of $Ca(OH)_2$ content.

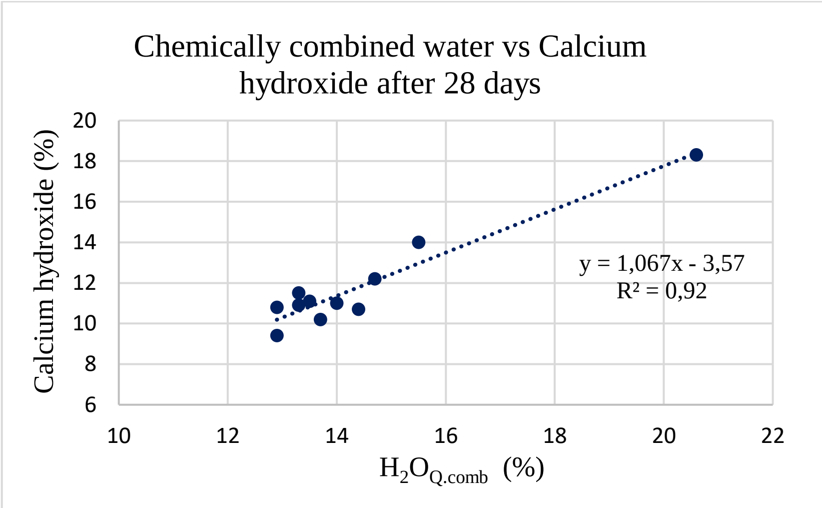

Figure 71: Correlation between chemically combined water and calcium hydroxide after 28 days of hydration

4.7.2. Correlation between compressive strength and calcium hydroxide

Figure 72 shows the trend between the compressive strength of all the mortar samples and the calcium hydroxide calculated for all cement pastes after 28 days of hydration. The trend curve shows a good correlation for the samples with R^2 = 0.70. A directly proportional relationship between the calcium hydroxide and compressive strength was obtained. The differences observed between blended mixes and the reference sample (showing the highest calcium hydroxide content and compressive strength) are attributed to the reduction of C_2S and C_3S compounds when secondary additions (FA and ISSA) were introduced. Secondly, FA and ISSA generally contained a relatively low amount of CaO content resulting in the reduced reactivity of the ashes compared to PC. This resulted in lower calcium hydroxide content and reduced compressive strength. Overall, the compressive strength results were related to the calcium hydroxide content.

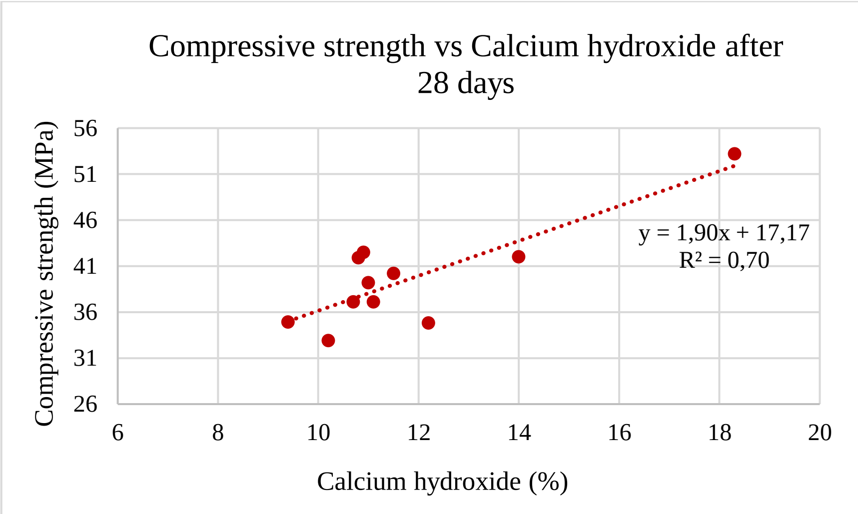

Figure 72: Correlation between compressive strength and calcium hydroxide after 28 days of hydration

4.7.3. Correlation between chemically combined water and compressive strength

Figure 73 shows the trend obtained for the compressive strength of mortar samples and the chemically combined water of cement paste mixes after 28 days of hydration. ISSA blended cement paste showed discrepancies between the $H_2O_{Q.comb}$ content obtained by thermogravimetric analysis and the compressive strength. As a result, an indirect correlation was obtained for ISSA blended samples with R^2 = 0.58. These results are attributed to the evaporation of PC which was high for the reference mix and FA blended mortar hence, the higher compressive strength. The indirect relation is also attributed to the fact that these properties are more related to the water–cement ratio (w/c) (Aitcin & Neville, 2003).

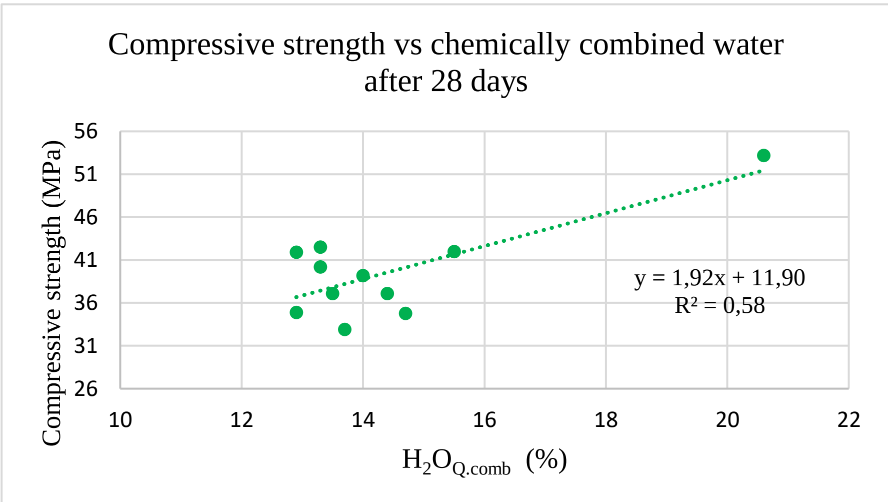

Figure 73: Correlation between compressive strength and chemically combined water after 28 days of hydration

4.8. Chapter summary

- The pozzolanicity of ISSA was studied for consideration as a partial replacement of PC. Physical and chemical characterization of DSS/ISSA was conducted. Particle size distribution and SEM results of ISSA were compared to those of FA (reference pozzolan) and PC (primary reference). It was found that ISSA had the largest particle size compared to FA and ISSA.
- SEM analysis showed evidence of both coarse and fine particles. Through this analysis it was also confirmed that ISSA had an irregular morphology with rare traces of spherical grains. In addition to this, large volumes of diatomite particles were traced in the ISSA before and after it was used as a partial replacement of PC.
- The chemical composition of the ISSA showed evidence of elements and compounds found in PC, in similar proportions to those of fly ash. The diatomite found in the ISSA is assumed to have contributed largely to the chemical composition of the ISSA, particularly to the high amount of SiO_2 found in the ISSA.
- The preparation method of the ISSA had an impact on the overall performance of the ISSA. An increase in the concentrations of compounds was established with an increase in the incineration temperature of the ISSA from 700ºC to 900ºC. However, the elemental composition of the ISSA varied with the different cooling methods.
- When used as a 30% replacement of PC in paste, ISSA showed evidence of hydration products. However, the hydration process was evidently slower than that of the reference samples. The diatomite found in the ISSA contributed largely to the hydration of ISSA blended cement pastes with evidence of hydration products strongly developed on its surfaces. Overall, the quenched ISSA showed better hydration with fewer traces of unhydrated surfaces.
- TGA analysis showed a reduction in mass loss of both FA blended cement paste and ISSA blended cement pastes. Unique results were obtained for cement paste samples S7Q and S8Q, with rapid mass losses having been observed, particularly at the highest temperatures during the TGA analysis. These observations were related to a high thermal reactivity after 6 hours and 7 days of hydration.
- Reductions in the calcium hydroxide content of ISSA blended cement pastes were obtained for samples FA30, S9F, S9A and S9Q after 28 days of hydration. This result led to the conclusion that ISSA is pozzolanic. Incinerating ISSA at 900ºC for 4 hours

was thus regarded as the best preparation method for enhancing the pozzolanicity of ISSA.

- A reduction in compressive strength was obtained with the addition of 30% ISSA and FA in the mortars. However, the level of reduction in compressive strength of ISSA blended mortar was similar to the reduction in compressive strength caused by the addition of FA in the mortar. Moreover, the rate of increase in compressive strength of ISSA blended mortar showed improvement with an increase in the curing age, with the compressive strength of sample MS9Q slightly exceeding that of sample MFA30 after 28 days of curing.

References

Abdul-Maula, S. and Odler, I., 1981, November. Hydration reactions in fly-ash-Portland cements. In *Proceedings of Symposium on Effects of Fly Ash Incorporation in Cement and Concrete, Materials Research Society, Boston* (pp. 102-111).

Aitcin, P.C. and Neville, A., 2003. How the water-cement ratio affects concrete strength. *Concrete International*, *25*(8), pp.51-58.

Alarcon-Ruiz, L., Platret, G., Massieu, E. and Ehrlacher, A., 2005. The use of thermal analysis in assessing the effect of temperature on a cement paste. *Cement and Concrete research*, *35*(3), pp.609-613.

Anderson, M., 2002. Encouraging prospects for recycling incinerated sewage sludge ash (ISSA) into clay-based building products. *Journal of Chemical Technology & Biotechnology: International Research in Process, Environmental & Clean Technology*, *77*(3), pp.352-360.

Anjos, M.A.S., Reis, R., Camões, A., Duarte, F. and Jesus, C., 2019. Evaluation of hydration of cement pastes containing high volume of mineral additions. *European Journal of Environmental and Civil Engineering*, *23*(8), pp.987-1002.

Baert, G., Hoste, S., De Schutter, G. and De Belie, N., 2008. Reactivity of fly ash in cement paste studied by means of thermogravimetry and isothermal calorimetry. *Journal of Thermal Analysis and Calorimetry*, *94*(2), pp.485-492.

Barry, E.E., 1989. Beneficiated fly ash: hydration, microstructure, and strength development in portland cement system. *International Concrete Abstracts*, *114*, pp.241-274.

Beaudoin, J. and Odler, I., 2019. Hydration, Setting and Hardening of Portland Cement. In: Hewlett, P.C. and Liska, M. (Ed), *Lea's Chemistry of Cement and Concrete*, 5th Ed, Butterworth-Heinemann, pp 157-250.

Boualleg, S., Bencheikh, M., Belagraa, L., Daoudi, A. and Chikouche, M.A., 2017. The combined effect of the initial cure and the type of cement on the natural carbonation, the portlandite content, and nonevaporable water in blended cement. *Advances in Materials Science and Engineering*, *2017*.

Bougara, A., Lynsdale, C. and Milestone, N.B., 2010. Reactivity and performance of blastfurnace slags of differing origin. *Cement and Concrete Composites*, *32*(4), pp.319-324.

Bhatty, J.I. and Reid, K.J., 1985. Use of thermal analysis in the hydration studies of a type 1 portland cement produced from mineral tailings. *Thermochimica Acta*, *91*, pp.95-105.

Chen, L. and Lin, D.F., 2009. Stabilization treatment of soft subgrade soil by sewage sludge ash and cement. *Journal of Hazardous Materials*, *162*(1), pp.321-327.

Chen, Y., He, X., Zhang, S., Tan, X. and Wan, Y., 2020. Strength and microstructure properties of solidified sewage sludge with two types of cement-based binders. *Scientific Reports*, *10*(1), pp.1-12.

Chen, Z. and Poon, C.S., 2017. Comparative studies on the effects of sewage sludge ash and fly ash on cement hydration and properties of cement mortars. *Construction and Building Materials*, *154*, pp.791-803.

Costa, U. and Massazza, F., 1983. Some properties of pozzolanic cements containing fly ashes. *International Concrete Abstracts*, *79*, pp.235-254.

Coutand, M., Cyr, M. and Clastres, P., 2006. Use of sewage sludge ash as mineral admixture in mortars. *Proceedings of the Institution of Civil Engineers-Construction Materials*, *159*(4), pp.153-162.

de Souza, L.M.S., Fairbairn, E.M.R., Filho, R.D.T. and Cordeiro, G.C., 2014. Influence of initial CaO/SiO_2 ratio on the hydration of rice husk ash-$Ca(OH)_2$ and sugar cane bagasse ash-$Ca(OH)_2$ pastes. *Química Nova*, *37*(10), pp.1600-1605.

Diamond, S., Sheng, Q. and Olek, J., 1988. Evidence for minimal pozzolanic reaction in a fly ash cement during the period of major strength development. *MRS Online Proceedings Library Archive*, *137*.

Dyer, T.D., Halliday, J.E. and Dhir, R.K., 2011. Hydration chemistry of sewage sludge ash used as a cement component. *Journal of materials in civil engineering*, *23*(5), pp.648-655.

Dweck, J., Buchler, P.M., Coelho, A.C.V. and Cartledge, F.K., 2000. Hydration of a Portland cement blended with calcium carbonate. *Thermochimica Acta*, *346*(1-2), pp.105-113.

El-Shimy, E., Abo-El-Enein, S.A., El-Didamony, H. and Osman, T.A., 2000. Physico-chemical and thermal characteristics of lime-silica fume pastes. *Journal of Thermal Analysis and Calorimetry*, *60*(2), pp.549-556.

Federal Highway Administration, 2012. User guidelines for waste and by-product materials in pavement construction.

Garcés, P., Carrión, M.P., García-Alcocel, E., Payá, J., Monzó, J. and Borrachero, M.V., 2008. Mechanical and physical properties of cement blended with sewage sludge ash. *Waste Management*, *28*(12), pp.2495-2502.

Halliday, J.E., Jones, M.R., Dyer, T.D. and Dhir, R.K., 2012, May. Potential use of UK sewage sludge ash in cement-based concrete. In *Proceedings of the Institution of Civil Engineers-Waste and Resource Management* (Vol. 165, No. 2, pp. 57-66). ICE Publishing.

Kappel, A., Ottosen, L.M. and Kirkelund, G.M., 2017. Colour, compressive strength and workability of mortars with an iron rich sewage sludge ash. *Construction and Building Materials*, *157*, pp.1199-1205.

Karayildirim, T., Yanik, J., Yuksel, M. and Bockhorn, H., 2006. Characterisation of products from pyrolysis of waste sludges. *Fuel*, *85*(10-11), pp.1498-1508.

Khan, R.I. and Ashraf, W., 2019. Effects of ground wollastonite on cement hydration kinetics and strength development. *Construction and Building Materials*, *218*, pp.150-161.

Li, H.L., Liu, G.L. and Cao, Y., 2014. Content and distribution of trace elements and polycyclic aromatic hydrocarbons in fly ash from a coal-fired CHP plant. *Aerosol and Air Quality Research*, *14*(4), pp.1179-1188.

Manjunatha M., 2017. Use of Sewage Sludge Ash & Fly Ash in Construction. *"International Journal of Latest Engineering Research and Applications", 8(2), pp.102-110.*

Massazza, F., 1998. Pozzolana and pozzolanic cements. *Lea's Chemistry of Cement and Concrete*, *4*, pp.471-631.

Mehta, P.K. and Monteiro, P.J., 2014. *Concrete: Microstructure, Properties, and Materials*. 4th Ed, McGraw-Hill Education, New York, USA.

Monzó, J., Paya, J., Borrachero, M.V. and Córcoles, A., 1996. Use of sewage sludge ash (SSA)-cement admixtures in mortars. *Cement and Concrete Research*, *26*(9), pp.1389-1398.

Naamane, S., Rais, Z. and Taleb, M., 2016. The effectiveness of the incineration of sewage sludge on the evolution of physicochemical and mechanical properties of Portland cement. *Construction and Building Materials*, *112*, pp.783-789.

Neville, A.M., 2008. In: J.J. (Ed.), Concrete Technology, third ed. Pearson Education, South Asia.

Pan, S.C., Tseng, D.H., Lee, C.C. and Lee, C., 2003. Influence of the fineness of sewage sludge ash on the mortar properties. *Cement and Concrete Research*, *33*(11), pp.1749-1754.

Pane, I. and Hansen, W., 2005. Investigation of blended cement hydration by isothermal calorimetry and thermal analysis. *Cement and Concrete Research*, *35*(6), pp.1155-1164.

Pekmezci, B.Y. and Akyüz, S., 2004. Optimum usage of a natural pozzolan for the maximum compressive strength of concrete. *Cement and Concrete Research*, *34*(12), pp.2175-2179.

Rizwan, S.A., 2006. High-performance mortars and concrete using secondary raw materials.

Roziere, E., Loukili, A. and Cussigh, F., 2009. A performance-based approach for durability of concrete exposed to carbonation. *Construction and Building Materials*, *23*(1), pp.190-199.

Scrivener, K.L., Juilland, P. and Monteiro, P.J., 2015. Advances in understanding hydration of Portland cement. *Cement and Concrete Research*, *78*, pp.38-56.

Scrivener, K., Bazzoni, A., Mota, B., and Rossen, J.E., 2018, Electron Microscopy. In: Scrivener, K., Snellings, R., and Lothenbach, B. (Eds): *A Practical Guide to Microstructural Analysis of Cementitious Materials*, CRC Press, p.351.

Scrivener, K.L., John, V.M. and Gartner, E.M., 2018. Eco-efficient cements: Potential economically viable solutions for a low-CO2 cement-based materials industry. *Cement and Concrete Research*, *114,* pp.2-26.

Sisomphon, K. and Franke, L., 2011. Evaluation of calcium hydroxide contents in pozzolanic cement pastes by a chemical extraction method. *Construction and Building Materials*, *25*(1), pp.190-194.

Tantawy, M.A., El-Roudi, A.M., Abdalla, E.M. and Abdelzaher, M.A., 2012. Evaluation of the pozzolanic activity of sewage sludge ash. *ISRN Chemical Engineering*, 2012.

Tantawy, M.A., El-Roudi, A.M., Abdalla, E.M. and Abdelzaher, M.A., 2013. Fire resistance of sewage sludge ash blended cement pastes. *Journal of Engineering*, *2013*.

Trník, A., Scheinherrová, L., Medveď, I. and Černý, R., 2015. Simultaneous DSC and TG analysis of high-performance concrete containing natural zeolite as a supplementary cementitious material. *Journal of Thermal Analysis and Calorimetry*, *121*(1), pp.67-73.

Van Beek, A. and Hilhorst, M.A., 1999. Dielectric measurements to characterize the microstructural changes of young concrete. *HERON-ENGLISH EDITION-*, *44*, pp.3-3.

Vouk, D., Serdar, M., Nakić, D. and Anić-Vučinić, A., 2016. Use of sludge generated at WWTP in the production of cement mortar and concrete. *Građevinar,* 68(03.), pp.199- 210.

Vouk, D., Nakic, D., Stirmer, N. and Cheeseman, C.R., 2017. Use of Sewage Sludge Ash in Cementitious Materials. *Reviews on Advanced Materials Science*, *49*(2).

Wang, A., Zhang, C. and Sun, W., 2004. Fly ash effects: II. The active effect of fly ash. *Cement and Concrete Research*, *34*(11), pp.2057-2060.

Wypych, G., 2016. Ch 2–Fillers-origin, Chemical Composition, Properties, and Morphology. *Handbook of Fillers (Fourth Edition), Chem Tec Publishing*, pp.13-266.

Yen, C.L., Tseng, D.H. and Lin, T.T., 2011. Characterization of eco-cement paste produced from waste sludges. *Chemosphere*, *84(2),* pp.220-226.

Yusuf, R.O., Noor, Z.Z., Din, M.D.F.M.D. and Abba, A.H., 2012. Use of sewage sludge ash (SSA) in the production of cement and concrete–a review. *International Journal of Global Environmental Issues*, *12*(2-4), pp.214-228.

Zeng, Q., Li, K., Fen-chong, T. and Dangla, P., 2012. Determination of cement hydration and pozzolanic reaction extents for fly-ash cement pastes. *Construction and Building Materials*, *27*(1), pp.560-569.

Zhang, W., Pinhua, R.A.O., Zhang, H. and Jingli, X.U., 2009. The role of diatomite particles in the activated sludge system for treating coal gasification wastewater. *Chinese Journal of Chemical Engineering*, *17*(1), pp.167-170.

Juala, RK., 2021. Turnitin report of MSc Report. Processed: 05 April 2021 https://www.turnitin.com/newreport_classic.asp?lang=en_us&oid=1551226682&ft=1&bypass_cv=1

CHAPTER 5

SUMMARY, CONCLUSION AND RECOMMENDATIONS

5.1. Summary

5.1.1. The effect of incineration on the performance of products containing ISSA

AA analysis (Table 14) showed that DSS and ISSA consisted mainly of Si, Ca, Al, Fe, Mg, Na, and K. The concentrations of these elements showed an increase with incineration due to the removal of volatile components. Heavy metals: Zn, Pb, Cu, Ti, Cr, Mn, V and Ni, and the light of metal TI, were present as minor constituents. A majority of the heavy metals were reduced by incineration. Considerable concentrations of cementitious compounds: SiO_2, CaO, Fe_2O_3 and Al_2O_3 were also found in ISSA through XRF analysis and increased with an increase in the incineration temperature of ISSA. The SiO_2 content in the ash was found to be higher than in Portland cement making ISSA a possible replacement of sand in mortar. Moreover, the relative CaO content in the ISSA (6.89% to 8.21%) was comparable to that of FA (4.2%). In general, more $Ca(OH)_2$ and $H_2O_{Q.comb}$ contents were obtained with an increase in the ISSA incineration temperature from 700ºC to 900ºC and as a result, a relationship was established between the ISSA incineration temperature and the reactivity of cement containing ISSA. Overall, ISSA incinerated at the highest temperature showed better performance compared to the ISSA incinerated at lower temperatures.

5.1.2. The effect of ISSA cooling rates on the performance of cement pastes

The concentration of cementitious compounds in the ISSA showed an increase in the order $A_{ISSA} < F_{ISSA} < Q_{ISSA}$ of the ISSA cooling rates. More $Ca(OH)_2$ and $H_2O_{Q.comb}$ contents were obtained for S7Q, S8Q and S9Q samples compared to the other ISSA blended cement paste samples. The high performance of samples containing quenched ISSA was also backed by the SEM analysis conducted for the cement pastes. The micrographs obtained showed that samples S8F and S8A contained potassium gel that retarded hydration of the ISSA when used as a replacement of PC in paste. The gel was not observed on samples containing quenched ISSA. This result also suggests that quenching ISSA suppressed possible crystal formation of the silica and maximised the amorphous silica content, thus improving its reactivity. From these results it can be deduced that the cement pastes containing quenched ISSA favoured the hydration of the paste more than the air-cooled and furnace cooled ISSA. The mass loss at elevated temperatures and $Ca(OH)_2$ determined by TGA analysis also suggested that quenching ISSA prior to incorporating it in cement products favoured the kinetics of the cement hydration and the pozzolanic reaction. This was seen through the high mass loss of S7Q and S8Q at elevated temperatures in the early stages of hydration.

5.1.3. The effect of ISSA on the hydration of cement paste

Evidence of hydration products, such as calcium hydroxide, ettringite and C-S-H were obtained on ISSA blended cement pastes. However, a reduction in hydration products was noted due to the reduced amount of PC in the samples. This means that the pastes developed less heat during their hydration. Reduced amounts of $Ca(OH)_2$ and $H_2O_{Q.comb}$ contents with the addition of ISSA compared to the reference cement paste mixes were obtained through TGA analysis. A reduction in $Ca(OH)_2$ after 28 days of hydration, particularly in samples: S9F, S9A and S9Q indicated that most of the calcium hydroxide content was consumed during the hydration, indicating that ISSA is a pozzolanic material. These results indicated that cement products containing ISSA may be more resistant and durable to shrinkage and some harmful reagents due to their reduced $Ca(OH)_2$ content.

5.1.4. The effect of ISSA on the workability and compressive strength of PC mortar

A reduction in the workability of mortar samples containing ISSA was obtained. An increase in incineration temperature of ISSA was found to improve the workability. The different cooling rates of the ISSA's had a varying effect on the flow percentage (Figure 66). In conclusion, the highest cooling rate (QISSA) yielded the best workability results, with the exception of sample MS7Q, which was surpassed by sample MS7A.

A reduction in compressive strength was obtained with the substitution of PC by ISSA in mortar. This was primarily due to the lower cementing power of the ISSA. A good relation between $Ca(OH)_2$ of ISSA blended cement paste obtained by thermogravimetric analysis and the compressive strength of mortar containing ISSA was obtained. This suggested that ISSA reduced the hydration reaction which consequently reduced the compressive strength. It was also noted that a reduction in the percentage decrease of the compressive strength with an increase in curing age of ISSA blended cement paste occurred. As a result, the long-term increase rate of ISSA blended mortar exceeded that of PC mortar and FA blended mortar. This result suggested that with an increase in curing age, the compressive strength of ISSA blended cement mortar became more comparable to PC mortar and FA blended mortar. Thus, it can be concluded that it is possible to achieve enhanced or even high compressive strength at later stages on mortar samples containing 30% ISSA with reduced PC contents.

5.2. Conclusion

The main purpose of incorporating SCM's into cement is to reduce the carbon dioxide emission from the production of cement. As described in chapter 2, pozzolanic materials, including pozzolanic waste materials, have the ability to increase the production of C-S-H due to their chemical composition and their capability to react with calcium hydroxide produced during cement hydration (Equations 2 and 3, Chapter 2). According to the $Ca(OH)_2$ results obtained from the TGA analysis in this study, ISSA showed a considerable level of pozzolanicity due to the reduction in $Ca(OH)_2$ content obtained (S9F, S9A and S9Q). These results indicate that ISSA has the ability to promote the pozzolanic reaction and eventually increase the durability of cement paste/mortar. Although the implication was that effective pozzolanic activity was only obtained with the use of ISSA incinerated at the highest temperature tested (900ºC), lower incineration temperatures were targeted for lower CO_2 emissions from the incineration process. Nevertheless, in seeing that 900ºC is less than the temperature of 1400ºC to 1500ºC used during cement production (see Section 2.1.2), the use of ISSA can still be beneficial in reducing the CO_2 emissions from cement production

5.3. Recommendations

This study provided information on the possible use of ISSA as a partial replacement of Portland cement. However, additional information on the use of ISSA can be obtained by further research. Areas for further studies on the topic may include:

i. The use of ISSA to partially replace PC using finer ISSA, as it is expected that smaller particles are the most reactive and would then show more binding properties.
ii. The inclusion of the colour of ISSA as an experimental parameter in future work
iii. A blend of FA and ISSA as a partial replacement of cement as means of improving ISSA fineness could also be studied
iv. There is also a need to investigate different water/binder ratios with the use of ISSA as a partial replacement of Portland cement.
v. The degree of the reduction in compressive strength of ISSA blended cement mortar also suggests that it may also be advantageous to study lower replacement levels of 20% or 25%.

Appendix

Table 18: Particle size distribution data

Size (µm)	PC Volume density (%)	FA Volume density (%)	ISSA Volume density (%)	PC Cumulative volume (%)	FA cumulative volume (%)	ISSA cumulative volume (%)
0.01	0	0	0	0	0	0
0.011482	0	0	0	0	0	0
0.013183	0	0	0	0	0	0
0.015136	0	0	0	0	0	0
0.017378	0	0	0	0	0	0
0.019953	0	0	0	0	0	0
0.022909	0	0	0	0	0	0
0.026303	0	0	0	0	0	0
0.0302	0	0	0	0	0	0
0.034674	0	0	0	0	0	0
0.039811	0	0	0	0	0	0
0.045709	0	0	0	0	0	0
0.052481	0	0	0	0	0	0
0.060256	0	0	0	0	0	0
0.069183	0	0	0	0	0	0
0.079433	0	0	0	0	0	0
0.091201	0	0	0	0	0	0
0.104713	0	0	0	0	0	0
0.120226	0	0	0	0	0	0
0.138038	0	0	0	0	0	0
0.158489	0	0	0	0	0	0
0.18197	0	0	0	0	0	0
0.20893	0	0	0	0	0	0
0.239883	0	0	0	0	0	0
0.275423	0	0	0	0	0	0
0.316228	0	0	0	0	0	0
0.363078	0	0	0	0	0	0
0.416869	0.071908	0	0	0.071908	0	0
0.47863	0.109183	0	0	0.18109	0	0
0.549541	0.13496	0	0	0.31605	0	0
0.630957	0.14036	0	0	0.45641	0	0
0.724436	0.134963	0	0	0.591373	0	0
0.831764	0.123559	0	0	0.714932	0	0
0.954993	0.116315	0	0	0.831246	0	0
1.096478	0.122567	0	0	0.953813	0	0

1.258925	0.149244	0	0	1.103057	0	0
1.44544	0.197192	0.0052	0.011973	1.300249	0.0052	0.011973
1.659587	0.261921	0.069152	0.334146	1.56217	0.07435	0.346119
1.905461	0.333453	0.396256	0.590703	1.895622	0.47061	0.936822
2.187762	0.401401	0.75878	0.877483	2.297023	1.22939	1.814305
2.511886	0.456263	1.14683	1.163406	2.753286	2.37622	2.977711
2.884031	0.492321	1.549911	1.433346	3.245607	3.92613	4.411056
3.311311	0.510927	1.945922	1.688333	3.756534	5.87205	6.099389
3.801894	0.523645	2.331738	1.926268	4.280179	8.20379	8.025657
4.365158	0.555123	2.709595	2.154262	4.835302	10.9134	10.17992
5.011872	0.641463	3.075302	2.371659	5.479764	13.9887	12.55158
5.754399	0.830821	3.432564	2.582489	6.307585	17.4212	15.13407
6.060934	1.167005	3.769412	2.781083	7.47459	21.1907	17.91515
7.585776	1.698911	4.087944	2.969575	9.173501	25.2786	20.88472
8.709636	2.430789	4.372493	3.139524	11.60429	29.6511	24.02425
10	3.371499	4.623945	3.293536	14.97579	34.275	27.31778
11.48154	4.437156	4.827156	3.425339	19.41294	39.1022	30.74312
13.18257	5.563098	4.981281	3.53989	24.97604	44.0835	34.28301
15.13561	6.594405	5.075602	3.63725	31.57045	49.1591	37.92026
17.37801	7.418374	5.107396	3.725181	38.98882	54.2665	41.64544
19.95262	7.899117	5.072928	3.808301	46.88794	59.3394	45.45374
22.90868	7.969125	4.971073	3.892918	54.85706	64.3105	49.34666
26.30268	7.613621	4.805136	3.978103	62.47068	69.11561	53.32476
30.19952	6.885152	4.578519	4.058197	69.35583	73.69413	57.38296
34.67369	5.900922	4.300464	4.117987	75.25676	77.99459	61.50095
39.81072	4.802114	3.94901	4.13587	80.05887	81.9736	65.63682
45.70882	3.734236	3.623334	4.086195	83.79311	85.59694	69.72301
52.48075	2.813852	3.241744	3.944786	86.60696	88.83868	73.6678
60.25596	2.101968	2.837943	3.694267	88.70893	91.67662	77.36207
69.1831	1.616889	2.420742	3.334839	90.32581	94.09737	80.69691
79.43282	1.32214	1.991056	2.877567	91.64795	96.08842	83.57447
91.20108	1.164994	1.565298	2.362289	92.81295	97.65372	85.93676
104.7129	1.079238	1.140714	1.824286	93.89219	98.79443	87.76105
120.2264	1.015387	0.747987	1.330586	94.90757	99.54242	89.09163
138.0384	0.939827	0.354186	0.896883	95.8474	99.89661	89.98852
158.4893	0.842976	0.094363	0.651398	96.69038	99.99097	90.633991
181.9701	0.724955	0.009031	0.603526	97.41533	100	91.24344
208.9296	0.601278	0	0.611412	98.01661	100	91.85485
239.8833	0.483637	0	0.662786	98.50025	100	92.51764
275.4229	0.387909	0	0.771031	98.88815	100	93.28867

316.2278	0.308233	0	0.915394	99.19639	100	94.20406
363.0781	0.26142	0	1.071696	99.45781	100	95.27576
416.8694	0.246301	0	1.169017	99.70411	100	96.44478
478.6301	0.19686	0	1.133305	99.90097	100	97.57808
549.5409	0.085593	0	0.957667	99.98656	100	98.53575
630.9573	0.013441	0	0.63374	100	100	99.16912
724.436	0	0	0.418004	100	100	99.58712
831.7638	0	0	0.270656	100	100	99.85778
954.9926	0	0	0.117589	100	100	99.97537
1096.478	0	0	0.024633	100	100	100
1258.925	0	0	0	100	100	100
1445.44	0	0	0	100	100	100
1659.587	0	0	0	100	100	100
1905.461	0	0	0	100	100	100
2187.762	0	0	0	100	100	100
2511.886	0	0	0	100	100	100
2884.032	0	0	0	100	100	100
3311.311	0	0	0	100	100	100
3801.894	0	0	0	100	100	100
4365.158	0	0	0	100	100	100
5011.872	0	0	0	100	100	100
5754.366	0	0	0	100	100	100
6606.934	0	0	0	100	100	100
7585.776	0	0	0	100	100	100
8709.696	0	0	0	100	100	100
10000	0	0	0	100	100	100

Table 19: Compressive strength data

	3 days	**7 days**	**28 days**
Mortar Samples	**Compressive strength (MPa)**		
MC100	33.3	45.9	53.2
MFA30	22.4	31.5	42.0
MS7F	14.3	26.2	32.9
MS7A	17.8	28.9	37.1
MS7Q	15.1	26.9	34.8
MS8F	16.2	27.6	34.9
MS8A	16.4	28.0	37.1
MS8Q	17.0	29.5	40.2
MS9F	17.4	29.7	41.9
MS9A	17.5	28.1	39.2
MS9Q	21.1	30.7	42.5

Table 20: Flow test data

Mortar samples	**Flow (%)**
MC100	38
MFA30	34,5
MS7F	19,8
MS7A	22
MS7Q	21
MS8F	21,1
MS8A	22,2
MS8Q	24,3
MS9F	26
MS9A	24
MS9Q	27,2

Table 21: Chemically combined water

	Uncombined water (30 - 100ºC)			Total mass loss (30 - 1000ºC)			Combined water (Uncombined - total mass loss)		
Paste	**6 hours**	**7 days**	**28 days**	**6 hours**	**7 days**	**28 days**	**6 hours**	**7 days**	**28 days**
C100	2,37	4,06	4,18	8,48	18,4	24,8	6,1	14,3	20,6
FA30	1,72	4,02	3,54	5,98	18,82	19,05	4,3	14,8	15,5
S7F	2,37	2,52	1,73	7,09	16,95	15,43	4,7	14,4	13,7
S7A	2,2	2,04	2,21	6,18	14,93	16,61	4,0	12,9	14,4
S7Q	1,94	3,18	2,1	8,63	18,43	16,79	6,7	15,3	14,7
S8F	2,04	2,67	2,34	6,92	17,03	15,24	4,9	14,4	12,9
S8A	1,75	2,75	2,08	5,85	15,66	15,62	4,1	12,9	13,5
S8Q	1,76	3,76	1,44	7,97	18,76	14,72	6,2	15,0	13,3
S9F	1,21	1,45	2,67	4,87	15,52	15,6	3,7	14,1	12,9
S9A	1,51	1,66	2,59	5,64	13,55	16,57	4,1	11,9	14,0
S9Q	1,46	2,23	2,44	5,01	14,71	15,78	3,6	12,5	13,3

Table 22: Calcium hydroxide content

	$Ca(OH)_2$ (400 - 450ºC)			$CaCO_3$ (600 - 710)			$CaCO_3$ %			mols (n)			$Ca(OH)_2$			Total Ca(OH)		
Paste	**6 hours**	**7 days**	**28 days**	**6 hours**	**7 days**	**28 days**	**6 hours**	**7 days**	**28 days**	**6 hours**	**7 days**	**28 days**	**6 hours**	**7 days**	**28 days**	**6 hours**	**7 days**	**28 days**
C100	0,65	3,77	3,83	1,94	1,27	1,54	4,40	2,88	3,50	0,044	0,029	0,035	3,26	2,13	2,59	5,9	17,6	18,3
FA30	0,51	3,09	3,01	1,31	1	0,95	2,98	2,27	2,17	0,030	0,023	0,022	2,20	1,68	1,60	4,3	14,4	14,0
S7F	0,17	1,93	1,7	1,14	1,18	1,93	2,59	2,68	4,38	0,026	0,027	0,044	1,92	1,98	3,24	2,6	9,9	10,2
S7A	0,21	2,16	1,97	1,02	0,79	1,56	2,32	1,79	3,54	0,023	0,018	0,035	1,71	1,33	2,62	2,6	10,2	10,7
S7Q	0,18	2,07	1,96	1,07	1,33	2,45	2,43	3,019	5,56	0,024	0,030	0,056	1,80	2,23	4,12	2,5	10,7	12,2
S8F	0,21	1,81	1,91	1,14	1,04	0,92	2,59	2,36	2,088	0,026	0,024	0,021	1,92	1,75	1,55	2,8	9,2	9,4
S8A	0,21	2,04	2,01	1,06	0,93	1,7	2,41	2,11	3,86	0,024	0,021	0,039	1,78	1,56	2,86	2,6	9,9	11,1

S8Q	0,21	2,17	2,03	1,25	1,02	1,86	2,84	2,32	4,22	0,028	0,023	0,042	2,10	1,71	3,13	3,0	10,6	11,5
S9F	0,28	2,08	2,26	1,21	2,28	0,9	2,75	5,18	2,043	0,027	0,052	0,020	2,033	3,83	1,51	3,2	12,4	10,8
S9A	0,27	2,14	2,31	1,24	1,97	0,92	2,82	4,47	2,088	0,02	0,045	0,021	2,083	3,31	1,55	3,2	12,1	11,0
S9Q	0,3	2,54	2,3	1,1	0,96	0,88	2,50	2,18	2,00	0,025	0,022	0,020	1,85	1,61	1,48	3,1	12,1	10,9

Table 23: Thermogravimetric analysis data

	C100-6h		**FA30-6h**		**S7F-6h**		**S7A-6h**		**S7Q-6h**		**S8F-6h**		**S8A-6h**		**S8Q-6h**		**S9F-6h**		**S9A-6h**		**S9Q-6h**	
Temp	wt	Deriv. wt	wt	Deriv. wt	wt	Deriv. wt	wt	Deriv. wt	wt	Deriv. wt	wt	Deriv. wt	wt	Deriv. wt	wt	Deriv. wt	wt	Deriv. wt	wt	Deriv. wt	wt	Deriv. wt
°C	%	%/°C	%	%/°C	%	%/°C	%	%/°C	%	%/°C	%	%/°C	%	%/°C	%	%/°C	%	%/°C	%	%/ºC	%	%/ºC
30	100	0,01133	100	0,004732	100	0,01437	100	0,01009	100	0,006401	100	0,005535	100	0,003476	100	0,00341	100	0,0063	100	0,005682	100	0,006105
40	99,89	0,01057	99,88	0,00556	99,9	0,01034	99,9	0,008626	99,93	0,009554	99,94	0,007523	99,98	0,006563	99,96	0,00645	99,91	0,01027	99,96	0,005649	99,96	0,005688
50	99,77	0,01665	99,81	0,01135	99,77	0,01757	99,83	0,01023	99,82	0,01613	99,83	0,01681	99,85	0,01622	99,85	0,01568	99,82	0,01286	99,87	0,01298	99,87	0,01339
60	99,52	0,03532	99,62	0,02879	99,52	0,03502	99,6	0,03534	99,59	0,03183	99,59	0,03354	99,64	0,03505	99,63	0,03097	99,64	0,01374	99,68	0,02747	99,66	0,02901
70	99,03	0,06529	99,19	0,05528	99,04	0,06098	99,11	0,03079	99,17	0,05257	99,13	0,05698	99,17	0,05636	99,21	0,05156	99,4	0,03578	99,3	0,04625	99,27	0,04568
80	98,3	0,06457	98,65	0,03927	98,37	0,06191	98,64	0,07731	98,6	0,04994	98,52	0,05345	98,65	0,03648	98,68	0,04357	99,1	0,02278	98,86	0,03337	98,87	0,0281
90	97,87	0,02886	98,41	0,01618	97,91	0,0339	98,07	0,03623	98,25	0,02467	98,15	0,02481	98,4	0,01877	98,39	0,01965	98,91	0,0143	98,63	0,01692	98,67	0,01607
100	97,63	0,01997	98,28	0,01181	97,64	0,02264	97,8	0,02099	98,06	0,02025	97,96	0,01569	98,25	0,01263	98,24	0,01266	98,79	0,01112	98,49	0,01179	98,54	0,01136
110	97,45	0,01628	98,17	0,009803	97,44	0,01786	97,62	0,01581	97,84	0,009429	97,83	0,01207	98,14	0,01029	98,13	0,009645	98,69	0,009314	98,39	0,00943	98,43	0,009023
120	97,3	0,01448	98,08	0,009184	97,27	0,0156	97,48	0,01386	97,73	0,0107	97,71	0,0107	98,04	0,009484	98,04	0,008217	98,6	0,008251	98,3	0,008416	98,36	0,007808
130	97,17	0,01273	97,99	0,007899	97,12	0,01509	97,35	0,01245	97,62	0,01099	97,61	0,01115	97,94	0,01021	97,96	0,008413	98,52	0,009781	98,22	0,008659	98,27	0,009213
140	97,04	0,01309	97,92	0,007417	96,95	0,02028	97,21	0,01596	97,5	0,01468	97,49	0,01248	97,82	0,01242	97,87	0,008438	98,43	0,01172	98,13	0,009511	98,17	0,00993
150	96,92	0,00977	97,85	0,00587	96,73	0,02042	97,06	0,01307	97,36	0,01071	97,38	0,008346	97,72	0,008484	97,8	0,006211	98,36	0,006535	98,05	0,006392	98,1	0,006613
160	96,84	0,00795	97,8	0,005043	96,57	0,01273	96,95	0,009162	97,27	0,007861	97,31	0,006967	97,64	0,006728	97,75	0,005436	98,29	0,006233	97,99	0,005207	98,02	0,004147
170	96,76	0,00688	97,75	0,004542	96,46	0,01035	96,87	0,007905	97,2	0,006831	97,24	0,006184	97,58	0,006021	97,7	0,004827	98,23	0,005705	97,94	0,00459	97,98	0,00456
180	96,7	0,00644	97,7	0,004178	96,36	0,008993	96,79	0,006974	97,14	0,006072	97,18	0,005678	97,52	0,005578	97,65	0,004444	98,18	0,004881	97,9	0,004477	97,93	0,004352
190	96,63	0,00592	97,66	0,004145	96,28	0,008286	96,73	0,006371	97,08	0,005696	97,13	0,005504	97,47	0,005304	97,61	0,004149	98,13	0,001977	97,86	0,004255	97,89	0,0042
200	96,58	0,00576	97,62	0,003909	96,2	0,007775	96,66	0,006145	97,02	0,005209	97,07	0,005169	97,42	0,005049	97,57	0,003879	98,2	0,004069	97,81	0,004049	97,85	0,00409

210	96,52	0,00549	97,59	0,003728	96,12	0,007446	96,59	0,003995	96,97	0,005087	97,02	0,005188	97,37	0,00496	97,53	0,003713	98,22	0,003726	97,77	0,004067	97,81	0,003987
220	96,47	0,00549	97,55	0,003667	96,05	0,007271	96,54	0,005298	96,93	0,004808	96,97	0,005277	97,32	0,004948	97,49	0,003839	98,18	0,005003	97,73	0,003943	97,77	0,004002
230	96,41	0,00549	97,51	0,003686	95,97	0,007365	96,5	0,005464	96,88	0,00518	96,92	0,005317	97,27	0,004838	97,45	0,003853	98,13	0,004676	97,69	0,003907	97,73	0,00376
240	96,36	0,00554	97,48	0,003733	95,9	0,007353	96,49	0,005946	96,82	0,005394	96,87	0,005418	97,22	0,004962	97,41	0,003851	98,08	0,004766	97,65	0,004608	97,69	0,004234
250	96,3	0,00558	97,44	0,003165	95,83	0,007386	96,43	0,006051	96,77	0,005494	96,81	0,005417	97,17	0,005144	97,37	0,00393	98,03	0,005318	97,6	0,004375	97,65	0,004136
260	96,24	0,00558	97,42	0,003827	95,75	0,007623	96,38	0,006395	96,71	0,005644	96,76	0,00556	97,12	0,005316	97,34	0,003859	97,98	0,005463	97,56	0,004538	97,6	0,004231
270	96,19	0,00550	97,38	0,003989	95,68	0,007698	96,36	0,005985	96,66	0,005525	96,7	0,005569	97,06	0,005396	97,29	0,003979	97,92	0,005707	97,51	0,004685	97,56	0,004743
280	96,13	0,00541	97,34	0,003944	95,6	0,007656	96,35	0,005955	96,6	0,005378	96,64	0,005481	97,01	0,005421	97,26	0,003986	97,86	0,005641	97,47	0,004636	97,52	0,004366
290	96,08	0,00516	97,3	0,00384	95,52	0,007324	96,29	0,00567	96,55	0,004883	96,59	0,005104	96,96	0,005263	97,22	0,003821	97,81	0,005746	97,42	0,004245	97,47	0,004334
300	96,03	0,00502	97,26	0,004008	95,45	0,006807	96,27	0,005086	96,5	0,004695	96,54	0,005041	96,91	0,00493	97,18	0,003895	97,75	0,004891	97,38	0,004482	97,43	0,004159
310	95,98	0,00500	97,22	0,004171	95,39	0,006195	96,24	0,004808	96,46	0,004246	96,49	0,005064	96,86	0,00463	97,14	0,003856	97,7	0,005125	97,34	0,003898	97,39	0,003885
320	95,93	0,00476	97,18	0,00429	95,33	0,005694	96,2	0,004748	96,42	0,004182	96,44	0,004866	96,81	0,00449	97,1	0,003982	97,66	0,004633	97,3	0,003165	97,36	0,003623
330	95,88	0,00457	97,13	0,004435	95,27	0,005353	96,19	0,004615	96,37	0,003948	96,39	0,004731	96,77	0,004263	97,06	0,004071	97,61	0,00431	97,26	0,003458	97,32	0,003381
340	95,84	0,00450	97,09	0,004682	95,22	0,005129	96,15	0,004443	96,34	0,003904	96,34	0,005014	96,73	0,004026	97,02	0,004307	97,57	0,004226	97,23	0,003464	97,29	0,002819
350	95,79	0,00448	97,04	0,005046	95,17	0,004802	96,11	0,004275	96,3	0,003256	96,29	0,005089	96,69	0,004097	96,97	0,005109	97,53	0,003949	97,2	0,003112	97,26	0,003046
360	95,75	0,00442	96,99	0,005404	95,13	0,004298	96,07	0,003735	96,27	0,00341	96,24	0,005086	96,65	0,003894	96,92	0,006136	97,49	0,003818	97,17	0,003124	97,22	0,003031
370	95,71	0,00428	96,93	0,005387	95,08	0,004076	96,03	0,003452	96,23	0,003255	96,19	0,005394	96,61	0,003641	96,85	0,006601	97,45	0,003541	97,14	0,002974	97,19	0,003702
380	95,66	0,00518	96,88	0,004526	95,05	0,003814	95,99	0,003312	96,2	0,003431	96,13	0,004868	96,57	0,003304	96,79	0,00532	97,42	0,003327	97,11	0,003004	97,16	0,003377
390	95,59	0,00960	96,84	0,003534	95,01	0,003515	95,96	0,00379	96,16	0,004235	96,09	0,00436	96,54	0,003232	96,74	0,004888	97,38	0,003473	97,08	0,002758	97,13	0,003241
400	95,47	0,01558	96,81	0,003767	94,97	0,003625	95,92	0,004959	96,11	0,005591	96,04	0,004886	96,51	0,003545	96,69	0,005677	97,35	0,004224	97,04	0,004486	97,09	0,004932
410	95,28	0,02262	96,76	0,004862	94,94	0,004113	95,86	0,006488	96,05	0,006038	95,99	0,005706	96,46	0,005236	96,63	0,006125	97,29	0,007594	96,98	0,007019	97,02	0,00878
420	95,04	0,02178	96,66	0,01684	94,89	0,004234	95,79	0,005629	96	0,004036	95,93	0,005892	96,4	0,006275	96,57	0,005536	97,2	0,008947	96,9	0,008463	96,92	0,009753
430	94,89	0,00688	96,46	0,01809	94,85	0,00341	95,76	0,003189	95,97	0,002433	95,88	0,003832	96,35	0,004185	96,52	0,003336	97,13	0,004666	96,83	0,006267	96,84	0,005045
440	94,85	0,00351	96,34	0,006743	94,82	0,002484	95,73	0,002601	95,95	0,002418	95,85	0,002581	96,32	0,002479	96,5	0,002282	97,1	0,002452	96,79	0,00271	96,81	0,002591
450	94,82	0,00301	96,3	0,003086	94,8	0,002383	95,71	0,002368	95,93	0,00194	95,83	0,002483	96,3	0,001966	96,48	0,002002	97,07	0,002441	96,77	0,001512	96,79	0,001975
460	94,79	0,00269	96,27	0,002359	94,78	0,002386	95,68	0,00212	95,91	0,001926	95,8	0,002345	96,28	0,001931	96,46	0,001965	97,05	0,001989	96,75	0,001422	96,77	0,001681
470	94,76	0,00265	96,25	0,00207	94,75	0,002425	95,66	0,002393	95,89	0,002019	95,78	0,002403	96,26	0,002057	96,44	0,001961	97,03	0,002216	96,73	0,001826	96,75	0,001661
480	94,74	0,00258	96,23	0,002205	94,73	0,002384	95,63	0,002157	95,87	0,002011	95,75	0,002477	96,24	0,002055	96,42	0,02126	97,01	0,002097	96,7	0,001342	96,74	0,001709

490	94,71	0,00268	96,21	0,001613	94,7	0,002549	95,61	0,002342	95,85	0,002146	95,73	0,002687	96,22	0,002209	96,4	0,002286	96,99	0,002274	96,7	0,00207	96,72	0,002013
500	94,68	0,00310	96,19	0,002392	94,68	0,002623	95,59	0,002331	95,83	0,002083	95,7	0,002637	96,19	0,002376	96,37	0,002209	96,97	0,002386	96,69	0,001945	96,7	0,001866
510	94,65	0,00332	96,16	0,002618	94,65	0,002874	95,56	0,001264	95,81	0,002161	95,67	0,002783	96,17	0,002492	96,35	0,002465	96,95	0,00241	96,66	0,001982	96,68	0,002117
520	94,62	0,00366	96,13	0,002865	94,62	0,003104	95,56	0,000121	95,78	0,002314	95,65	0,002886	96,14	0,002611	96,33	0,002504	96,92	0,0027	96,64	0,002396	96,66	0,002088
530	94,58	0,00402	96,1	0,002835	94,59	0,003469	95,52	0,00279	95,76	0,00274	95,62	0,00288	96,11	0,003007	96,3	0,00252	96,89	0,00283	96,62	0,002399	96,64	0,002081
540	94,54	0,00420	96,07	0,00354	94,55	0,003679	95,5	0,002835	95,73	0,002834	95,59	0,00318	96,08	0,003092	96,27	0,002948	96,86	0,002187	96,59	0,002772	96,61	0,002267
550	94,49	0,00494	96,03	0,004009	94,52	0,003863	95,48	0,00262	95,7	0,003145	95,55	0,003388	96,05	0,003425	96,24	0,003224	96,84	0,003283	96,56	0,003137	96,58	0,003003
560	94,44	0,00570	95,99	0,004516	94,48	0,004055	95,46	0,003585	95,67	0,003036	95,52	0,003582	96,02	0,003754	96,21	0,004055	96,81	0,003569	96,53	0,003659	96,55	0,003382
570	94,38	0,00651	95,94	0,005294	94,43	0,004342	95,44	0,003513	95,64	0,003656	95,48	0,003942	95,97	0,004207	96,16	0,004077	96,77	0,004207	96,49	0,004147	96,51	0,003858
580	94,31	0,00724	95,88	0,005994	94,39	0,004533	95,4	0,004008	95,6	0,003873	95,44	0,004216	95,93	0,004515	96,12	0,004842	96,73	0,004509	96,44	0,004589	96,47	0,004249
590	94,23	0,00827	95,82	0,006611	94,34	0,004845	95,39	0,003801	95,56	0,003918	95,39	0,00489	95,88	0,005057	96,07	0,005001	96,68	0,005045	96,4	0,004396	96,43	0,00444
600	94,14	0,00889	95,75	0,007219	94,29	0,005097	95,38	0,00434	95,52	0,00408	95,34	0,00531	95,83	0,005399	96,02	0,005545	96,63	0,005393	96,35	0,005474	96,38	0,00463
610	94,05	0,00934	95,68	0,007479	94,24	0,005388	95,34	0,004213	95,47	0,004544	95,29	0,005954	95,78	0,005845	95,96	0,006151	96,57	0,005889	96,29	0,005786	96,33	0,00508
620	93,96	0,00996	95,6	0,008214	94,18	0,005788	95,29	0,00678	95,46	0,001229	95,22	0,006615	95,71	0,006499	95,89	0,007019	96,51	0,006311	96,22	0,006928	96,28	0,005934
630	93,85	0,01129	95,51	0,008754	94,12	0,00671	95,23	0,006349	95,4	0,006668	95,16	0,007186	95,65	0,007136	95,82	0,007911	96,44	0,007432	96,15	0,007867	96,21	0,007378
640	93,73	0,01338	95,42	0,01011	94,05	0,007629	95,16	0,007333	95,33	0,007549	95,08	0,007776	95,57	0,007728	95,73	0,008596	96,36	0,008833	96,07	0,009017	96,14	0,007921
650	93,58	0,01617	95,31	0,0127	93,97	0,008886	95,08	0,009688	95,25	0,009831	94,99	0,009771	95,48	0,01087	95,64	0,01017	96,27	0,01028	95,98	0,01049	96,05	0,0103
660	93,4	0,02195	95,16	0,01751	93,86	0,01332	94,96	0,01361	95,13	0,01338	94,88	0,01302	95,35	0,01616	95,53	0,01304	96,15	0,01476	95,85	0,01452	95,93	0,01425
670	93,14	0,02925	94,95	0,02319	93,7	0,01904	94,8	0,0185	94,97	0,01724	94,73	0,01647	95,16	0,02131	95,38	0,0168	95,98	0,01912	95,68	0,02011	95,76	0,01923
680	92,81	0,03603	94,71	0,02449	93,48	0,02266	94,61	0,01982	94,79	0,01916	94,56	0,01763	94,94	0,01947	95,19	0,01963	95,75	0,02404	95,45	0,02423	95,55	0,02225
690	92,45	0,03265	94,51	0,01171	93,27	0,01736	94,44	0,01162	94,61	0,01555	94,39	0,01516	94,81	0,006023	95	0,018	95,52	0,01807	95,22	0,01866	95,35	0,01316
700	92,24	0,00862	94,46	0,00251	93,17	0,003524	94,38	0,002538	94,49	0,006561	94,26	0,009424	94,79	0,001422	94,85	0,01173	95,43	0,003056	95,12	0,00364	95,29	0,001929
710	92,2	0,00326	94,44	0,001856	93,15	0,001089	94,36	0,0009781	94,45	0,003147	94,2	0,004542	94,77	0,001279	94,77	0,005496	95,42	0,001192	95,11	0,001038	95,28	0,0009797
720	92,17	0,00287	94,42	0,001757	93,15	0,000955	94,35	0,0009015	94,42	0,003394	94,16	0,003133	94,76	0,001081	94,72	0,003794	95,41	0,001096	95,09	0,001173	95,27	0,0009845
730	92,14	0,00263	94,4	0,001636	93,14	0,0007473	94,34	0,001084	94,39	0,003844	94,13	0,003006	94,75	0,001109	94,68	0,004134	95,4	0,0007361	95,08	0,001041	95,26	0,001068
740	92,11	0,00252	94,39	0,001379	93,13	0,0006863	94,33	0,001098	94,34	0,00482	94,1	0,003169	94,74	0,000971	94,64	0,04676	95,39	0,001259	95,07	0,001261	95,25	0,0009235
750	92,09	0,00243	94,37	0,001164	93,12	0,0006254	94,32	0,0009574	94,29	0,006331	94,07	0,003196	94,73	0,000989	94,59	0,05729	95,38	0,0008342	95,07	0,0005817	95,24	0,0007583
760	92,06	0,00260	94,36	0,001117	93,12	0,000527	94,31	0,0005575	94,21	0,00832	94,04	0,003118	94,72	0,000986	94,52	0,00714	95,37	0,0007362	95,06	0,001225	95,23	0,0007688

770	92,04	0,00279	94,35	0,001111	93,11	0,0003739	94,31	0,001416	94,12	0,01053	94,01	0,003039	94,71	0,009916	94,45	0,007565	95,36	0,0005918	95,05	0,0008099	95,22	0,0005745
780	92,01	0,00284	94,34	0,001094	93,11	0,0002895	94,29	0,0008989	94	0,01384	93,98	0,003106	94,7	0,001157	94,37	0,009039	95,36	0,0007675	95,04	0,0004356	95,21	0,001671
790	91,98	0,00291	94,33	-0,00044	93,1	0,0004256	94,29	0,001059	93,84	0,017	93,95	0,003084	94,69	0,001132	94,27	0,01089	95,35	0,00096	95,03	0,0005822	95,21	0,0006946
800	91,95	0,00291	94,33	0,001113	93,1	0,0004898	94,27	0,001146	93,65	0,02013	93,92	0,003163	94,68	0,001116	94,15	0,01294	95,34	0,0007701	95,03	0,000488	95,2	0,000642
810	91,92	0,00273	94,32	0,000915	93,1	0,0006189	94,26	0,001146	93,44	0,02193	93,88	0,002931	94,67	0,001137	94,01	0,01465	95,33	0,000715	95,02	0,001171	95,2	0,0006876
820	91,9	0,00261	94,31	0,001046	93,09	0,0006694	94,25	0,001646	93,23	0,02138	93,85	0,003236	94,66	0,00115	93,86	0,01575	95,33	0,0006731	95,01	0,00208	95,19	0,0006153
830	91,87	0,00237	94,3	0,000984	93,08	0,0005436	94,24	0,001223	93,02	0,01952	93,82	0,002896	94,64	0,001434	93,7	0,01623	95,32	0,0007658	95,01	0,002373	95,18	0,0005154
840	91,85	0,00240	94,29	0,001028	93,08	0,0005497	94,22	0,001442	92,84	0,01764	93,79	0,003232	94,63	0,001573	93,53	0,01604	95,31	0,0005778	95,05	0,004302	95,18	0,0005412
850	91,83	0,00223	94,28	0,001003	93,07	0,0006492	94,2	0,001861	92,67	0,01602	93,76	0,003086	94,61	0,001506	93,37	0,01593	95,3	0,000684	94,97	0,004054	95,17	0,0005906
860	91,8	0,00202	94,27	0,000852	93,07	0,0005537	94,18	0,001925	92,51	0,01539	93,73	0,003165	94,45	0,004971	93,22	0,01554	95,3	0,0009145	94,96	0,02535	95,16	0,0007166
870	91,78	0,00192	94,26	0,001074	93,06	0,00057	94,16	0,002066	92,36	0,0156	93,7	0,003331	94,43	0,002125	93,06	0,0152	95,29	0,0009658	94,72	0,001474	95,15	0,0009964
880	91,77	0,00163	94,25	0,001009	93,06	0,000618	94,14	0,002286	92,2	0,01516	93,66	0,003604	94,41	0,00147	92,91	0,01511	95,28	0,001002	94,69	0,001262	95,14	0,0005354
890	91,75	0,00181	94,24	0,001098	93,05	0,0007582	94,12	0,002475	92,06	0,01257	93,63	0,003669	94,34	0,009835	92,76	0,01417	95,27	0,000803	94,66	0,02432	95,14	0,001003
900	91,73	0,00197	94,23	0,000998	93,04	0,0008659	94,09	0,002507	91,95	0,009555	93,59	0,003635	94,31	0,001654	92,63	0,01178	95,26	0,001144	94,49	0,001023	95,13	0,001089
910	91,71	0,00172	94,22	0,001148	93,03	0,0007578	94,07	0,002607	91,86	0,007364	93,55	0,003672	94,33	0,001621	92,53	0,008745	95,25	0,0008852	94,48	0,0009303	95,12	0,0009866
920	91,69	0,00194	94,21	0,001286	93,02	0,0007854	94,04	0,002803	91,8	0,00619	93,52	0,003766	94,31	0,002526	92,45	0,00661	95,24	0,0009516	94,47	0,0008834	95,11	0,0009575
930	91,67	0,00208	94,19	0,001485	93,01	0,001101	94,02	0,002678	91,74	0,005732	93,48	0,003632	94,33	0,003312	92,39	0,005242	95,23	0,001008	94,46	0,001071	95,1	0,0009631
940	91,65	0,00204	94,18	0,001761	93	0,001018	93,99	0,002797	91,69	0,00703	93,44	0,003745	94,3	0,003124	92,34	0,004579	95,22	0,00129	94,45	0,0005995	95,09	0,001148
950	91,63	0,00198	94,16	0,001879	92,99	0,001221	93,96	0,002578	91,62	0,005485	93,41	0,003756	94,27	0,003262	92,3	0,004124	95,21	0,001102	94,44	0,001295	95,07	0,001299
960	91,61	0,00212	94,14	0,002204	92,98	0,001329	93,93	0,002797	91,56	0,004689	93,37	0,003913	94,23	0,003651	92,26	0,004147	95,19	0,001512	94,43	0,001422	95,06	0,001474
970	91,59	0,00235	94,11	0,00264	92,97	0,001527	93,89	0,004673	91,52	0,005166	93,33	0,004017	94,2	0,003463	92,22	0,003946	95,18	0,001319	94,42	0,001608	95,05	0,001272
980	91,57	0,00246	94,09	0,003178	92,95	0,001765	93,86	0,003164	91,47	0,00444	93,29	0,004413	94,16	0,003746	92,18	0,003741	95,17	0,001637	94,4	0,001393	95,03	0,001918
990	91,54	0,00273	94,05	0,003785	92,93	0,001763	93,82	0,005497	91,42	0,005467	93,24	0,004443	94,12	0,004421	92,14	0,003596	95,15	0,002041	94,38	0,001548	95,01	0,002192
1000	91,52	0,00270	94,02	0,003786	92,91	0,00176	93,82	0,005489	91,37	0,005486	93,08	0,004412	94,15	0,004316	92,03	0,003458	95,13	0,00213	94,36	0,001564	94,99	0,002298
	C100-7d		**FA30-7d**		**S7F-7d**		**S7A-7d**		**S7Q-7d**		**S8F-7d**		**S8A-7d**		**S8Q-7d**		**S9F-7d**		**S9A-7d**		**S9Q-7d**	
Temp	wt	Deriv. wt	wt	Deriv. wt	wt	Deriv. wt	wt	Deriv. wt	wt	Deriv. wt	wt	Deriv. wt	wt	Deriv. wt	wt	Deriv. wt	wt	Deriv. wt	wt	Deriv. wt	wt	Deriv. wt
°C	%	%/°C	%	%/°C	%	%/°C	%	%/°C	%	%/°C	%	%/°C	%	%/°C	%	%/°C	%	%/°C	%	%/°C	%	%/°C
30	100	0,03823	100	0,03518	100	0,03013	100	0,03722	100	0,03624	100	0,01286	100	0,03079	100	0,03521	100	0,001224	100	0,02748	100	0,03976

40	99,17	0,05378	99,23	0,04646	99,71	0,0311	99,95	0,03823	99,2	0,04349	99,38	0,0115	99,62	0,0385	99,25	0,04473	99,97	0,004894	99,79	0,02041	99,67	0,03167
50	98,55	0,06915	98,7	0,05824	99,36	0,03575	99,74	0,03882	98,72	0,04885	98,99	0,01628	99,22	0,04072	98,77	0,05075	99,9	0,0103	99,58	0,02243	99,36	0,03194
60	97,83	0,06985	98,09	0,06287	99,01	0,03688	99,62	0,03822	98,24	0,0457	98,58	0,02293	98,81	0,04094	98,11	0,0623	99,76	0,01791	99,34	0,02352	99,04	0,03165
70	97,2	0,05594	97,47	0,05947	98,63	0,0375	99,22	0,04004	97,82	0,03956	98,2	0,02942	98,4	0,04057	97,63	0,04836	99,54	0,026	99,1	0,02572	98,72	0,03151
80	96,71	0,04383	96,91	0,05161	98,25	0,0381	98,79	0,04173	97,45	0,03425	97,88	0,03354	98,01	0,03828	97,15	0,04638	99,25	0,03132	98,84	0,02592	98,41	0,03157
90	96,31	0,03784	96,42	0,04532	97,87	0,03892	98,37	0,04173	97,12	0,03153	97,59	0,03635	97,63	0,03851	96,69	0,04499	98,92	0,03496	98,58	0,02544	98,09	0,03234
100	95,94	0,03517	95,98	0,04258	97,48	0,03829	97,96	0,04042	96,82	0,02891	97,33	0,03423	97,25	0,03732	96,24	0,04496	98,55	0,03777	98,34	0,02346	97,77	0,03017
110	95,6	0,03336	95,58	0,03898	97,1	0,03632	97,54	0,04059	96,54	0,02665	97,09	0,0321	96,87	0,03602	95,8	0,0439	98,17	0,03829	98,11	0,02165	97,48	0,02846
120	95,27	0,03353	95,2	0,0379	96,73	0,03732	97,16	0,03703	96,28	0,0269	96,86	0,03242	96,52	0,03689	95,36	0,04449	97,78	0,04013	97,89	0,02228	97,2	0,02929
130	94,93	0,03525	94,82	0,03865	96,35	0,04064	96,75	0,0418	96	0,03038	96,61	0,03555	96,13	0,04124	94,9	0,04825	97,36	0,04393	97,66	0,02456	96,89	0,03288
140	94,56	0,03646	94,43	0,03857	95,93	0,04365	96,33	0,04402	95,68	0,03439	96,31	0,03819	95,69	0,04449	94,39	0,05282	96,9	0,04749	97,4	0,02769	96,55	0,03481
150	94,19	0,03953	94,03	0,0414	95,48	0,04668	95,89	0,04607	95,31	0,03897	95,98	0,0436	95,25	0,04414	93,88	0,0479	96,43	0,04536	97,1	0,03165	96,18	0,03845
160	93,79	0,03638	93,63	0,03534	94,99	0,04756	95,41	0,0452	94,91	0,03818	95,59	0,04082	94,82	0,03959	93,43	0,04144	96	0,04049	96,78	0,0308	95,81	0,03389
170	93,47	0,02978	93,33	0,02744	94,56	0,03731	95,02	0,03449	94,56	0,03267	95,23	0,03193	94,46	0,03257	93,06	0,03349	95,63	0,0334	96,49	0,02799	95,5	0,02845
180	93,19	0,02616	93,08	0,02325	94,22	0,03237	94,7	0,03023	94,25	0,02985	94,92	0,02753	94,16	0,02899	92,75	0,02881	95,32	0,02863	96,22	0,02548	95,23	0,02534
190	92,94	0,02309	92,86	0,02019	93,92	0,0282	94,41	0,02574	93,97	0,0271	94,62	0,02409	93,89	0,02507	92,48	0,02513	95,06	0,02463	95,98	0,02354	95	0,02241
200	92,73	0,0209	92,67	0,0182	93,65	0,02529	94,17	0,02299	93,71	0,02411	94,34	0,02148	93,66	0,02248	92,24	0,02243	94,83	0,02237	95,76	0,02124	94,78	0,02035
210	92,52	0,01936	92,49	0,01697	93,41	0,02354	93,95	0,02091	93,48	0,02241	94,09	0,01979	93,44	0,02074	92,03	0,02083	94,61	0,02052	95,55	0,02014	94,59	0,01892
220	92,33	0,01856	92,33	0,01631	93,19	0,02136	93,75	0,01955	93,26	0,02144	93,85	0,01865	93,24	0,01979	91,83	0,01989	94,41	0,01973	95,35	0,01858	94,4	0,01806
230	92,15	0,01815	92,17	0,01593	92,98	0,02069	93,55	0,01937	93,05	0,02066	93,61	0,01808	93,05	0,01908	91,63	0,01931	94,22	0,01913	95,17	0,01794	94,22	0,01776
240	91,97	0,01842	92,01	0,01621	92,77	0,02059	93,36	0,01908	92,84	0,02066	93,38	0,01836	92,86	0,0191	91,43	0,01927	94,03	0,0191	94,98	0,01836	94,05	0,01811
250	91,78	0,01892	91,84	0,0166	92,57	0,02099	93,17	0,01958	92,64	0,0207	93,15	0,01874	92,67	0,01939	91,24	0,01918	93,84	0,01923	94,8	0,01881	93,86	0,01842
260	91,59	0,01972	91,68	0,01713	92,35	0,02128	92,96	0,02058	92,43	0,02128	92,9	0,01901	92,48	0,01939	91,05	0,01946	93,64	0,0194	94,61	0,0191	93,67	0,01907
270	91,39	0,02005	91,5	0,01719	92,14	0,02169	92,75	0,02155	92,22	0,02145	92,64	0,01943	92,28	0,01934	90,85	0,01911	93,45	0,01953	94,41	0,0197	93,48	0,01973
280	91,19	0,01999	91,33	0,01709	91,92	0,02192	92,54	0,02131	92	0,02143	92,37	0,01939	92,09	0,01902	90,67	0,01828	93,25	0,01939	94,22	0,01965	93,28	0,02001
290	90,99	0,01952	91,16	0,01689	91,7	0,02092	92,33	0,02056	91,79	0,02102	92,1	0,01856	91,91	0,01801	90,48	0,01781	93,06	0,01881	94,02	0,0199	93,08	0,01989
300	90,79	0,01909	91	0,01655	91,5	0,02021	92,13	0,01971	91,58	0,02017	91,83	0,01769	91,73	0,01765	90,31	0,01722	92,88	0,01842	93,82	0,01895	92,89	0,01921
310	90,61	0,01892	90,83	0,01643	91,3	0,0192	91,94	0,01893	91,38	0,0192	91,58	0,01677	91,56	0,01684	90,14	0,01647	92,7	0,01779	93,64	0,018	92,7	0,01863
320	90,42	0,01886	90,67	0,01643	91,11	0,01873	91,75	0,01814	91,2	0,01835	91,34	0,01631	91,39	0,0162	89,98	0,01594	92,52	0,01716	93,46	0,01702	92,51	0,01809

330	90,23	0,01925	90,5	0,01649	90,93	0,01825	91,57	0,01803	91,02	0,01782	91,11	0,01604	91,23	0,0159	89,82	0,01577	92,35	0,01642	93,3	0,01604	92,33	0,01825
340	90,03	0,01953	90,34	0,01656	90,75	0,01808	91,4	0,01758	90,84	0,01785	90,88	0,01615	91,07	0,01627	89,66	0,01554	92,19	0,01609	93,14	0,01583	92,15	0,01853
350	89,84	0,01974	90,17	0,01671	90,57	0,0181	91,22	0,01736	90,66	0,01734	90,66	0,01609	90,91	0,01623	89,5	0,01572	92,03	0,01653	92,98	0,01614	91,96	0,01905
360	89,64	0,0193	90,01	0,01631	90,39	0,01795	91,05	0,01712	90,49	0,01723	90,44	0,0158	90,75	0,01598	89,34	0,01706	91,86	0,01644	92,81	0,01594	91,77	0,01898
370	89,45	0,01819	89,85	0,015	90,21	0,01734	90,88	0,01646	90,32	0,01662	90,23	0,01488	90,59	0,01553	89,19	0,01639	91,7	0,01694	92,66	0,01537	91,58	0,01851
380	89,28	0,01682	89,7	0,01424	90,04	0,01549	90,72	0,01477	90,16	0,01544	90,03	0,01324	90,44	0,01436	88,89	0,01907	91,53	0,01633	92,51	0,01445	91,4	0,01654
390	89,11	0,02019	89,55	0,02011	89,9	0,01387	90,59	0,01304	90,01	0,01346	89,86	0,01341	90,31	0,01296	88,76	0,01235	91,37	0,01524	92,37	0,013	91,25	0,01472
400	88,85	0,03344	89,28	0,03312	89,75	0,01774	90,45	0,01824	89,89	0,01333	89,52	0,02347	90,17	0,01528	88,64	0,01296	91,23	0,01385	92,25	0,0117	91,09	0,0199
410	88,43	0,05077	88,87	0,05066	89,52	0,03238	90,2	0,03275	89,87	0,02146	89,5	0,03931	89,97	0,02876	88,47	0,0217	91,09	0,01302	92,14	0,0113	90,82	0,0364
420	87,8	0,07821	88,24	0,07762	89,09	0,05477	89,76	0,0552	89,39	0,04994	89,15	0,05863	89,55	0,05599	88,13	0,05174	90,96	0,01481	92,02	0,01807	90,33	0,06201
430	86,85	0,1096	87,33	0,09906	88,44	0,06521	89,08	0,07451	88,73	0,07449	88,57	0,05362	88,87	0,07341	87,42	0,08384	90,72	0,0454	91,65	0,06521	89,59	0,08393
440	85,7	0,1027	86,44	0,05646	87,97	0,02441	88,53	0,03515	88,11	0,0356	87,84	0,01288	88,28	0,03165	86,68	0,04541	89,96	0,09437	90,78	0,09039	88,8	0,05427
450	85,08	0,02509	86,19	0,0134	87,82	0,01183	88,29	0,01048	87,82	0,01101	87,71	0,008969	88,13	0,0106	86,47	0,01163	89,15	0,04656	90,11	0,03169	88,55	0,01298
460	84,93	0,01263	86,08	0,00956	87,77	0,003328	88,19	0,009192	87,8	0,008618	87,42	0,007686	88,04	0,008378	86,38	0,008368	88,99	0,005138	90	0,00543	88,44	0,009749
470	84,81	0,01048	86	0,008052	87,69	0,007594	88,11	0,007876	87,77	0,007453	87,31	0,006777	87,96	0,007813	86,29	0,007638	88,96	0,00201	89,96	0,002852	88,35	0,00836
480	84,71	0,008995	85,92	0,007048	87,63	0,004414	88,03	0,007004	87,7	0,006876	87,22	0,00619	87,89	0,006896	86,22	0,006729	88,94	0,001013	89,94	0,001837	88,27	0,007649
490	84,63	0,007992	85,85	0,006421	87,57	0,006531	87,97	0,006706	87,63	0,006261	87,14	0,005704	87,82	0,006506	86,16	0,006903	88,94	0,00044	89,92	0,001485	88,2	0,006881
500	84,55	0,007229	85,79	0,005786	87,52	0,003573	87,9	0,006357	87,57	0,005942	87,06	0,005268	87,76	0,00623	86,1	0,005868	88,93	0,0002149	89,91	0,0009877	88,13	0,006308
510	84,49	0,006617	85,74	0,005497	87,47	0,005458	87,84	0,005447	87,51	0,005999	86,98	0,005058	87,7	0,005747	86,04	0,005759	88,93	0,0003682	89,9	0,0009819	88,07	0,006082
520	84,42	0,006127	85,68	0,005341	87,38	0,008746	87,79	0,00622	87,45	0,006021	86,9	0,005086	87,64	0,005652	85,98	0,00658	88,93	0,0001247	89,89	0,001407	88,01	0,00599
530	84,36	0,005993	85,63	0,005254	87,33	0,006572	87,72	0,005963	87,39	0,006407	86,83	0,005032	87,58	0,005709	85,92	0,00623	88,92	0,001481	89,87	0,001927	87,95	0,005876
540	84,3	0,006015	85,58	0,005168	87,27	0,006657	87,66	0,006313	87,32	0,006939	86,75	0,005262	87,52	0,006537	85,85	0,006619	88,9	0,002557	89,85	0,002953	87,89	0,006119
550	84,24	0,006081	85,52	0,00544	87,2	0,007085	87,6	0,006414	87,25	0,007235	86,67	0,005465	87,46	0,006308	85,79	0,006689	88,87	0,003745	89,82	0,003602	87,83	0,006379
560	84,18	0,005973	85,47	0,005367	87,12	0,007701	87,54	0,006753	87,18	0,00798	86,59	0,00568	87,39	0,007136	85,71	0,007546	88,82	0,005198	89,78	0,004612	87,76	0,00684
570	84,12	0,00636	85,42	0,005702	87,04	0,008164	87,56	0,008161	87,09	0,008942	86,5	0,005765	87,31	0,007504	85,64	0,008384	88,77	0,006465	89,72	0,006011	87,69	0,007459
580	84,06	0,006459	85,36	0,005768	86,96	0,008681	87,48	0,007671	87	0,009994	86,4	0,005807	87,29	0,008926	85,55	0,009738	88,69	0,008026	89,66	0,007182	87,61	0,008092
590	83,99	0,006599	85,3	0,005837	86,87	0,00887	87,4	0,007733	86,89	0,01127	86,3	0,005708	87,28	0,01054	85,45	0,01019	88,6	0,009771	89,58	0,008874	87,53	0,008552
600	83,92	0,006628	85,24	0,005736	86,78	0,00892	87,33	0,007905	86,77	0,0125	86,19	0,008427	87,23	0,006734	85,35	0,01059	88,5	0,012	89,48	0,01114	87,44	0,008702
610	83,86	0,006958	85,18	0,006102	86,69	0,008615	87,25	0,002341	86,64	0,01298	86,09	0,006078	87,17	0,009296	85,24	0,01041	88,36	0,01472	89,35	0,01353	87,36	0,008318

620	83,78	0,007765	85,12	0,00673	86,61	0,008485	87,23	0,006275	86,51	0,01249	85,99	0,005297	87,13	0,008024	85,15	0,009068	88,2	0,01807	89,2	0,01672	87,28	0,007771
630	83,7	0,009662	85,05	0,008509	86,52	0,008111	87,18	0,006522	86,4	0,0112	85,9	0,005973	87,03	0,007968	85,06	0,008082	88	0,02193	89,02	0,02028	87,2	0,007914
640	83,59	0,01279	84,95	0,01133	86,44	0,009255	87,09	0,009376	86,29	0,009839	85,8	0,01012	86,97	0,008683	84,97	0,009745	87,76	0,02604	88,8	0,02308	87,12	0,009468
650	83,44	0,01629	84,82	0,01386	86,33	0,01176	86,99	0,01218	86,19	0,01122	85,74	0,01121	86,86	0,0144	84,86	0,01382	87,48	0,02964	88,56	0,02463	87,01	0,01203
660	83,27	0,01863	84,67	0,01483	86,19	0,01537	86,87	0,01179	86,06	0,01536	85,61	0,01173	86,71	0,01381	84,72	0,01459	87,17	0,03018	88,32	0,0208	86,88	0,01372
670	83,08	0,01903	84,53	0,01337	86,03	0,01666	86,76	0,01165	85,89	0,01796	85,55	0,00971	86,57	0,01322	84,57	0,013	86,9	0,0218	88,15	0,0147	86,74	0,01276
680	82,89	0,01612	84,41	0,009483	85,86	0,01564	86,66	0,006907	85,71	0,01603	85,41	0,005763	86,45	0,009387	84,48	0,005735	86,71	0,02167	87,98	0,02091	86,63	0,009244
690	82,76	0,009663	84,34	0,006134	85,73	0,009937	86,61	0,00433	85,58	0,01008	85,32	0,003284	86,39	0,005794	84,42	0,0064	86,47	0,02301	87,76	0,02154	86,56	0,00528
700	82,69	0,005367	84,28	0,004598	85,66	0,006032	86,57	0,003511	85,5	0,006839	85,26	0,002537	86,34	0,004408	84,38	0,002687	86,29	0,01099	87,59	0,01195	86,52	0,003606
710	82,65	0,003714	84,24	0,004381	85,6	0,00497	86,54	0,003051	85,44	0,006443	85,15	0,002033	86,3	0,004151	84,33	0,005214	86,22	0,005727	87,51	0,005353	86,48	0,003045
720	82,62	0,0033	84,19	0,004523	85,55	0,005615	86,5	0,003502	85,37	0,006897	85	0,002159	86,26	0,004186	84,28	0,005347	86,17	0,005261	87,46	0,004004	86,45	0,002933
730	82,58	0,003293	84,15	0,004843	85,49	0,006222	86,47	0,003394	85,3	0,007434	84,94	0,002235	86,22	0,004419	84,23	0,00531	86,11	0,005506	87,42	0,003978	86,42	0,00288
740	82,55	0,003185	84,1	0,00538	85,43	0,00674	86,44	0,003243	85,22	0,008491	84,8	0,002378	86,17	0,00465	84,17	0,005899	86,06	0,005578	87,38	0,004213	86,4	0,002831
750	82,52	0,002973	84,04	0,005819	85,42	0,007856	86,4	0,003398	85,13	0,009804	84,75	0,002455	86,13	0,005012	84,11	0,006282	86	0,005709	87,34	0,004109	86,37	0,002876
760	82,49	0,00253	83,98	0,006329	85,33	0,01531	86,37	0,003809	85,02	0,0118	84,63	0,002317	86,07	0,005441	84,04	0,006773	85,95	0,005655	87,3	0,003913	86,34	0,002774
770	82,47	0,002138	83,91	0,00698	85,31	0,00945	86,33	0,004145	84,89	0,01457	84,57	0,002388	86,02	0,006133	83,97	0,00718	85,89	0,005318	87,26	0,003714	86,31	0,002676
780	82,45	0,001965	83,84	0,007929	85,27	0,01238	86,29	0,003575	84,73	0,01782	84,43	0,002261	85,95	0,0069	83,89	0,008116	85,84	0,005012	87,23	0,003486	86,29	0,002259
790	82,43	0,002194	83,76	0,009185	85,18	0,01251	86,26	0,004096	84,53	0,02106	84,32	0,002151	85,88	0,007474	83,81	0,0099	85,79	0,004884	87,2	0,003142	86,26	0,002094
800	82,4	0,002625	83,66	0,01048	85,04	0,01191	86,21	0,005393	84,31	0,02217	84,21	0,002159	85,8	0,00761	83,7	0,01172	85,74	0,005067	87,16	0,003355	86,24	0,002033
810	82,38	0,003126	83,55	0,01163	84,93	0,01177	86,15	0,006068	84,09	0,02162	84,12	0,00259	85,72	0,007987	83,57	0,01362	85,69	0,005563	87,13	0,003591	86,22	0,00222
820	82,34	0,00375	83,43	0,01238	84,82	0,01154	86,09	0,006082	83,88	0,02031	84	0,002788	85,64	0,008555	83,43	0,01447	85,63	0,005736	87,09	0,003729	86,2	0,002563
830	82,3	0,004176	83,3	0,01325	84,7	0,01187	86,02	0,01409	83,69	0,01876	83,93	0,003086	85,56	0,007798	83,29	0,01478	85,57	0,005882	87,05	0,004005	86,17	0,002911
840	82,26	0,004273	83,16	0,01439	84,58	0,01175	85,91	0,006484	83,51	0,01783	83,8	0,003434	85,48	0,008027	83,14	0,01471	85,51	0,006015	87,01	0,004126	86,14	0,002963
850	82,22	0,004092	83,01	0,01515	84,45	0,01269	85,83	0,007594	83,33	0,01685	83,78	0,003443	85,39	0,008612	83	0,01532	85,45	0,005592	86,97	0,004053	86,11	0,003013
860	82,18	0,003807	82,86	0,01557	84,33	0,01271	85,76	0,006754	83,17	0,0165	83,74	0,003622	85,31	0,008681	82,84	0,01414	85,4	0,005445	86,93	0,00387	86,08	0,002815
870	82,14	0,003861	82,7	0,01545	84,2	0,01295	85,69	0,006696	83,01	0,01615	83,69	0,004163	85,23	0,008547	82,7	0,01345	85,34	0,005356	86,9	0,003605	86,05	0,002746
880	82,1	0,003598	82,55	0,01527	84,07	0,01302	85,63	0,006743	82,85	0,01571	83,53	0,004122	85,14	0,008087	82,57	0,0133	85,29	0,005329	86,86	0,003475	86,03	0,002699
890	82,07	0,003553	82,4	0,01506	83,94	0,006975	85,56	0,006461	82,69	0,01554	83,46	0,004539	85,06	0,008489	82,44	0,01321	85,24	0,005506	86,82	0,003557	86	0,002708
900	82,03	0,00374	82,25	0,01444	83,89	0,01146	85,49	0,006801	82,54	0,01522	83,39	0,004565	84,97	0,008032	82,32	0,02104	85,18	0,005884	86,79	0,003425	85,97	0,002578

910	81,99	0,003954	82,11	0,01425	83,77	0,01288	85,42	0,006365	82,39	0,01463	83,31	0,004462	84,9	0,008507	81,99	0,0146	85,12	0,006279	86,76	0,003139	85,95	0,002781
920	81,95	0,004278	81,96	0,01396	83,65	0,01045	85,36	0,006016	82,25	0,0137	83,25	0,004422	84,81	0,007278	81,88	0,0111	85,06	0,006765	86,72	0,003405	85,92	0,002585
930	81,9	0,004607	81,83	0,01355	83,55	0,01027	85,31	0,006015	82,11	0,01284	83,2	0,004267	84,74	0,007321	81,78	0,009576	84,99	0,007283	86,69	0,003299	85,89	0,002627
940	81,86	0,004701	81,7	0,01276	83,45	0,009159	85,24	0,003407	81,99	0,01173	83,18	0,004133	84,67	0,006931	81,69	0,008931	84,91	0,007816	86,66	0,003226	85,87	0,002501
950	81,81	0,004695	81,57	0,01149	83,37	0,008347	85,2	0,007759	81,88	0,01067	83,12	0,004517	84,6	0,006399	81,6	0,008267	84,83	0,008228	86,63	0,003223	85,84	0,002796
960	81,76	0,00486	81,47	0,01	83,28	0,007732	85,2	0,005208	81,78	0,009829	83,07	0,004596	84,54	0,006182	81,52	0,007522	84,75	0,008209	86,6	0,003182	85,81	0,002848
970	81,71	0,004914	81,37	0,00911	83,2	0,007759	85,15	0,005636	81,68	0,009436	83,02	0,004903	84,47	0,006906	81,45	0,006977	84,66	0,008325	86,56	0,003417	85,79	0,002908
980	81,67	0,004711	81,28	0,00815	83,12	0,007618	85,12	0,0058	81,59	0,009244	83	0,005211	84,41	0,008134	81,38	0,006976	84,58	0,008258	86,52	0,003713	85,76	0,003057
990	81,62	0,004767	81,21	0,007817	83,05	0,007373	85,09	0,004953	81,58	0,00924	82,9	0,005443	84,34	0,006077	81,32	0,006201	84,5	0,008587	86,48	0,003897	85,68	0,003059
1000	81,6	0,00477	81,18	0,007815	83,05	0,00721	85,07	0,004	81,57	0,009238	82,97	0,005452	84,34	0,006012	81,24	0,00614	84,48	0,008478	86,45	0,003907	85,29	0,003061
	C100-7d		**FA30-28d**		**S7F-28d**		**S7A-28d**		**S7Q-28d**		**S8F-28d**		**S8A-28d**		**S8Q-28d**		**S9F-28d**		**S9A-28d**		**S9Q-28d**	
Temp	wt	Deriv. Wt	Weight	Deriv. Weight	Weight	Deriv. Weight	Weight	Deriv. Weight	Weight	Deriv. Weight	Weight	Deriv. Weight	Weight	Deriv. Weight	Weight	Deriv. Weight	Weight	Deriv. Weight	Weight	Deriv. Weight	Weight	Deriv. Weight
°C	%	%/°C	%	%/°C	%	%/°C	%	%/°C	%	%/°C	%	%/°C	%	%/°C	%	%/°C	%	%/°C	%	%/°C	%	%/°C
30	100	0,03542	100	0,05357	100	0,02334	100	0,03051	100	0,01077	100	0,01562	100	0,02245	100	0,01488	100	0,04035	100	0,0347	100	0,03005
40	99,57	0,05367	99,47	0,05778	99,85	0,0148	99,77	0,02591	99,87	0,01589	99,83	0,02028	99,79	0,02261	99,89	0,01117	99,66	0,03352	99,72	0,0286	99,69	0,02923
50	98,91	0,07711	98,85	0,06558	99,69	0,01819	99,48	0,02982	99,67	0,02329	99,6	0,02669	99,55	0,02507	99,76	0,01347	99,31	0,0374	99,41	0,03396	99,38	0,03303
60	98,07	0,0847	98,21	0,05971	99,48	0,02331	99,15	0,03363	99,4	0,03141	99,3	0,03343	99,26	0,03044	99,62	0,02017	98,91	0,04078	99,04	0,03879	99,03	0,03632
70	97,29	0,06918	97,66	0,0489	99,22	0,02737	98,8	0,03466	99,05	0,03697	98,92	0,04105	98,96	0,03203	99,39	0,02288	98,5	0,0409	98,64	0,04143	98,66	0,03742
80	96,69	0,0515	97,22	0,04048	98,93	0,03135	98,46	0,03466	98,67	0,0385	98,5	0,04277	98,63	0,03215	99,14	0,02821	98,1	0,03907	98,22	0,04109	98,29	0,03671
90	96,23	0,04222	96,84	0,03753	98,61	0,03102	98,12	0,03361	98,28	0,03868	98,08	0,04135	98,3	0,03399	98,85	0,02907	97,72	0,0384	97,82	0,04046	97,92	0,03673
100	95,82	0,04004	96,46	0,03696	98,27	0,03511	97,79	0,02898	97,9	0,03767	97,66	0,04211	97,92	0,03836	98,56	0,02782	97,33	0,03855	97,41	0,04087	97,56	0,03659
110	95,43	0,03934	96,1	0,036	97,94	0,03272	97,51	0,02931	97,54	0,03567	97,24	0,04158	97,58	0,03287	98,3	0,02582	96,95	0,03755	97,01	0,04002	97,2	0,03543
120	95,03	0,04006	95,74	0,03691	97,64	0,03292	97,21	0,0313	97,19	0,03521	96,82	0,0423	97,25	0,03478	98,04	0,02626	96,57	0,03846	96,61	0,04083	96,84	0,03669
130	94,62	0,04315	95,35	0,04139	97,27	0,03883	96,87	0,03602	96,82	0,03863	96,39	0,04547	96,88	0,0396	97,76	0,02978	96,17	0,04287	96,18	0,04495	96,46	0,04067
140	94,16	0,04736	94,91	0,0448	96,85	0,04523	96,48	0,04114	96,4	0,0434	95,91	0,04934	96,46	0,04448	97,44	0,034	95,71	0,04758	95,7	0,05011	96,02	0,04461
150	93,7	0,04594	94,47	0,04278	96,38	0,04818	96,06	0,04418	95,96	0,04444	95,63	0,03677	96,01	0,04611	97,08	0,03705	95,24	0,04676	95,21	0,04858	95,58	0,04434
160	93,23	0,04705	94,05	0,0389	95,88	0,04978	95,6	0,04432	95,52	0,04308	95,12	0,04861	95,57	0,04237	96,7	0,03827	94,78	0,04359	94,72	0,04549	95,14	0,0419
170	92,8	0,03865	93,71	0,03119	95,43	0,04195	95,19	0,03965	95,11	0,03806	94,68	0,03942	95,16	0,03826	96,33	0,03683	94,39	0,03538	94,32	0,0359	94,76	0,03436
180	92,44	0,03331	93,42	0,02745	95,02	0,03798	94,81	0,03619	94,75	0,03474	94,32	0,03338	94,8	0,03423	95,87	0,0466	94,06	0,03082	93,99	0,03046	94,44	0,0299

190	92,12	0,03003	93,16	0,0242	94,66	0,03398	94,46	0,03269	94,42	0,03094	94,01	0,02957	94,47	0,03047	95,54	0,0307	93,77	0,02701	93,71	0,02633	94,16	0,0264
200	91,84	0,02696	92,93	0,02141	94,35	0,02955	94,15	0,02927	94,12	0,02791	93,73	0,02621	94,18	0,02699	95,25	0,02758	93,52	0,02361	93,46	0,02287	93,91	0,02331
210	91,58	0,02458	92,73	0,01997	94,07	0,02615	93,88	0,02677	93,85	0,02619	93,48	0,024	93,93	0,02435	94,99	0,02537	93,29	0,02169	93,25	0,02103	93,69	0,02122
220	91,35	0,02339	92,53	0,01912	93,81	0,02508	93,62	0,02527	93,6	0,02463	93,24	0,02281	93,7	0,02158	94,74	0,02396	93,08	0,02059	93,04	0,02017	93,49	0,02016
230	91,11	0,02286	92,34	0,01914	93,57	0,02393	93,37	0,02443	93,36	0,02419	93,02	0,0222	93,48	0,02199	94,51	0,02307	92,88	0,0201	92,84	0,01991	93,29	0,01969
240	90,89	0,02286	92,15	0,01919	93,33	0,02325	93,13	0,02388	93,12	0,02387	92,8	0,02183	93,26	0,02167	94,28	0,02265	92,68	0,02027	92,64	0,01983	93,09	0,01971
250	90,66	0,02338	91,96	0,01973	93,1	0,02342	92,89	0,02355	92,88	0,02417	92,59	0,0219	93,05	0,0217	94,05	0,02266	92,47	0,02058	92,44	0,02015	92,89	0,02017
260	90,42	0,02399	91,76	0,02007	92,88	0,02405	92,65	0,02394	92,64	0,02487	92,37	0,02202	92,83	0,02225	93,82	0,02298	92,26	0,021	92,24	0,0203	92,69	0,02051
270	90,18	0,0246	91,55	0,02019	92,62	0,02403	92,42	0,02394	92,39	0,02524	92,15	0,02203	92,6	0,02255	93,59	0,02298	92,05	0,02128	92,04	0,02035	92,48	0,02104
280	89,93	0,0246	91,35	0,02002	92,38	0,0243	92,17	0,02439	92,13	0,02518	91,92	0,02203	92,38	0,02247	93,36	0,02334	91,84	0,02103	91,84	0,02018	92,27	0,02128
290	89,68	0,0243	91,16	0,01965	92,14	0,02365	91,93	0,02405	91,88	0,02462	91,71	0,02118	92,16	0,02183	93,13	0,02293	91,63	0,02069	91,64	0,01964	92,06	0,02075
300	89,44	0,02383	90,96	0,01925	91,89	0,02401	91,69	0,02329	91,64	0,02337	91,5	0,0206	91,94	0,02116	92,91	0,02218	91,43	0,01995	91,44	0,01889	91,85	0,02025
310	89,21	0,0232	90,77	0,01871	91,67	0,0217	91,46	0,02205	91,42	0,02197	91,3	0,01939	91,73	0,0205	92,69	0,02109	91,23	0,01924	91,26	0,01827	91,65	0,01939
320	88,98	0,02313	90,58	0,01875	91,5	0,01602	91,25	0,0213	91,2	0,02102	91,11	0,01855	91,53	0,01986	92,48	0,02005	91,04	0,01878	91,08	0,01777	91,46	0,01893
330	88,74	0,02357	90,4	0,01875	91,3	0,01938	91,05	0,02002	90,99	0,01991	90,93	0,01807	91,34	0,01864	92,29	0,0192	90,86	0,01871	90,9	0,01793	91,28	0,01901
340	88,51	0,02394	90,21	0,01932	91,1	0,01901	90,85	0,01934	90,8	0,01928	90,75	0,01793	91,16	0,01822	92,1	0,01864	90,67	0,019	90,72	0,01808	91,08	0,01921
350	88,27	0,02441	90,01	0,01957	90,91	0,01908	90,66	0,01917	90,6	0,01925	90,57	0,01774	90,97	0,01837	91,91	0,01856	90,48	0,01923	90,54	0,0183	90,89	0,01936
360	88,02	0,02481	89,82	0,01954	90,72	0,01832	90,46	0,01925	90,41	0,01934	90,39	0,01783	90,79	0,01817	91,73	0,01834	90,28	0,01938	90,35	0,01872	90,7	0,01963
370	87,77	0,02414	89,62	0,01851	90,54	0,01846	90,27	0,01904	90,22	0,01936	90,21	0,01755	90,61	0,01795	91,55	0,01811	90,09	0,01896	90,17	0,0186	90,5	0,01935
380	87,54	0,02227	89,45	0,01644	90,36	0,0178	90,09	0,01835	90,02	0,01905	90,04	0,01669	90,43	0,01722	91,37	0,01736	89,91	0,01738	89,98	0,01719	90,31	0,01743
390	87,33	0,01976	89,29	0,01532	90,18	0,0162	89,91	0,01699	89,84	0,01812	89,89	0,01493	90,27	0,01599	91,2	0,01589	89,75	0,01516	89,82	0,01536	90,15	0,01543
400	87,24	0,01911	89,13	0,01865	90,03	0,01428	89,74	0,01531	89,66	0,01609	89,74	0,01362	90,12	0,01379	91,05	0,01431	89,6	0,01598	89,67	0,0176	89,99	0,01886
410	86,93	0,02434	88,88	0,03508	89,9	0,01308	89,6	0,01457	89,51	0,01525	89,61	0,01367	89,98	0,01293	90,91	0,01313	89,39	0,02785	89,44	0,03068	89,75	0,03292
420	86,58	0,05094	88,41	0,06017	89,76	0,01589	89,44	0,0229	89,35	0,02071	89,41	0,03351	89,85	0,01891	90,78	0,01742	89	0,05187	89,02	0,05401	89,31	0,05453
430	85,88	0,09129	87,66	0,09	89,47	0,05392	89,01	0,06889	88,98	0,06262	88,87	0,07126	89,46	0,0669	90,44	0,05909	88,35	0,07685	88,36	0,0759	88,65	0,07497
440	84,76	0,1296	86,66	0,09181	88,73	0,07027	88,16	0,07358	88,17	0,07688	88,15	0,0574	88,59	0,08344	89,65	0,08313	87,6	0,05274	87,63	0,05313	87,94	0,05004
450	83,41	0,1165	86,12	0,02034	88,33	0,01587	87,77	0,0164	87,7	0,01948	87,83	0,01495	88,11	0,02126	89,02	0,03177	87,34	0,01425	87,36	0,01399	87,69	0,01433
460	82,77	0,0237	85,99	0,01121	88,22	0,007046	87,66	0,008029	87,6	0,00656	87,72	0,009322	88	0,005952	88,89	0,007423	87,23	0,009868	87,25	0,01032	87,57	0,01049
470	82,61	0,01321	85,89	0,009459	88,19	0,003264	87,6	0,006284	87,55	0,004063	87,64	0,007998	87,95	0,004139	88,83	0,004739	87,14	0,008512	87,15	0,009015	87,47	0,009149

480	82,49	0,01126	85,8	0,008523	88,16	0,002584	87,53	0,00563	87,51	0,002585	87,56	0,007453	87,91	0,003217	88,79	0,003419	87,06	0,007532	87,07	0,008129	87,39	0,008306
490	82,39	0,009687	85,72	0,007439	88,13	0,002314	87,48	0,004807	87,49	0,00181	87,49	0,006801	87,88	0,002677	88,76	0,002679	86,99	0,006971	86,99	0,007433	87,31	0,007564
500	82,3	0,008664	85,65	0,006857	88,11	0,00144	87,44	0,004369	87,47	0,001693	87,42	0,006291	87,85	0,002108	88,74	0,002145	86,92	0,006415	86,92	0,006919	87,23	0,006998
510	82,21	0,008091	85,59	0,006339	88,09	0,002117	87,39	0,00447	87,46	0,001187	87,36	0,00636	87,83	0,002216	88,72	0,001974	86,86	0,006094	86,85	0,006607	87,17	0,006722
520	82,13	0,007863	85,52	0,006281	88,08	0,001841	87,35	0,004514	87,45	0,001533	87,3	0,006139	87,81	0,002463	88,7	0,002156	86,8	0,006033	86,79	0,00647	87,1	0,006554
530	82,06	0,007795	85,46	0,006346	88,05	0,002771	87,3	0,004565	87,43	0,002349	87,24	0,0061	87,78	0,002877	88,67	0,002574	86,74	0,006059	86,72	0,006514	87,04	0,006333
540	81,98	0,007985	85,4	0,006628	88,02	0,003767	87,25	0,005291	87,4	0,003484	87,17	0,006464	87,75	0,003584	88,65	0,003232	86,68	0,006102	86,66	0,006411	86,97	0,006381
550	81,9	0,00842	85,33	0,007111	87,98	0,004291	87,2	0,005873	87,36	0,004994	87,11	0,007131	87,71	0,004311	88,61	0,004223	86,61	0,006424	86,59	0,006673	86,91	0,006555
560	81,81	0,009019	85,25	0,007642	87,93	0,005715	87,13	0,006844	87,31	0,005536	87,03	0,007736	87,66	0,005547	88,56	0,005762	86,55	0,006924	86,52	0,007129	86,84	0,006708
570	81,71	0,009795	85,18	0,008004	87,86	0,006872	87,06	0,007809	87,24	0,008299	86,94	0,004653	87,6	0,006648	88,5	0,006355	86,47	0,007757	86,45	0,007641	86,77	0,007295
580	81,61	0,01061	85,09	0,008202	87,79	0,008275	86,98	0,008989	87,14	0,01009	86,9	0,006219	87,53	0,007722	88,43	0,007983	86,39	0,008548	86,37	0,007984	86,7	0,007488
590	81,5	0,0112	85,01	0,007968	87,69	0,01091	86,88	0,0106	87,03	0,01169	86,88	0,009496	87,45	0,009434	88,34	0,0109	86,3	0,009262	86,29	0,008148	86,62	0,007594
600	81,39	0,01182	84,93	0,007912	87,58	0,01131	86,77	0,01274	86,91	0,01321	86,78	0,009349	87,34	0,01136	88,22	0,01111	86,21	0,009463	86,21	0,008112	86,55	0,007472
610	81,27	0,01191	84,86	0,007489	87,46	0,01355	86,63	0,0174	86,77	0,01523	86,71	0,008423	87,22	0,01386	88,1	0,01408	86,12	0,008694	86,13	0,007521	86,47	0,006958
620	81,15	0,0124	84,78	0,007946	87,31	0,01591	86,44	0,0179	86,6	0,01831	86,66	0,00717	87,07	0,01669	87,95	0,0166	86,04	0,007473	86,06	0,006838	86,41	0,006486
630	81,02	0,01424	84,69	0,009606	87,13	0,01998	86,25	0,01961	86,4	0,02182	86,58	0,007655	86,89	0,0196	87,76	0,01981	85,97	0,006729	85,99	0,006973	86,34	0,007052
640	80,86	0,0172	84,59	0,01164	86,92	0,02297	86,06	0,0187	86,16	0,02598	86,49	0,01054	86,68	0,02222	87,55	0,02312	85,89	0,008333	85,91	0,008834	86,26	0,008941
650	80,67	0,02042	84,46	0,01394	86,67	0,02563	85,87	0,01668	85,88	0,03058	86,38	0,0123	86,45	0,0229	87,3	0,02513	85,8	0,01127	85,81	0,0116	86,16	0,01131
660	80,45	0,02275	84,32	0,01419	86,42	0,0236	85,74	0,01056	85,56	0,03398	86,3	0,01179	86,23	0,01816	87,06	0,02255	85,67	0,01299	85,68	0,01327	86,04	0,01285
670	80,23	0,02122	84,18	0,01129	86,22	0,01604	85,63	0,01461	85,22	0,03171	86,26	0,005819	86,1	0,0114	86,87	0,01405	85,54	0,0121	85,55	0,0131	85,91	0,01222
680	80,05	0,01372	84,09	0,006717	86,08	0,01642	85,46	0,01609	84,96	0,01914	86,2	0,004646	85,95	0,01714	86,73	0,01751	85,44	0,008198	85,43	0,0097	85,8	0,00845
690	79,95	0,00682	84,04	0,004084	85,89	0,01962	85,32	0,01069	84,76	0,02238	86	0,00348	85,78	0,01441	86,54	0,01692	85,38	0,004728	85,36	0,005222	85,74	0,004638
700	79,9	0,004924	84,01	0,003258	85,72	0,01136	85,25	0,004947	84,56	0,01573	85,89	0,002804	85,68	0,006258	86,41	0,008505	85,34	0,003387	85,32	0,003572	85,7	0,003267
710	79,85	0,004558	83,98	0,003164	85,65	0,004351	85,21	0,003891	84,46	0,006014	85,86	0,002578	85,64	0,003792	86,36	0,003954	85,31	0,002769	85,29	0,003162	85,67	0,003121
720	79,8	0,004491	83,95	0,003135	85,6	0,004942	85,17	0,004125	84,41	0,004732	85,84	0,002878	85,6	0,004209	86,32	0,003575	85,28	0,002594	85,25	0,003373	85,64	0,003037
730	79,76	0,004493	83,91	0,003442	85,56	0,004446	85,13	0,004101	84,37	0,004473	85,81	0,002934	85,57	0,003655	86,29	0,003651	85,25	0,002684	85,22	0,003329	85,61	0,002961
740	79,72	0,004506	83,88	0,003452	85,52	0,003749	85,08	0,004177	84,32	0,004854	85,78	0,002881	85,53	0,003616	86,25	0,003956	85,23	0,002854	85,18	0,003649	85,58	0,002893
750	79,67	0,004287	83,84	0,003694	85,48	0,00431	85,04	0,004389	84,27	0,004477	85,76	0,003124	85,49	0,003739	86,21	0,003645	85,2	0,002848	85,15	0,003964	85,55	0,002948
760	79,63	0,004076	83,81	0,003699	85,44	0,004196	85	0,004613	84,22	0,004617	85,72	0,003242	85,46	0,003678	86,18	0,003798	85,17	0,002993	85,11	0,004132	85,52	0,003192

770	79,59	0,004453	83,77	0,00385	85,4	0,003532	84,95	0,004739	84,18	0,004397	85,7	0,003285	85,42	0,003484	86,14	0,003796	85,14	0,002951	85,06	0,004547	85,49	0,003187
780	79,54	0,005258	83,73	0,004365	85,36	0,00372	84,9	0,005184	84,13	0,004231	85,68	0,003635	85,38	0,003359	86,1	0,003732	85,11	0,002713	85,01	0,005327	85,46	0,003429
790	79,48	0,006963	83,68	0,005076	85,32	0,003821	84,85	0,006228	84,09	0,003991	85,63	0,003146	85,35	0,003275	86,06	0,003372	85,08	0,00271	84,96	0,006245	85,42	0,004055
800	79,4	0,009912	83,63	0,006293	85,29	0,004777	84,78	0,006826	84,05	0,004018	85,58	0,003694	85,31	0,003741	86,03	0,003657	85,06	0,002681	84,89	0,006777	85,38	0,004637
810	79,28	0,01415	83,56	0,007546	85,23	0,001015	84,71	0,007651	84,01	0,004463	85,51	0,003223	85,28	0,004182	85,99	0,004114	85,03	0,002893	84,82	0,006976	85,33	0,00511
820	79,12	0,01757	83,47	0,008872	85,22	0,004807	84,63	0,007398	83,96	0,00465	85,48	0,003192	85,23	0,004355	85,95	0,004308	85	0,003064	84,75	0,007017	85,27	0,005233
830	78,93	0,01908	83,38	0,01004	85,17	0,0041	84,56	0,007093	83,91	0,004839	85,41	0,02322	85,19	0,004379	85,91	0,004112	84,97	0,003249	84,68	0,007031	85,22	0,005317
840	78,74	0,01969	83,27	0,01138	85,13	0,004337	84,49	0,007124	83,86	0,004952	85,4	0,01842	85,14	0,004541	85,87	0,004172	84,93	0,003329	84,61	0,00733	85,17	0,005615
850	78,54	0,02026	83,15	0,01269	85,08	0,00434	84,42	0,007077	83,81	0,0048	85,31	0,003102	85,1	0,004003	85,82	0,003953	84,9	0,003104	84,53	0,007551	85,11	0,005868
860	78,33	0,02166	83,02	0,0139	85,04	0,003124	84,35	0,007348	83,77	0,004701	85,28	0,004484	85,06	0,004632	85,78	0,003988	84,87	0,003079	84,46	0,007609	85,05	0,006163
870	78,1	0,024	82,87	0,01512	85	0,004278	84,28	0,007116	83,72	0,004724	85,21	0,007691	85,01	0,004369	85,75	0,003991	84,84	0,002822	84,38	0,007851	84,99	0,006288
880	77,85	0,02667	82,72	0,01624	84,96	0,003953	84,21	0,007546	83,68	0,0044	85,2	0,002337	84,96	0,004688	85,71	0,003852	84,81	0,003064	84,3	0,007967	84,92	0,006434
890	77,57	0,02953	82,55	0,01728	84,93	0,003584	84,13	0,007273	83,63	0,004286	85,18	0,003173	84,91	0,004864	85,67	0,003898	84,78	0,002781	84,22	0,007937	84,86	0,006395
900	77,26	0,03175	82,37	0,01817	84,89	0,003659	84,06	0,007201	83,59	0,004177	85,14	0,003479	84,86	0,005075	85,63	0,003981	84,76	0,002811	84,14	0,007944	84,79	0,006612
910	76,93	0,0328	82,18	0,01886	84,85	0,00359	83,99	0,00714	83,55	0,003948	85,11	0,003227	84,81	0,004819	85,59	0,00386	84,73	0,002729	84,07	0,007894	84,73	0,00692
920	76,61	0,0296	82	0,01878	84,82	0,003266	83,92	0,007294	83,52	0,003844	85,07	0,003499	84,77	0,004733	85,55	0,00378	84,7	0,002766	83,99	0,007897	84,66	0,00685
930	76,36	0,02184	81,81	0,01796	84,78	0,003382	83,85	0,006719	83,48	0,003584	85,04	0,003187	84,72	0,004669	85,51	0,003548	84,67	0,003092	83,91	0,007822	84,59	0,006342
940	76,16	0,01814	81,64	0,01659	84,75	0,003311	83,78	0,006953	83,44	0,003464	85	0,00362	84,67	0,005127	85,48	0,003448	84,64	0,003135	83,83	0,007474	84,53	0,006126
950	75,98	0,01772	81,48	0,01482	84,72	0,003266	83,71	0,007867	83,41	0,00365	84,97	0,003721	84,62	0,004764	85,44	0,003422	84,61	0,003405	83,76	0,007585	84,47	0,005831
960	75,8	0,01817	81,34	0,01272	84,68	0,003516	83,63	0,006821	83,37	0,003541	84,93	0,003941	84,58	0,004552	85,41	0,003301	84,57	0,003441	83,68	0,007493	84,42	0,005347
970	75,62	0,0183	81,23	0,0107	84,66	0,002945	83,56	0,006636	83,34	0,003733	84,89	0,003863	84,52	0,004985	85,38	0,00331	84,54	0,003635	83,61	0,007521	84,36	0,005239
980	75,44	0,01821	81,13	0,009289	84,62	0,00339	83,5	0,007206	83,31	0,003486	84,85	0,004528	84,47	0,0053	85,34	0,003303	84,5	0,003975	83,53	0,006784	84,31	0,005342
990	75,26	0,01803	81,04	0,009176	84,59	0,00368	83,42	0,007222	83,27	0,002886	84,8	0,004781	84,41	0,005431	85,31	0,003704	84,46	0,004174	83,47	0,006828	84,26	0,005458
1000	75,2	0,01801	80,95	0,009165	84,57	0,00371	83,39	0,007432	83,21	0,002878	84,76	0,004802	84,38	0,005567	85,28	0,003812	84,4	0,004151	83,43	0,006621	84,22	0,005321